REGULATION OF COHESIN AND PLK1 FUNCTION IN MOUSE OOCYTES

Submitted by

Dimitrios Kalleas

Institute for Ageing and Health

Newcastle University

A thesis submitted for the degree of Doctor of Philosophy
Newcastle upon Tyne, December 2012

Abstract

Faithful segregation of homologous chromosomes during the first meiotic division (MI) is essential for the formation of haploid gametes. Recent research in our lab and others has shown that female ageing is associated with depletion of chromosomal cohesin and is accompanied by a marked decline in the ability of oocytes to segregate chromosomes synchronously during MI. This mechanism likely underlies the dramatic increase in infertility, miscarriage and birth defects that accompany female reproductive ageing. Here, I have used a mouse model and the transgenic *Rec8-myc* mouse strain to investigate mechanisms regulating chromosome segregation in oocytes and to identify pathways leading to missegregation during MI.

I show for the first time that Plk1 is required for stepwise removal of cohesin, which is essential for normal segregation of chromosomes during meiosis. I found that a highly specific small-molecule inhibitor of Plk1 (BI 2536) inhibited APC/C-mediated degradation of securin, thereby preventing cleavage of cohesin by separase, which in turn prevents anaphase onset during MI. By using a lower concentration of BI 2536, which was permissive for securin degradation, I unmasked a function for Plk1 in protecting centromeric cohesin during anaphase of MI. My findings indicate that loss of centromeric cohesin in the presence of BI 2536 is due to mislocalisation of the cohesin protector Sgo2. These data indicate that PLK1 kinase activity is essential for two key events required for normal segregation of chromosomes during MI.

In somatic cells, Plk1 is involved in removal of cohesin by the separase-independent prophase pathway, which removes the bulk of arm cohesin during prophase/prometaphase. My findings indicate that removal of cohesin during prophase is particularly relevant to the problem of female reproductive ageing. I show that age-related depletion of chromosomal cohesin occurs during the prolonged period of prophase arrest experienced by oocytes from older

females. I also find that the cohesin protector Sgo2 is not recruited to chromosomes until the transition from prophase to prometaphase of MI and that its recruitment is impaired in cohesin-deficient oocytes. Moreover, I present data indicating that removal of cohesin by a Plk1-mediated mechanism is unlikely to contribute to the age-related loss of cohesin during progression through prometaphase of MI.

Taken together the data indicate that Plk1 is essential for stepwise removal of cohesin in oocytes, but is not likely to be a major contributor to its loss during mammalian female ageing. Overall, these findings advance our understanding of the molecular mechanisms controlling chromosome segregation during meiosis I in mammalian oocytes, and how these are influenced by female reproductive ageing.

Acknowledgments

I would like to thank my supervisors Prof Mary Herbert and Dr Gordon Strathdee for their helpful advice and guidance throughout the duration of my research.

I am deeply grateful to all my colleagues in the lab, Rez "the biker" Prathalingham, Randy "the blocker" Ballesteros, Qi "the slipper" Zang, Laura "eee God" Irving, Lyndsey "the OCD hand-washer" Butterworth and Daniel "the rookie" Cooney for their support and the fun times inside and outside the lab.

I am particularly thankful to Lisa Lister for introducing me to the lab-world of meiosis, for being patient and for being an excellent collaborator in a number of experiments presented in this thesis.

Many thanks go to Tania Papoutsi and Morten Ritso for their friendly support and advice and to Eleni Filipou for nominating me as David Attenborough's successor.

A whole-hearted thank you to Alan Burns and Paul Hooley for being great lecturers and excellent mentors.

Ancora un passo più avanti Tonino. Facciamo come ci hanno insegnato ed Io ho avuto un grande maestro. Un abbraccio forte.

Στην αδερφή μου Σοφία και στους γονείς μου Βασιλική και Στέφανο το μόνο που μπορώ να πω είναι οτι χωρίς το κουράγιο σας, την συμπαράστασή σας και την αγάπη σας, τίποτα δεν θα ήταν το ίδιο.

Finally, I want to thank Marilena for keeping me clean, well-fed and sane throughout the 13th herculean labour known as PhD write-up.

CHAPTER 1 : INTRODUCTION 1

1.1 MEIOSIS, ANEUPLOIDY AND AGEING: AN OVERVIEW 1

1.2 MECHANISMS FOR SUCCESSFUL CHROMOSOME SEGREGATION 3

1.2.1 The Spindle 4

1.2.2 The Anaphase Promoting Complex / Cyclosome 6

1.2.3 The Spindle Assembly Checkpoint 8

1.2.4 Establishment and resolution of cohesion in mitosis 10

1.2.5 Establishment and resolution of cohesion in meiosis 14

1.3 DEVELOPMENT OF MAMMALIAN GERM CELLS 18

1.3.1 Oogenesis 18

1.3.2 Spermatogenesis 21

1.4 MEIOTIC MATURATION IN MOUSE OOCYTES 22

1.5 POLO-LIKE KINASE 1 23

1.6 FAILURE OF MEIOTIC DIVISION AND ASSOCIATED REPERCUSSIONS 29

1.7 AIMS 32

CHAPTER 2 : MATERIALS AND METHODS 33

2.1 MOUSE STRAINS 33

2.2 HARVEST, CULTURE AND DRUG TREATMENT OF MOUSE OOCYTES 33

2.3 ISOLATION OF OOCYTES FROM PRE-ANTRAL FOLLICLES 34

2.4 MICROINJECTION 35

2.5 OOCYTE IMMUNO-FLUORESCENCE STAINING 36

2.5.1 Whole oocyte Ca^{2+}-buffer treatment and fixation 36

2.5.2 Indirect immuno-fluorescence staining of whole oocytes 36

2.6 CHROMOSOME SPREADS THAT PRESERVE CHROMOSOME-ASSOCIATED PROTEINS 37

2.6.1 Paraformaldehyde and slide preparation 37

2.6.2 Removal of zona pellucida, fixation and spreading 38

2.6.3 Indirect immunofluorescence staining of chromosome spreads 38

2.7 FLUORESCENT CONSTRUCTS 39

2.8 PREPARATION OF MRNAS 41

2.9 MICROSCOPIC METHODS 41

2.9.1 Time-lapse (4D) Microscopy 41

2.9.2 Epifluorescence Imaging of Chromosome Spreads 42

2.9.3 Confocal Imaging 43

2.10 IMAGE PROCESSING AND QUANTIFICATION 43

2.10.1 Time-lapse 44

2.10.2 Chromosome spreads 44

2.10.3 Confocal 45

2.11 Statistical Analysis 45
2.12 Reagents 46

CHAPTER 3 . THE EFFECT OF FEMALE AGEING ON CHROMOSOMAL COHESIN IN OOCYTES 47

3.1 Introduction 47
3.2 Cohesin is depleted in oocytes of aged mice 48
3.3 Cohesin depletion in aged oocytes is linked with disruption of bivalent chromosome structure 48
3.4 Mechanisms of cohesin depletion and the role of Sgo2 52
3.4.1 Sgo2 levels are reduced in aged mouse oocytes 52
3.4.2 Sgo2 becomes enriched on chromosomes during the transition from prophase to metaphase of MI 53
3.4.3 Sgo2 levels are reduced in Smc1β$^{-/-}$ mouse oocytes 54
3.5 Discussion 56
3.5.1 Cohesin depletion in oocytes of aged mice 56
3.5.2 Female ageing is associated with loss of the closely apposed structure of sister kinetochores required for their monopolar attachment 59
3.5.3 The role of Sgo2 in cohesin depletion 60

CHAPTER 4 . CHARACTERISATION OF PLK1 MEDIATING CHROMOSOME SEGREGATION DURING MEIOSIS I OF THE MOUSE OOCYTE 62

4.1 Introduction 62
4.2 Plk1 is recruited to the kinetochore after release from prophase I arrest 63
4.3 BI 2536 does not prevent recruitment of Plk1 to the kinetochore during MI 66
4.4 BI 2536 does not affect the timing of entry into prometaphase of MI in mouse oocytes 67
4.4.1 Effect on the timing of GVBD with short exposure to BI 2536 67
4.4.2 Effect on the timing of GVBD with prolonged exposure to BI 2536 67
4.5 BI 2536 inhibits exit from MI in a dose-dependent manner 70
4.5 Oocytes arrested in MI in the presence of BI 2536 do not undergo anaphase. 71
4.5.1 BI 2536 increases inter-centromere distance during prometaphase of MI 73
4.5.2 BI 2536 increases the number of erroneous Kt-Mt attachments at prometaphase of MI 75
4.6 Plk1 is required for efficient activation of APC/C^{Cdc20} during exit from MI. 78
4.6.1 BI 2536 inhibits securin degradation in MI. 78
4.6.1 BI 2536 inhibits the activation of APC/C^{Cdc20} in MI. 81
4.6.2 Exogenous cyclin B1 relieves inhibition of securin degradation in the presence of BI 2536. 85

4.7 Discussion 87
4.7.1 Plk1 is recruited to the kinetochore of meiotic chromosomes 87
4.7.2 BI 2536 does not affect the timing of entry into prometaphase of MI, but prevents initiation of anaphase of MI in a dose-dependent manner 88
4.7.3 BI 2536 inhibits anaphase of MI, disrupts sister-centromere integrity and promotes misalignment of bivalents. 89
4.7.4 Plk1 prevents degradation of exogenous securin and is required for efficient activation of APC/C^{cdc20} in MI 90

CHAPTER 5 . PLK1 IS REQUIRED FOR STEPWISE REMOVAL OF COHESIN IN MOUSE MEIOSIS 94

5.1 Introduction 94
5.2 Securin profile of oocytes that exit MI in the precence of BI 2536 96
5.3 BI 2536 promotes separation sister chromatids in a dose-dependent manner 98
5.4 Post-PBE treatment with BI 2536 does induce premature separation of sister chromatids 100
5.5 Centromeric cohesin is not depleted during in BI 2536-treated oocytes. 102
5.6 BI 2536 compromises the centromeric localisation of Sgo2-PP2A at late prometaphase of MI 104
5.7 BI 2536 does not affect the levels of chromosome-associated cohesin during prometaphase of MI. 107
5.8 Discussion 110
5.8.1 The role of Plk1 in the protection of centromeric cohesion 110
5.8.2 No evidence of prophase pathway-like activity in MI 114

CHAPTER 6 . CONCLUSION & FUTURE DIRECTIONS 117

6.1 Cohesin and female reproductive ageing 117
6.2 Plk1 function in mouse oocytes and its association with cohesin 119
6.3 Clinical Relevance 121
Abbreviations 122
References 124

List of Figures and Tables

Figure 1.1 Incidence of trisomy in relation to maternal age. 2
Figure 1.2 Regulation of the APC/C by the SAC 10
Figure 1.3 Chromosome segregation during Mitosis and Meiosis 12
Figure 1.4 The cohesin complex 13
Figure 1.5 Protection of centromeric cohesin by shugoshin-PP2A in mitosis and meiosis. 15
Figure 1.6 The development of human germ cells 20
Figure 1.7 Meiosis in mouse oocytes 21
Figure 1.8 Plk1 structure and functions in mitosis and meiosis 27
Figure 2.1 Schematic representation of the constructs made using a pRN3 vector backbone 40
Figure 2.2 Conserved domains and motifs of Cdc20 40
Figure 3.1 Cohesin depletion in oocytes of aged mice. 49
Figure 3.2 Reduced cohesin is associated with splitting of sister centromeres 51
Figure 3.3 Age-related decline in chromosome-associated Sgo2 levels 53
Figure 3.4 Localisation of Sgo2 in GV-stage mouse oocytes 54
Figure 3.5 Reduced levels of chromosome-associated Sgo2 in *Smc1β*$^{-/-}$ mouse oocytes 55
Figure 4.1 Experimental design. 64
Figure 4.2 Plk1 is enriched at the centromere upon meiotic resumption. 65
Figure 4.3 BI 2536 does not prevent recruitment of Plk1 to the kinetochore during MI. 66
Figure 4.4 BI 2536 does not affect the timing of entry into prometaphase of MI 69
Figure 4.5 BI 2536 inhibits exit from MI in a dose-dependent manner 71
Figure 4.6 BI 2536 inhibits anaphase I 72
Figure 4.7 BI 2536 increases inter-centromere distance in prometaphase of MI 74
Figure 4.8 BI 2536 increases the frequency of erroneous Kt-Mt attachments at late prometaphase of MI. 77
Figure 4.9 BI 2536 inhibits the degradation of securin in late metaphase of MI 80
Figure 4.10 Cdc20^{R132A} allows degradation of securin in the presence of nocodazole. 83
Figure 4.11 BI 2536 inhibits degradation of securin in Cdc20^{R132A}-injected oocytes in the presence of nocodazole. 84
Figure 4.12 Exogenous cyclin B1 relieves inhibition of securin degradation in the presence of BI 2536. 86

Figure 5.1 Degradation of securin-YFP during exit from MI in the presence of low concentrations (6.25 nM) of BI 2536 97
Figure 5.2 Sister chromatid separation in the presence of BI 2536 99
Figure 5.3 BI 2536 does not induce premature separation of sisters during MetII arrest 101
Figure 5.4 Effect of BI 2536 on inter-centromere distance and centromeric cohesin in Rec8-myc oocytes 103
Figure 5.5 The effect of BI 2536 on centromeric localisation of Sgo2-PP2A in late prometaphase of MI 106
Figure 5.6 The effect of BI 2536 on chromosome-associated cohesin levels in late prometaphase I 109

Table 2.1 Antibodies used for immunofluorescence staining 37

Chapter 1 : Introduction

1.1 Meiosis, aneuploidy and ageing: an overview

Sexual reproduction is a means for the continuation of most eukaryotic species and in the same time the pinnacle of their evolutionary course in life. Sexual reproduction requires the fusion of two gametes, the specialised reproductive cells, one from each parent, which produces a single cell, the zygote, from which the new organism develops. To prevent duplication of the genomic material at each generation, sexual reproduction relies on a specialised form of cellular division, known as meiosis, which as the name implies in Greek (μείωσης), it reduces the genomic material of gametes by half. In diploid organisms, such as mammals, meiosis gives rise to haploid gametes via two sequential rounds of chromosome segregation – meiosis I (MI) and meiosis II (MII) – without an intervening round of DNA replication. MI is the reductional part of the meiotic programme, during which the recombinant paternal and maternal homologous chromosomes are segregated into two different cells. MII is the equational part, where sister-chromatid pairs are segregated by mechanisms that are almost similar to those used in mitotic division of somatic cells (Petronczki *et al.*, 2003; Marston and Amon, 2004).

As with every physiological process, cell division can fail. Deregulation of the mitotic programme has been identified as the malignant factor of a significant number of solid human cancers (Nakayama and Nakayama, 2006) and has been associated with neurodegenerative diseases, such as Alzheimer's (Aulia and Tang, 2006). In most sexually reproducing organisms, meiotic errors are rare. However, in humans they appear to be more common and lead to the generation of gametes carrying an abnormal number of chromosomes, known as aneuploid gametes. Such abnormal gametes can give rise to embryos, which generally are non-viable and account for almost 50% of miscarriages occurring during the first semester of pregnancy (Suzumori *et al.*, 2010). The few

aneuploid zygotes that are viable produce progeny with genetic birth defects, most common being the Down syndrome (trisomy 21).

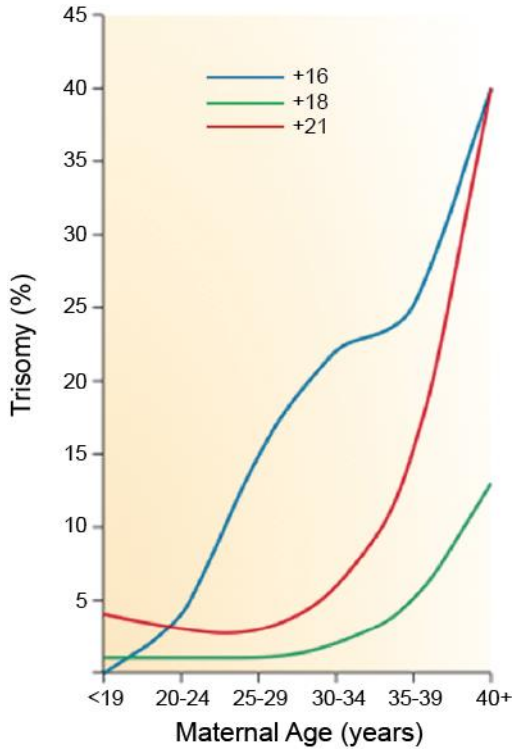

Figure 1.1 Incidence of trisomy in relation to maternal age.
A graphical representation of the percentage of clinically recognized trisomic pregnancies in relation to maternal age. The risk for a trisomic pregnancy is exponentially increased after the late 30s for both trisomies 18 (green) and 21 (red), whereas for trisomy 16 (blue) it increases in an almost linear manner [modified from (Nagaoka *et al.*, 2012)].

The majority of embryonic aneuploidies originate from the oocyte, rather than the sperm, and in particular from segregation errors during MI (Hassold and Hunt, 2001). More importantly, it appears that the frequency of meiotic errors increases rapidly as women age. Indeed, the probability of a trisomic pregnancy is known to reach 35% at the age of forty, from a mere 2% for a woman in her early twenties (Fig. 1.1) (Hunt and Hassold, 2010). Given that, if we also consider that it has become more commonplace for modern women to postpone childbirth, it would be easy to understand why in the last twenty years the incidence of Down syndrome pregnancies has increased by 71% in the UK (Morris and Alberman, 2009). The link between aneuploidies and ageing is most likely related to the extended meiotic arrest that occurs during mammalian female meiosis. As I will explain in more detail later, oocytes enter

meiosis during foetal development and remain arrested at MI until ovulation is triggered. In humans this state of limbo may last more than 40 years.

Whilst the phenomenon of age-related aneuploidies has been well established, the meiotic programme is so intricate that the molecular basis of segregation errors is not yet well defined. In this otherwise magically tuned and flawlessly orchestrated dance of chromosomes that takes place on the meiotic stage, there has to be at least one culprit responsible for the aneuploid confusion in the grand finale. Like a passionate lover of the theatre of life, this thesis sets out to uncover this felon.

1.2 Mechanisms for successful chromosome segregation

Chromosome segregation is essentially a mechanical process involving a structural lattice of microtubules (Mts) known as the spindle, which segregate chromosomes under the control of biochemical signals. The biochemical signals are largely generated from the kinetochore (Kt), a complex assembly of proteins at the primary constriction (centromere), which forms the attachment site between chromosomes and the Mts of the spindle. The biochemical signals generated from unattached Kts act as a surveillance mechanism known as the spindle assembly checkpoint (SAC). The SAC monitors the attachment of the spindle to all Kts, thereby ensuring the genomic material will be accurately segregated between daughter cells upon the onset of anaphase (Musacchio and Salmon, 2007). Most importantly, during mitosis, sister chromatids need to be tightly aligned on the metaphase plate (spindle equator) and establish correctly oriented attachments with the spindle microtubules. In order to accomplish that sister chromatids are held together by sister chromatid cohesion, which is mediated by protein complexes known as cohesins (Nasmyth and Haering, 2009) . Upon SAC satisfaction and the onset of anaphase, chromosome disjunction is triggered through the cleavage of cohesin by a protease known as separase (Uhlmann *et al.*, 2000; Waizenegger *et al.*, 2000). Until that point and

for most of the cell cycle, separase is kept inactive by being sequestered by an inhibitory chaperon known as securin and through phosphorylation by Cdk1/cyclin B (Yamamoto *et al.*, 1996; Stemmann *et al.*, 2001a). Activation of separase is achieved when all chromosomes have bioriented, through the ubiquitination of securin and cyclin B by the anaphase-promoting complex or cyclosome (APC/C) and their subsequent degradation by the proteasome [reviewed by (Peters, 2006)].

1.2.1 The Spindle

The spindle is a complex, highly dynamic structure made up off tubulin polymers (microtubules) and microtubule-associated proteins, such as molecular motors that use chemical energy to perform mechanical labour. The meiotic spindle in mammalian oocytes differs from the somatic cell mitotic spindle in several aspects. In somatic cells spindle positioning is mediated by astral microtubules in both symmetric and asymmetric divisions, whereas astral microtubules are absent in meiosis and the spindle is asymmetrically positioned through the action of the actin-filament network (Verlhac *et al.*, 2000; Schuh and Ellenberg, 2008). Another major difference is that mammalian oocytes do not have "traditional" centrosomes, as they lack centriole pairs. Instead, microtubule nucleation and coordination is performed by microtubule organising centres (MTOCs), which undergo a striking cell-cycle dependent remodeling (Maro *et al.*, 1985; Messinger and Albertini, 1991). As discussed below, recent 3D live-cell (4D) imaging studies have verified the significance of MTOCs in the assembly of the meiotic spindle and have provided a unique insight into spindle-chromosome interactions during meiotic maturation (Schuh and Ellenberg, 2007; Kitajima *et al.*, 2011).

The first phenotypical hallmark of meiosis I resumption is germinal vesicle breakdown (GVBD), the equivalent of nuclear envelope breakdown (NEB) in somatic cells. Before GVBD, chromosomes are partially condensed around the

nucleolus, although not to an extent where homologue pairs can be microscopically distinguished. In a study by Schuh and Ellenberg, the authors have used 4D confocal fluorescence microscopy to quantitatively analyse the functional dynamics of single MTOCs, bivalent chromosomes, and microtubule plus ends during meiosis I spindle assembly at high spatial and temporal resolution (Schuh and Ellenberg, 2007). According to this study, in mice, the first few hours following GVBD chromosomes condense further and a bipolar spindle is gradually formed through the coalescence of MTOCs. Approximately 80 MTOCs, which form during prophase from a network of cytoplasmic microtubules, migrate to the centre of the oocyte and gradually merge from a multipolar spindle into a bipolar spindle that elongates and captures the condensed chromosomes. During most of prometaphase I, chromosome movement is performed by microtubules associated with chromosome arms. Finally, at 4 hours after GVBD, at metaphase of MI, chromosomes appear to have aligned on the metaphase plate of a centrally localized, barrel-shaped spindle structure. Interestingly, the bipolar meiosis I spindle appears to form due to the actions of MTOCs, rather than due to any chromosome-induced effect (Brunet *et al.*, 1998; Schuh and Ellenberg, 2007). Moreover, stable end-on Kt-Mt interactions appear to be established just a short time prior to anaphase (Brunet *et al.*, 1999; Schuh and Ellenberg, 2007).

In another study, Kitajima and Ellenberg have performed 4D confocal fluorescence imaging of meiosis I in mouse oocytes expressing kinetochore proteins fused to GFP (Kitajima *et al.*, 2011). Using a kinetochore tracking approach, where distances between centromeres in paired homologues were monitored, the authors reported that chromosomes form an intermediate configuration, the prometaphase belt; initially, condensing chromosomes arrange as a spherical shell around microtubules and then congress and become gradually ordered to form a ring structure in the equatorial region surrounding microtubules. A similar phenomenon has also been observed during mitosis

(Magidson *et al.*, 2011). Next, chromosomes invade the elongating spindle structure centre, align on the metaphase plate and gradually become bi-oriented. Furthermore, it was shown that multiple Kt-Mt attachment attempts are required to achieve biorientation of homologous chromosomes in late metaphase I and that Aurora B kinase is essential for the correction of erroneous Kt-Mt attachments. This finding is of particular interest, given the high incidence of aneuploidies of mammalian oocytes, due to meiosis I chromosome segregation errors.

1.2.2 The Anaphase Promoting Complex / Cyclosome

Under physiological conditions, the cell cycle comprises a predefined sequence of irreversible biochemical phenomena. One of the ways that this irreversible character is established is through the proteolytic degradation of the proteins that regulate the transitions along the stages of the cell cycle. The leading cellular mechanism that controls proteolysis is the process of ubiquitination (Hershko, 2005). The APC/C is a major component of this mechanism; therefore its activity is intimately associated with the progress of the cell cycle.

The APC/C is composed of 11-13 different subunits most of which have been conserved from yeast to animal cells (Baker *et al.*, 2007). Phosphorylation of these subunits at multiple sites is also required for APC/C activation (Pines, 2006). The functions of most other APC/C subunits is not clear, and although it has been suggested that some of them may play a more essential role in meiosis than in mitosis, the question why APC/C is so complex still remains open.

Another fact that underlines the highly important role of APC/C is that its activity is finely tuned by a complex system of kinases, activators and inhibitors. Activators are essential for APC/C activity, bind to it at different times during mitosis/meiosis and control its substrate specificity. Two activators, Cdc20 and Cdh1 which belong to the family of WD40 proteins, give

rise to APC/C^{Cdc20} and APC/C^{Cdh1} respectively, and are of particular importance. Other activators include Mfr1 and Ama1 (in yeast) and Fzr2 and Cortex (in *Drosophila*), which are meiosis-specific and their functions have not been fully understood (Acquaviva and Pines, 2006). APC/C inhibitors include the mitotic checkpoint complex (MCC), the early mitotic inhibitor 1 (Emi1) and its homologue Emi2/XErp1, the tumour suppressor Ras association domain family 1 (Rassf1A), the APC/C^{Cdh1} modulator 1 (Acm1), the nuclear transport factors Nup98 and Rae1, and Mes1 (Pesin and Orr-Weaver, 2008). Most of these inhibitors act by directly binding activators, thus restricting APC/C activation.

In addition to the well investigated mechanism of modulation of APC/C activity through control of Cdh1 and Cdc20 levels, there is evidence that APC/C activity is also regulated by direct phosphorylation. A number of kinases, including Cdk1/cyclin B, Polo-like kinase 1 (Plk1) and protein kinase A (PKA) are known to regulate APC/C function through the phosphorylation of numerous residues (Kraft *et al.*, 2003; Baker *et al.*, 2007). Once somatic cells have entered mitosis, the APC/C is partially activated by Cdk1/cyclin-dependent phosphorylation (Rudner and Murray, 2000; Kraft *et al.*, 2003). In particular, B-type cyclins phosphorylate numerous APC/C subunits, thereby increasing the affinity of Cdc20 to the APC/C (Shteinberg *et al.*, 1999; Rudner *et al.*, 2000; Rudner and Murray, 2000; Kraft *et al.*, 2003). In *S. cerevisiae*, phosphorylation by Cdk1/cyclin B has been reported to determine APC/C activator-binding specificity, thus promoting Cdc20 binding during mitosis and Cdh1 binding during mitotic exit and interphase. Indeed, mutating the Cdk1/cyclin B phosphorylation sites on the APC/C promotes Cdh1 binding during mitosis, instead of Cdc20 (Cross, 2003).

Nevertheless, it is still unclear whether Cdk1/cyclin-dependent phosphorylation is the sole mechanism of APC/C activation in mitosis. Early studies have shown that APC/C activation may require phosphorylation by

Plk1 (Kotani *et al.*, 1998). Moreover, the APC/C inhibitor Emi1 has been proposed to be targeted for degradation by the $SCF^{\beta TrCP}$ once phosphorylated by Plk1 (Reimann *et al.*, 2001a; Hansen *et al.*, 2004; Moshe *et al.*, 2004). However, recent studies have shown that in the presence of a non-degradable form of Emi1 (Di Fiore and Pines, 2007), or with chemical Plk1-inhibition (Lenart *et al.*, 2007), the activation of APC/C is not obstructed.

Although it is still unclear which characteristics of a target protein allow its recognition by the ACP/C complex, it has been shown that the target proteins contain specific sequence motifs, known as degradation motifs (or degrons), which are necessary for their ubiquitination. One important motif is RxxLxxxxN (R for arginine; X any amino-acid; L for leucine; N for asparagine), which is known as the destruction box (D-box) (Prinz *et al.*, 1998). Another motif is KENxxxN (K for lysine; E for glutamate) which is given the name KEN-box (Pfleger and Kirschner, 2000). The KEN-box is preferentially recognised by ACP/C^{Cdh1}, whereas ACP/C^{Cdc20} can recognise only the D-box. Other degrons, such as the A-box, the O-box and the CRY-box have also been described [reviewed in (Barford, 2011)].

1.2.3 The Spindle Assembly Checkpoint

During mitosis separase activity is highly regulated by the inhibitory binding of securin (Yamamoto *et al.*, 1996) and the Cdk1/cyclin B complex (Stemmann *et al.*, 2001b; Gorr *et al.*, 2005). The APC/C together with its activator Cdc20, promotes the ubiquitination and subsequent degradation of securin and cyclin B, thus promoting separase activation (Fig 1.2). However, before APC/C^{Cdc20} can degrade its substrates to promote anaphase, the SAC has to be satisfied. In general, this is achieved through the activity of the MCC, a complex comprising the conserved checkpoint proteins Mad2, Bub3, BubR1 and Cdc20, which inhibits APC/C^{Cdc20} from targeting cyclin B and securin for degradation [reviewed in (Musacchio and Salmon, 2007)] (Fig 1.2). The exact mechanism of

inhibition has not been fully unveiled yet and recent evidence suggests that different inhibitory protein complexes may operate during the SAC in different organisms and that the MCC is just a transient step in the activation of the SAC (Eytan *et al.*, 2008; Nilsson *et al.*, 2008; Kulukian *et al.*, 2009).

Although the SAC is the principal regulatory mechanism of APC/C activity during mitosis [reviewed in (Nasmyth, 2005; Musacchio and Salmon, 2007)], in meiosis its role still remains controversial. Studies focusing on SAC function in vertebrate oocytes have proven it to be present and active. Preliminary experiments using XO mice (mice carrying a single X chromosome), suggested that the vertebrate meiotic SAC was inefficient in detecting misaligned chromosomes (LeMaire-Adkins *et al.*, 1997). However, later evidence showed that biorientation of sister chromatids, instead of bivalents, is probably the reason XO oocytes evade the SAC (Kouznetsova *et al.*, 2007). Mad2, Bub1 and BubR1 are present in vertebrate oocytes and perturbation or loss of their function leads to premature resolution of chiasmata, failure to biorient bivalents, premature onset of anaphase and chromosome missegregation in MI (Wassmann *et al.*, 2003; Zhang *et al.*, 2004; Homer *et al.*, 2005a; Homer *et al.*, 2005b; Niault *et al.*, 2007; Homer *et al.*, 2009a; McGuinness *et al.*, 2009). In contrast to mitosis, where the presence of a single unattached kinetochore effectively inhibits anaphase (Rieder *et al.*, 1994; Rieder *et al.*, 1995), in MI the SAC appears to be notoriously error-prone (Hassold and Hunt, 2009) and various hypotheses have been proposed to explain this paradox (Hoffmann *et al.*, 2011; Nagaoka *et al.*, 2011; Gui and Homer, 2012; Lane *et al.*, 2012).

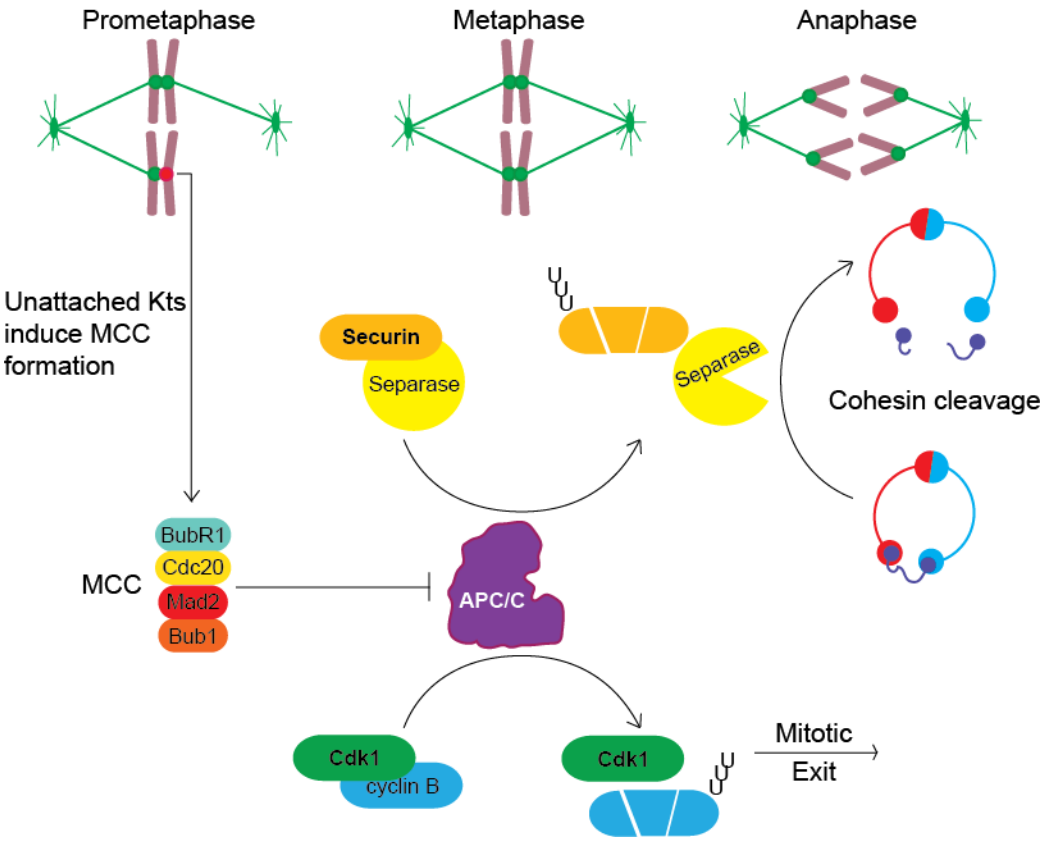

Figure 1.2 Regulation of the APC/C by the SAC

During early mitosis unattached kinetochores (Kts) promote the formation of the mitotic checkpoint complex (MCC), which consists of BubR1, Cdc20, Mad2 and Bub1. The MCC leads to inhibition of the APC/C by sequestering its activator Cdc20. Once all Kts establish end-on attachments with spindle microtubules and align on the metaphase plane, Cdc20 is released and activates the APC/C, which ubiquitinates securin and cyclin B, thereby tagging them for degradation by the 26S proteasome. Degradation of securin releases separase, which cleaves cohesin and allows anaphase to occur. Cyclin B degradation inactivates Cdk1, thus leading to exit from mitosis.

1.2.4 Establishment and resolution of cohesion in mitosis

Mitosis is a complex process during which the duplicated genome coming from the S-phase (DNA replication) is equationally segregated into two new daughter nuclei (Fig. 1.3.A). Following mitosis, the cell divides by cytokinesis to produce two daughter cells with identical genomes. This process is repeated in mammalian somatic cells contributing to the growth, development and maintenance of the organism.

During mitosis, sister chromatid cohesion is mediated by the multi-subunit cohesin complex (Fig. 1.4). Cohesin was first identified in *Saccharomyces*

cereviciae (Guacci *et al.*, 1997; Michaelis *et al.*, 1997; Toth *et al.*, 1999) and was found to comprise of four core subunits: two subunits of the structural maintenance of chromosomes (SMC) protein family, Smc1 (also known as Smc1α in vertebrates) and Smc3; the kleisin family protein Scc1/Rad21; and an accessory subunit Scc3. According to the currently prevalent model, cohesin fulfills its role by forming a ring-like structure which encircles sister chromatids (Fig 1.4) (Gruber *et al.*, 2003; Uhlmann, 2004; Nasmyth and Haering, 2005; Nasmyth, 2011). Cohesin protein subunits are highly conserved among eukaryotes, from yeasts to vertebrates. In vertebrates two isoforms of Scc3 are expressed and are known as SA1 and SA2 (Losada *et al.*, 2000). The important role of cohesin subunits has been underscored in various experiments, where their depletion leads to chromosome segregation errors and increased levels of aneuploidy (Sonoda *et al.*, 2001; Hoque and Ishikawa, 2002).

Cohesin is recruited to chromosomes before S-phase, a process mediated by the Scc2/Scc4 cohesin-loading complex (Ciosk *et al.*, 2000; Tomonaga *et al.*, 2000), and appears to be enriched around the centromeres and at several sites along chromosome arms (Blat and Kleckner, 1999; Tanaka *et al.*, 1999). During S-phase, other factors including Ctf4, Ctf18 and the acetyl-transferase Eco1 facilitate the cohesin-dependent pairing of the emerging sister chromatids (Toth *et al.*, 1999) and consistently colocalise with DNA replication forks (Lengronne *et al.*, 2006). In fission yeast and mammals, the heterochromatin protein HP1/Swi6 facilitates the enrichment of cohesin at pericentromeric regions suggesting that the establishment of strong centromeric cohesion to counteract the pulling forces of spindle microtubules is of outmost importance, as this mechanical phenomenon essentially ensures the bipolar attachment of chromosomes (Pidoux and Allshire, 2004).

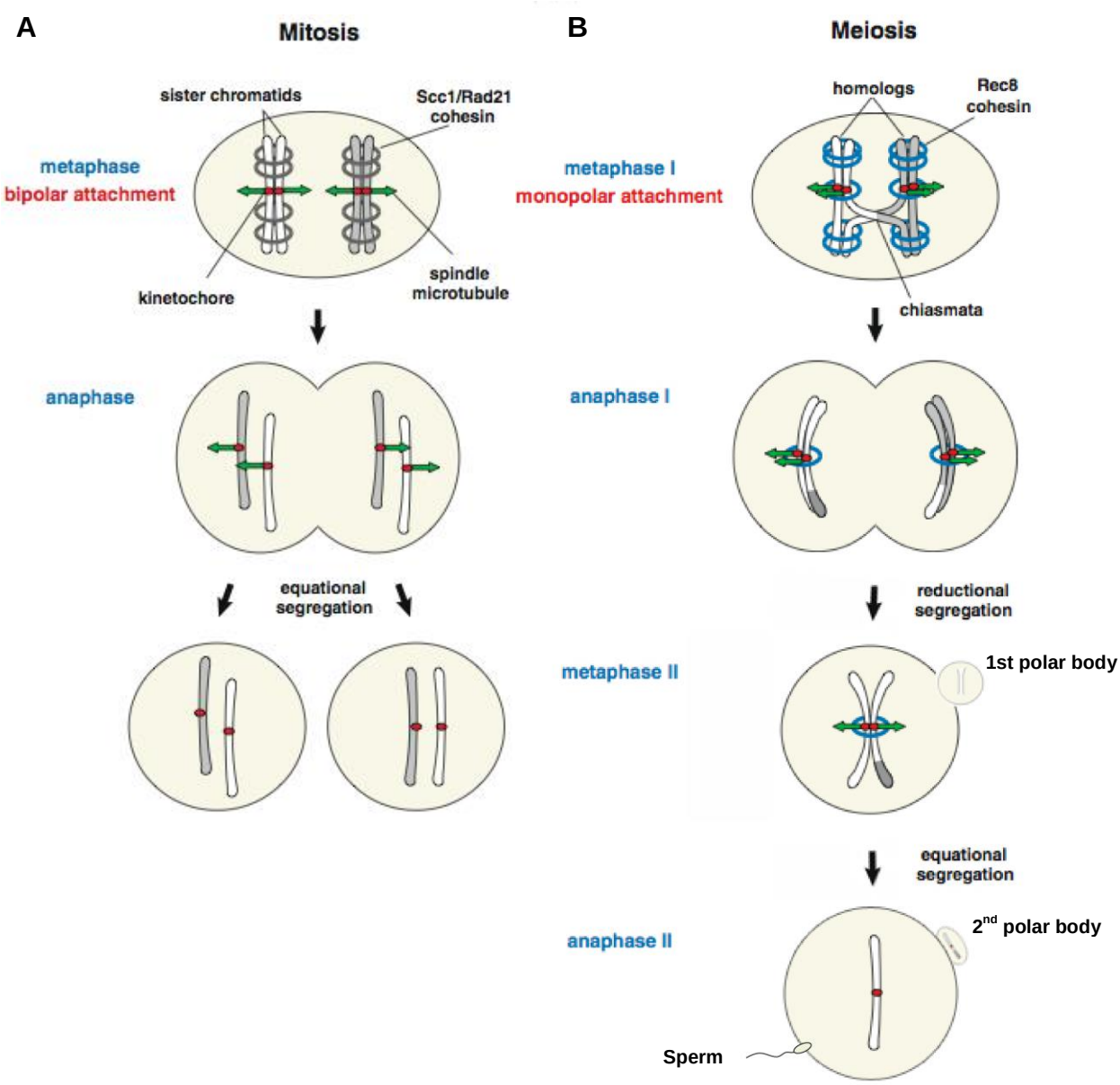

Figure 1.3 Chromosome segregation during Mitosis and Meiosis

A simplified schematic representation of chromosome segregation in mitosis and meiosis: **(A)** In vertebrate somatic mitosis, sister kinetochores are attached to spindle microtubules emanating from opposite poles. Prior to anaphase, sister chromatid cohesion mediated by Scc1/Rad21-cohesin is removed, allowing sister chromatid separation. **(B)** In mammalian female meiosis, the Scc1/Rad21 subunit is replaced by Rec8. During prometaphase I, sister kinetochores of recombined homologues attach to spindle microtubules emanating from the same pole. Cleavage of chromosome-arm cohesin allows separation of homologues, with one of them being extruded within the 1st polar body. Upon fertilisation, centromeric cohesin is removed and sister chromatids separate as in mitosis, with one sister chromatid being extruded within the 2nd polar body [modified from (Sakuno and Watanabe, 2009)].

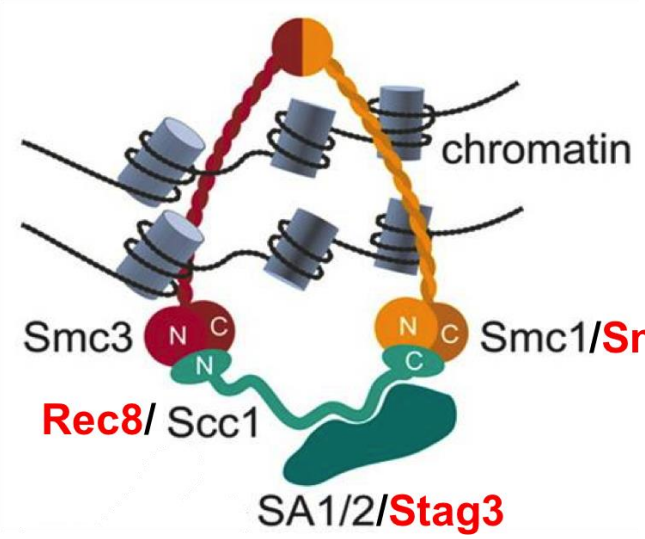

Figure 1.4 The cohesin complex

In somatic vertebrate cells, the cohesin core complex consists of the subunits Smc1, Smc3, Scc1, and either SA1 or SA2. In mammalian meiosis the synthesis of cohesin alters, with Scc1 being substituted by Rec8 or Rad21L, Smc1 by Smc1β and SA1/2 by SA3/Stag3. According to the "ring" model, cohesin mediates SCC by forming a tripartite ring that entraps sister chromatids [modified from (Peters *et al.*, 2008)].

In order for sister chromatids to separate during anaphase, cohesin needs to be removed (Fig 1.5). In yeast, a specific protease known as separase (Esp1 in *S. cerevisiae*, Cut1 in *S. pombe*) is activated at the onset of anaphase and cleaves the Scc1/Rad21 subunit, thus breaking open the cohesin ring and allowing sister chromatids to be pulled apart (Uhlmann *et al.*, 1999; Uhlmann *et al.*, 2000; Uhlmann, 2003). In vertebrates, however, the bulk of cohesin is removed from chromosome arms during prophase prior to separase activation, via a process known as the "prophase pathway" (Losada *et al.*, 1998; Sumara *et al.*, 2002). This process does not require the cleavage of Scc1/Rad21 by separase, as cohesin dissociation is achieved through phosphorylation of SA1/2 by Polo-like kinase 1(Plk1) mediated by Aurora B (Hauf *et al.*, 2005) and Wapl (Gandhi *et al.*, 2006; Kueng *et al.*, 2006). During this process, centromeric cohesin is protected by the protein shugoshin (Sgo; Japanese 守護神 for "guardian spirit"), which together with protein phosphatase 2A (PP2A) counteract cohesin phosphorylation until the onset of anaphase (Katis *et al.*, 2004; McGuinness *et al.*, 2005; Kitajima *et al.*, 2006; Riedel *et al.*, 2006). Once the cell reaches the metaphase-anaphase

transition, separase is activated to cleave the remainder centromeric cohesin and allow sister chromatid segregation.

1.2.5 Establishment and resolution of cohesion in meiosis

Meiotic division (Fig. 1.3.B) is fundamental for the production of functional gametes and is a much more intricate and specialised programme than mitosis. Its level of complexity is well reflected by the increased levels of cohesin regulation through the activity of both mitotic and meiosis-specific mechanisms.

As in mitosis, meiotic cohesion is established during the pre-meiotic S-phase, however meiosis-specific cohesin subunits are also employed. In budding yeast, fission yeast and mammals, Scc1/Rad21 is largely replaced by its meiotic counterpart Rec8 (Klein *et al.*, 1999; Watanabe and Nurse, 1999; Pasierbek *et al.*, 2001) and the mammal-specific Rad21L (Gutierrez-Caballero *et al.*, 2011; Herran *et al.*, 2011; Ishiguro *et al.*, 2011; Lee and Hirano, 2011). In mammalian germ cells further alterations include the replacement of SA1/2 by SA3/STAG3 (Pezzi *et al.*, 2000; Prieto *et al.*, 2001), and Smc1α by Smc1β (Revenkova *et al.*, 2001). Various localization studies on these meiosis-specific cohesin variants have revealed differential chromosome distribution patterns throughout meiosis (Prieto *et al.*, 2004; Revenkova and Jessberger, 2005; Sakuno and Watanabe, 2009; Jessberger, 2011), suggesting that different cohesin complexes might have unique functions. However, across all organisms Rec8 appears to play a predominantly significant role. Whereas Rad21L is not detectable in metaphase I oocytes (Ishiguro *et al.*, 2011), Rec8 is recruited earlier than other cohesin subunits, is removed later from chromosome arms in MI and remains at the core centromeric regions until the metaphase-anaphase II transition (Fig. 1.5) (Eijpe *et al.*, 2003). In addition, various experiments involving RNAi depletion of Rec8 and Rec8 mutations have revealed several effects including premature loss of cohesion, reduction or failure of recombination and increased aneuploidy and

infertility (Klein *et al.*, 1999; Watanabe and Nurse, 1999; Pasierbek *et al.*, 2001; Xu *et al.*, 2005).

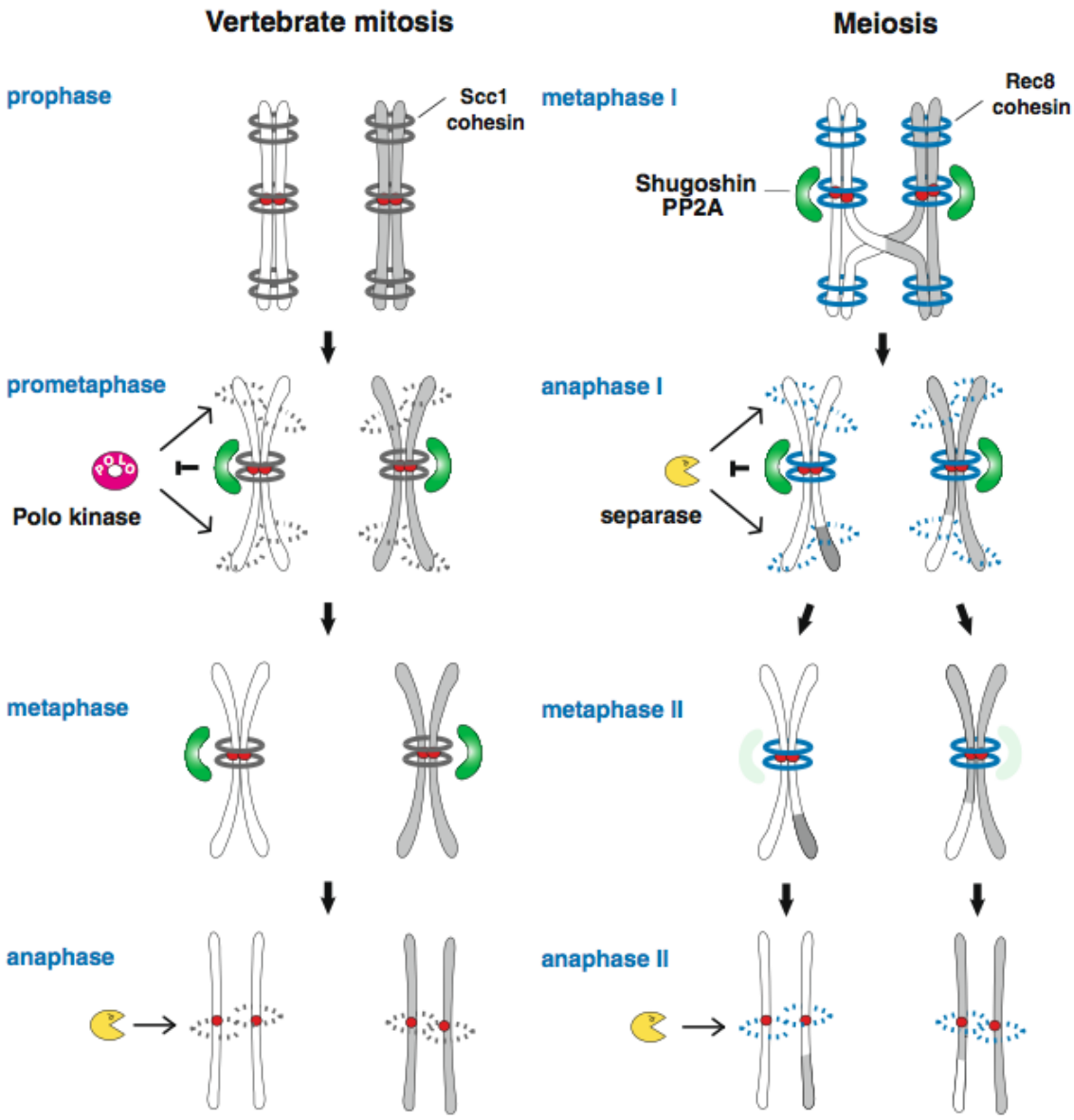

Figure 1.5 Protection of centromeric cohesin by shugoshin-PP2A in mitosis and meiosis.

During prometaphase of vertebrate meiosis, cohesin is removed from chromosome arms via Plk1-mediated phosphorylation. This mechanism is known as the "prophase pathway". The shugoshin-PP2A complex protects pericentromeric cohesin until the onset of anaphase, when it is removed to allow the cleavage of cohesin by separase. In meiosis, during anaphase I, shugoshin-PP2A protects centromeric cohesin from cleavage by separase, until metaphase II, thus allowing accurate segregation of homologous chromosomes. With the onset of anaphase II, protection is removed and sister chromatids are separated into individual gametes [adapted from (Sakuno and Watanabe, 2009)].

One of the issues in meiosis is that segregation of the genomic material has to occur twice, without being interrupted by an S-phase. This is essential for haploid gametes to be generated. This scenario requires that homologous chromosome pairs (bivalents) and sister chromatids must be segregated separately in MI (reductional segregation) and MII (equational segregation), respectively, thereby imposing specific adaptations to the meiotic process.

As with sister chromatids, the pairs of homologous chromosomes must be somehow bonded to establish tension between them to counteract the pulling force of spindle microtubules. The establishment of physical linkages between paternal and maternal homologues occurs during early meiotic prophase, and is known as meiotic recombination or crossover formation, which involves reciprocal exchange of DNA between non-sister chromatids (Kleckner, 2006). Following crossover formation the physical linkages between recombined homologues become visible at cytologically distinct structures known as chiasmata. However, chiasmata hold homologues together in MI only because they are stabilized by sister chromatid cohesion on chromosome arms, distal to the chiasmata (Moore and Orr-Weaver, 1998; Petronczki *et al.*, 2003). Furthermore, studies on Rec8 and Smc1β deficient mice have shown that these proteins are involved in meiotic recombination and stabilisation of chiasmata (Bannister *et al.*, 2004; Revenkova *et al.*, 2004; Xu *et al.*, 2005).

Proper homologue segregation during MI means that sister chromatids need to attach to microtubules that will pull them towards the same spindle pole. This is known as monopolar kinetochore-microtubule attachment of sister chromatids (Fig. 1.3.B) (Hauf and Watanabe, 2004; Brar and Amon, 2008) and depends on sister centromeres being closely apposed. In this case, centromeric cohesin is responsible for keeping sister centromeres tightly bound. In yeast, proteins known as monopolins have also been shown to be essential for monopolar attachment (Toth *et al.*, 2000; Yokobayashi and Watanabe, 2005).

Finally, cohesin on chromosome arms of sister chromatids must be cleaved for MI to occur, whereas centromeric cohesin must remain intact until the onset of anaphase II, as it is essential for biorientation of sister chromatids before anaphase of MII. In both MI and MII, segregation is achieved by the breakdown of cohesin complexes through the same mechanism that has been described in mitosis, involving APC/C-dependent activation of separase (Buonomo *et al.*, 2000; Kudo *et al.*, 2006). However, to achieve chromosome arm-specific loss of sister chromatid cohesion in meiosis I, centromeric cohesin is protected from cleavage by either of two shugoshin isoforms, Sgo1 and Sgo2 (paralogs of MEI-S332 in Drosophila melanogaster) (Kitajima *et al.*, 2004). This allows homologues to separate, while sister chromatids remain attached together (Fig. 1.5). In MII, protection is removed from the centromeres and separase is able to cleave cohesin and promote the segregation of sister chromatids (Watanabe, 2005). *S. cerevisiae* and *D. melanogaster* have only one known shugoshin (Sgo1 and MEI-S332, respectively), whereas *S. pompe*, *Xenopus laevis* and mammals have two (Sgo1/SGOL1 and Sgo2/SGOL2) (Gutierrez-Caballero *et al.*, 2012). Although shugoshins are considered orthologs, they share little sequence homology and exhibit divergence in their functions among different species. For example, whereas Sgo1 is considered to be the guardian of meiotic centromere cohesion in yeast (Kitajima *et al.*, 2004) and flies (Kerrebrock *et al.*, 1995), resent studies have shown that in mammals Sgo2 is solely responsible and Sgo1 dispensable for protection of centromeric cohesin during meiosis (Lee *et al.*, 2008; Llano *et al.*, 2008).

It is evident that cohesin is a key component of all the fundamental meiotic mechanisms described above. Consequently, it is easy to understand why cohesin-related anomalies can cause chromosome missegregation and thus aneuploidy. In other words, accurate regulation of the cohesin complex is one

of the most central features of faithful chromosome segregation therefore it is important to understand the precise molecular mechanisms that surround it.

1.3 Development of mammalian germ cells

Mammalian germ cells (female oogonia and male spermatogonia) originate from primordial germ cells (PGCs), which migrate to the genital ridge during embryonic development to form the gonad. There, expression of sex-determining genes on the Y chromosome promote testicular development, whereas in their absence a female gonad develops (Gilbert, 2006).

1.3.1 Oogenesis

The development of female germ cells into mature oocytes is known as oogenesis and is initiated before birth (Fig. 1.6). In mice, oocytes start undergoing meiosis (primary oocytes) in the fetal ovary from embryonic day 13.5. In the human embryo, primary oocytes appear around the second month of gestation and oogonia continue to divide mitotically until the seventh month (Peters, 1970). During this developmental stage, maternal and paternal homologues pair and undergo reciprocal exchange of DNA. After birth, primary oocytes enter arrest in prophase of meiosis I, which is also known as the dictyate arrest. For the most part, prophase arrest is spent in the primordial stage, when the oocytes are not yet been recruited for growth. The fully grown oocytes becomes responsive to hormonal signals, which trigger exit from prophase arrest and entry into prometaphase of MI. Ovulation occurs once MI has been completed and the oocyte arrests at metaphase of MII until it is fertilized or otherwise activated. At this stage oocytes have a visible nucleus, called the germinal vesicle (GV; Fig. 1.7.A) and remain arrested there, until they receive the necessary hormonal signals to resume meiosis, or become atretic and perish (Jones, 2008).

With the onset of puberty, cyclical hormone stimuli are activated that promote oocyte maturation and ovulation. The effects of periodically secreted gonadotropins (follicle-stimulating hormone, FSH; luteinising hormone, LH) stimulate fully grown oocytes to make the transition from prophase arrest to prometaphase of MI, until they become arrested again at metaphase of MII prior to ovulation (Jones, 2008). Resumption of MI is marked by germinal vesicle breakdown (GVBD; Fig. 1.7.B). The completion of MI yields a secondary oocyte, in which half the chromosomes have been "discarded" into a tiny structure known as the first polar body (Fig. 1.7.C). Upon fertilisation, the secondary oocyte quickly completes MII to produce a second polar body and a haploid oocyte. The latter, together with the sperm will form the zygote, giving rise to a new organism (Gilbert, 2006).

Overall, during vertebrate oogenesis, meiosis is arrested twice, in prophase I and in metaphase II. Although the exact mechanisms have not been elucidated yet, it is known that APC/C activity must be highly regulated during both meiotic arrests. In mouse oocytes APC/C^{Cdh1}-mediated degradation of substrates appears to be necessary for maintaining prophase I arrest and its inhibition by Emi1 contributes to resumption of MI (Reis *et al.*, 2006a; Marangos *et al.*, 2007; Reis *et al.*, 2007). The metaphase II arrest is also known as the cytostatic factor (CSF) arrest and its function is to prevent egg activation prior to fertilisation. According to the currently accepted model, the MetII arrest is generated primarily due to the inhibition of APC/C^{Cdc20} by the protein Emi2/XErp1 (Gui and Homer, 2012) (Madgwick *et al.*; Lane *et al.*, 2012)

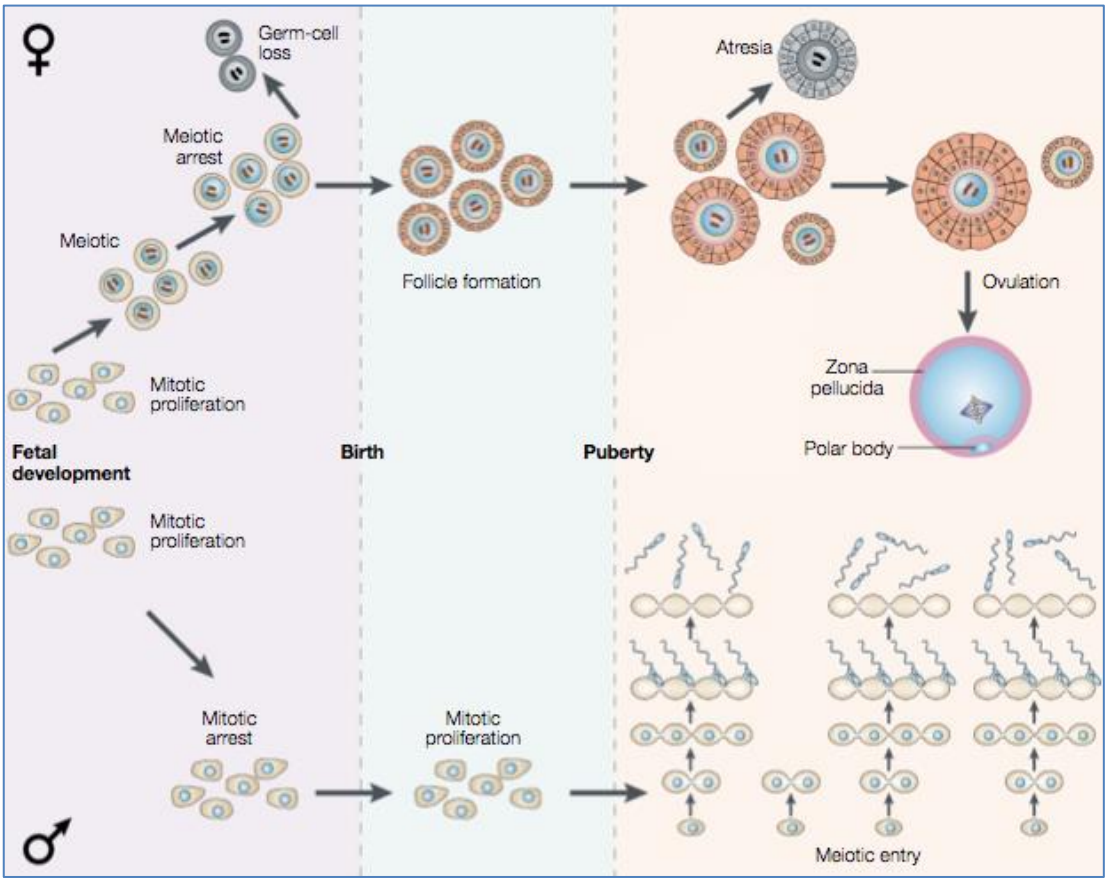

Figure 1.6 The development of human germ cells

In both foetal testis and ovary, germ cells proliferate mitotically. However, they enter meiosis at markedly different stages through their development. **Males**: In the foetal testis male germ cells initially proliferate mitotically for a short period and then enter mitotic arrest. After birth spermatogonia resume mitotic proliferation and with the onset of puberty they begin to differentiate and mitotically divide into sperm cells. Spermatogonia continue to proliferate and produce sperm virtually throughout the lifetime of a male. **Females**: In the foetal ovary the brief period of proliferation is directly followed by entry into meiosis, while in the same time a significant number of oogonia become apoptotic. The remaining oogonia enter dictyate arrest prior to birth and begin forming primordial follicles by being surrounded with somatic cells. At puberty, small cohorts of primary follicles are periodically induced to mature via hormonal stimuli and typically each month a single secondary oocyte is ovulated, while the rest of the primary oocytes succumb to atresia. This process continues until the pool of oocytes is depleted and the female enters menopause [modified from (Hassold and Hunt, 2001)].

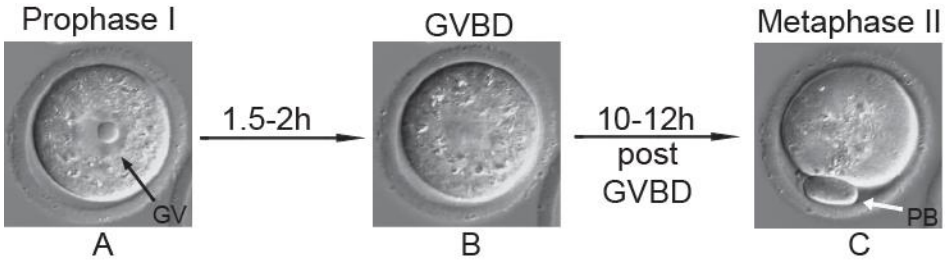

Figure 1.7 Meiosis in mouse oocytes

A timeline of oocyte maturation: **(A)** A primary oocyte at dictyate arrest, with a visible germinal vesicle (GV) and nucleolus. **(B)** Germinal vesicle breakdown (GVBD) marks the resumption of meiosis I. **(C)** Polar body (PB) extrusion signals completion of MI and arrest at metaphase II.

As mentioned previously, cohesin is recruited during S-phase, which takes place during fetal development, and is totally removed at the onset of anaphase II, which occurs upon fertilisation. Considering the developmental profile of mammalian oocytes, the time interval between recruitment and removal of cohesin is amazingly long, as in humans it could last until the onset of reproductive senescence (~40-50 years long). During such a prolonged period, cohesin might degrade and become defective, thus causing destabilisation of chiasmata and premature segregation of sister chromatids. From that perspective, cohesin could be the perfect link between reproductive age and aneuploidy.

1.3.2 Spermatogenesis

Spermatogenesis is the process by which male spermatogonia develop into mature spermatozoa, also known as sperm cells (Fig. 1.6). In the mammalian embryonic testis, immature spermatogonia enter a phase of mitotic arrest at G0/G1 early during development (~13.5 days *post coitum* in mice) and remain there until birth (de Rooij and Grootegoed, 1998). In mice, a few days after birth, spermatogonia begin to proliferate mitotically and through successive differentiation steps they enter MI and initiate spermatogenesis. Development from stem cell to spermatozoon takes 34.5 days. In human males, spermatogenesis begins with the onset of puberty and development takes almost twice as long. Nevertheless, each day nearly 100 million "fresh"

spermatozoa are made in each testicle and during his lifetime a human male can produce 10^{12} to 10^{13} sperm (Reijo *et al.*, 1995; Gilbert, 2006).

1.4 Meiotic Maturation in Mouse Oocytes

Meiosis is the process by which diploid germ cells generate haploid gametes. As previously described, in females meiosis begins during fetal development and exhibits two arrest stages (Prophase I and Metaphase II). According to the widely accepted dogma, females are born with a finite cohort of oocytes, a big part of which become apoptotic during prophase I arrest (Beaumont and Mandl, 1961; Byskov, 1974; Coucouvanis *et al.*, 1993). Developing oocytes are surrounded by granulosa cells, which support their growth (Eppig, 2001). During the prolonged prophase I arrest, granulosa cells increase in numbers and oocytes grow in size, while accumulating the necessary transcripts to support meiotic maturation, fertilisation, and preimplantation development (Moore, 1975; Sorensen and Wassarman, 1976; Moore and Lintern-Moore, 1978). Fully-grown, meiotically competent oocytes are contained within large antral follicles. Upon receiving ovulatory signals, these oocytes escape prophase arrest, complete MI, extrude the first polar body polar body and arrest at metaphase II. Upon fertilization, a second polar body is extruded and MII is completed. The stages between MI resumption and Met-II arrest are collectively referred to as meiotic maturation.

During meiotic maturation a plethora of protein kinases and phosphatases engage in a highly dynamic play in order to regulate the process (Schultz *et al.*, 1983; Bornslaeger *et al.*, 1986; Bornslaeger *et al.*, 1988). At the moment we know that the mouse genome encodes a total of 162 protein phosphatases and 561 protein kinases (Roy and Cyert, 2009). During recent years research has focused on key players of these protein groups and a constantly increasing number of them appear to be essential in the regulatory pathways that control oocyte meiotic maturation. Among the many kinases, Plk1 has been shown to have a

multitude of functions during mitosis and is therefore established as an important regulator of mitotic phenomena. However, very little is known to date about the meiosis-specific functions of Plk1.

1.5 Polo-like kinase 1

The serine/threonine kinase known as Polo was discovered almost 25 years ago in *Drosophila* (Sunkel and Glover, 1988; Llamazares *et al.*, 1991). Polo kinase is highly conserved among eukaryotes and its orthologues include Plk1 in mammals (Fig 1.8), Plx1 in *Xenopus*, Cdc5 in *S. cerevisiae* and Plo1 in *S. pombe* (Archambault and Glover, 2009). Extensive research has established Plks as key regulators of cell proliferation in all model organisms where they have been studied to date. Currently, in humans, the PLK family includes five members (PLK1-5), with PLK1 being arguably the most important member in regulating mitotic and meiotic divisions (Lens *et al.*, 2010). All Plks contain a C-terminal Polo-box domain (PBD), which allows them to interact with target proteins. In vertebrate cells Plk1 controls a number of processes, including mitotic entry, centrosome maturation, bipolar spindle assembly, microtubule (Mt)-kinetochore (Kt) attachments, release of cohesin from chromosome arms (prophase pathway), APC/C activation and cytokinesis (Fig 1.8) [reviewed in (van de Weerdt and Medema, 2006; Petronczki *et al.*, 2008; Archambault and Glover, 2009)]. Consistent with its multiple functions, Plk1 localises to various subcellular sites, mediated by its phospho-binding PBD (Elia *et al.*; Elia *et al.*, 2003b).

Most of research on Plk1 has focused on its multiple functions in mitosis. During interphase Plk1 is diffusely distributed throughout the cell (Taniguchi *et al.*, 2002; Acquaviva and Pines, 2006). In late G2 phase Plk1 localises at the centrosomes and then becomes enriched at kinetochores in prometaphase and metaphase, where it persists throughout most of mitosis (Golsteyn *et al.*, 1995).

In anaphase Plk1 localises on the central spindle and finally accumulates on the midbody in telophase (Golsteyn *et al.*, 1995).

One of the major functions attributed to Plk1 is promoting mitotic entry. Plk1 achieves that by promoting Cdk1/cyclin B activation in three ways: (1) It phosphorylates and thereby promotes nuclear translocation of Cdc25C, a kinase activator of Cdk1/cyclin B (Roshak *et al.*, 2000; Toyoshima-Morimoto *et al.*, 2002). (2) It phosphorylates and so promotes the degradation of the Cdk1/cyclin B-inhibiting kinases Wee1 and Myt1 (Nakajima *et al.*, 2003; Watanabe *et al.*, 2004). (3) It phosphorylates cyclin B at the centrosome, which is the primary site where Cdk1/cyclin B is known to be activated (Toyoshima-Morimoto *et al.*, 2001; Jackman *et al.*, 2003). However, Plk1 activity has been shown to be non-essential for mitotic entry as its inhibition does not block mitotic entry, but significantly delays it (Lenart *et al.*, 2007).

Plk1 is also involved in centrosome maturation and subsequently the formation and elongation of the bipolar spindle. It has been suggested that Nlp phosphorylation by Plk1 leads to dissociation of the former from the centrosome, thereby allowing the recruitment of various proteins, most importantly γ-tubulin, which are essential for microtubule nucleation (Casenghi *et al.*, 2003; Casenghi *et al.*, 2005; Rapley *et al.*, 2005).

Plk1 is also implicated in regulating chromosome alignment on the mitotic spindle. A number of studies have shown that Plk1 activity and localisation at the kinetochore are required for the formation of Kt-Mt attachments and thereby chromosome congression (Casenghi *et al.*, 2003; Sumara *et al.*, 2004; Lenart *et al.*, 2007). It has also been observed that Plk1 levels are increased on the kinetochores of chromosomes that have not established bipolar attachments and are not under tension (Ahonen *et al.*, 2005; Lenart *et al.*, 2007). Plk1 also phosphorylates proteins that are involved in the SAC, including BubR1 and

Bub1, but these phosphorylations appear to be non-essential for SAC activation (Sumara *et al.*, 2004; Burkard *et al.*, 2007; Lenart *et al.*, 2007; Santamaria *et al.*, 2007). Nonetheless, BubR1 is required for Kt-Mt attachments (Lampson and Kapoor, 2005) and its levels of phosphorylation by Plk1 are higher at kinetochores that are not under tension (Elowe *et al.*, 2007).

Plk1 is also involved in direct and indirect activation of the APC/C. Several APC/C subunits are phosphorylated by Plk1, including Cdc16, Cdc27, Tsg24 the Apc1 subunits (Kotani *et al.*, 1998; Golan *et al.*, 2002; Kraft *et al.*, 2003). Indirect activation of the APC/C by Plk1 involves the phosphorylation of the APC/C-activator Cdk1/cyclin B (Golan *et al.*, 2002), together with the phosphorylation of the APC/C-inhibitor Emi1, which promotes its subsequent targeting for degradation by the ubiquitin ligase $SCF^{\beta Trcp1}$ (Hansen *et al.*, 2004; Moshe *et al.*, 2004). However, APC/C activation appears to occur even in the absence of Plk1 activity (Kraft *et al.*, 2003; Lenart *et al.*, 2007).

Cytokinesis is also highly sensitive to Plk1 activity. Recent studies have shown that the onset of cytokinesis in human cells is blocked when Plk1 activity is inhibited at the metaphase to anaphase transition (Brennan *et al.*, 2007b; Burkard *et al.*, 2007; Petronczki *et al.*, 2007; Santamaria *et al.*, 2007). In particular, cells treated with different Plk1 inhibitors failed to form a contractile ring at the equatorial cortex during anaphase and to accumulate RhoA, the upstream regulator of the contractile function. The reason behind this phenotype appeared to be the abolishment of Ect2 recruitment to the spindle midzone, an essential activator of the RhoA network linking the anaphase spindle to the cellular cortex and stimulating cytokinesis (Brennan *et al.*, 2007b; Burkard *et al.*, 2007; Petronczki *et al.*, 2007; Santamaria *et al.*, 2007).

Finally, as already described in detail in section 1.2.3, Plk1 is involved in the removal of cohesin from chromosome arms of sister chromatids prior to anaphase (Sumara *et al.*, 2002; Hauf *et al.*, 2005).

Of particular interest is the study by Lenart *et al*. (Lenart *et al.*, 2007) where the authors have used BI 2536, a small-molecule inhibitor of Plk1, to delineate some of the known functions of Plk1 in mitosis and uncover novel ones. According to this study, treatment of HeLa cells with BI 2536 induces a delay in prophase, consistent with a previously reported role for Plk1 in promoting activation of Cdk1/Cyclin B (Dehapiot *et al.*, 2013). Once into mitosis, cells were arrested in late prophase, due to SAC activation, with abnormal monopolar spindles, which could not attach stably to chromosomes. Moreover, consistent with previous reports (Hansen *et al.*, 2004; Moshe *et al.*, 2004), BI 2536 inhibited the degradation of Emi1. However, cyclin A degradation was not perturbed, showing that Emi1 degradation is not required for Cyclin A to be degraded. This also shows that the prophase arrest caused by BI 2536 does not depend on Cyclin A not being degraded, which has been previously reported to inhibit exit from mitosis (den Elzen and Pines, 2001). Another significant observation made possible by the use BI 2536 was that Plk1 activity is essential not just for the establishment, but also for the maintenance of chromosome biorientation (Peters *et al.*, 2006; Lenart *et al.*, 2007).

Studies in mouse oocytes have revealed that Plk1 exhibits a highly dynamic localisation pattern also during mammalian meiosis (Fig 1.8). Plk1 is known to be activated by phosphorylation shortly prior to GVBD (Pahlavan *et al.*, 2000) suggesting it could be involved in promoting meiotic resumption/Cdk1 activation. Consistent with that, its inhibition either by antibody-microinjection

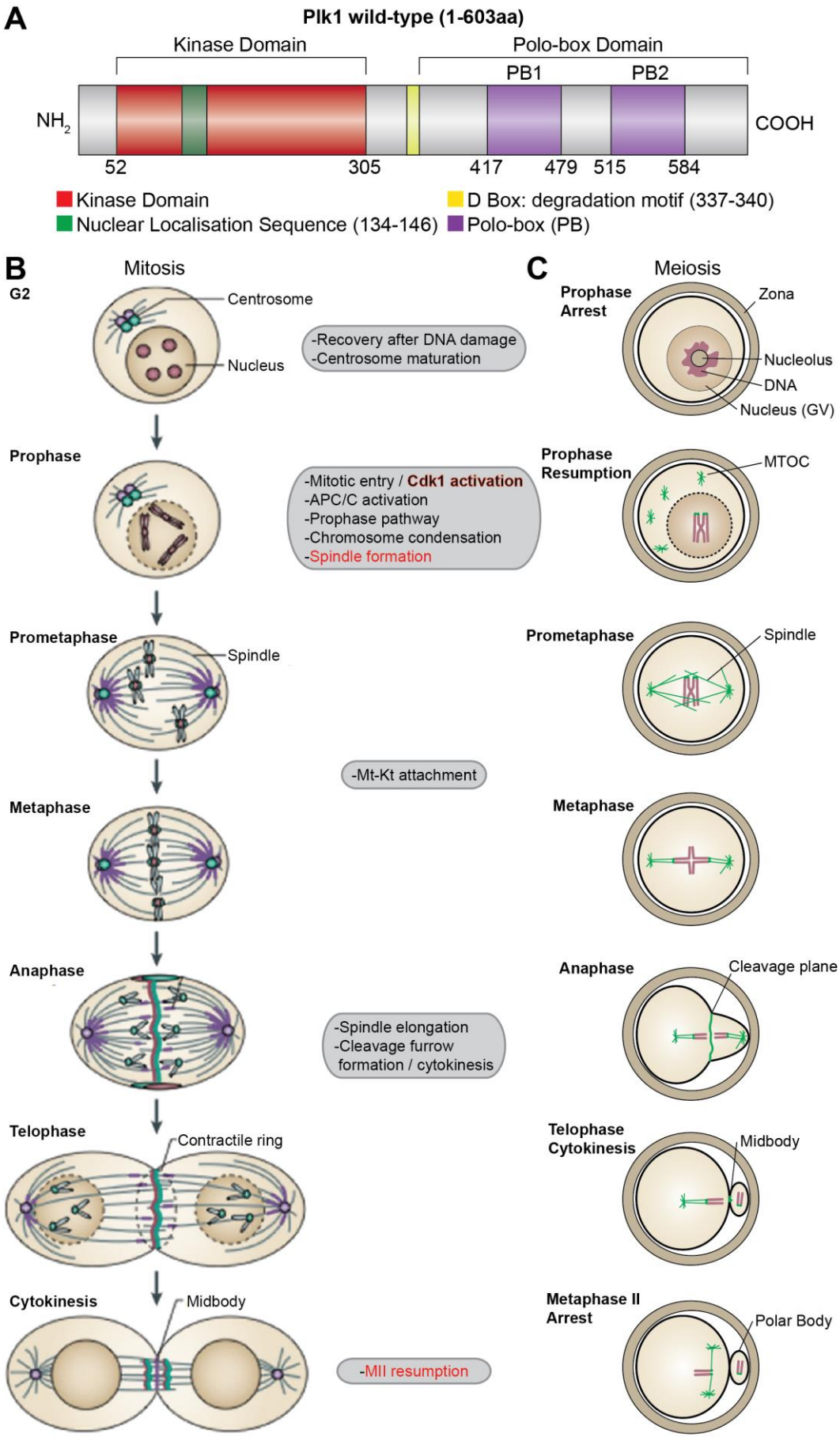

Figure 1.8 Plk1 structure and functions in mitosis and meiosis

(See legend on next page)

Figure 1.8 Plk1 structure and functions in mitosis and meiosis

(A) Schematic representation of mouse Plk1. The positions of the kinase domain (red) and polo-boxes 1 and 2 (purple) are depicted. The amino acid (aa) sequences that mediate its nuclear localization (green) and its destruction by the proteasome (D-box; yellow) are also shown. The amino- and carboxyl- termini are also indicated. Numbers indicate amino acid positions.

(B) Schematic representation of human mitosis indicating PLK1 localisation (green). During interphase PLK1 is diffusely distributed throughout the cell (Acquaviva and Pines, 2006). In late G2 phase PLK1 localises at the centrosomes and then becomes enriched at kinetochores in prometaphase and metaphase, where it persists throughout most of mitosis. In anaphase PLK1 localises on the central spindle and finally accumulates on the midbody in telophase. Major functions of PLK1 are listed in gray boxes (black lettering) at the corresponding cell cycle stages:
-Recovery after DNA damage: Turns off the DNA damage checkpoint by promoting the degradation of Claspin (Prinz *et al.*, 1998; Pfleger and Kirschner, 2000; Barford, 2011).
-Centrosome maturation: Recruits γ-Tubulin, which is essential for microtubule nucleation (Lane and Nigg, 1996; Nasmyth, 2005; Schreiber *et al.*, 2011).
-Mitotic entry/ Cdk1 activation: Activates Cdc25C, an activator of Cdk1/cyclin B (Toyoshima-Morimoto *et al.*, 2002; Hershko, 2005). Promotes the degradation of the Cdk1/cyclin B-inhibiting kinases Wee1 and Myt1(Watanabe *et al.*, 2004; Baker *et al.*, 2007). Phosphorylates cyclin B at the centrosome (Toyoshima-Morimoto *et al.*, 2001; Jackman *et al.*, 2003).
-APC/C activation: Stimulates APC/C activity by phosphorylating its Apc1, Cdc16, Cdc27 and Tsg24 subunits (Kotani *et al.*, 1998; Golan *et al.*, 2002; Kraft *et al.*, 2003). Induces the destruction of APC/C^{Cdh1} inhibitor Emi1 (Hansen *et al.*, 2004; Moshe *et al.*, 2004). However, PLK1 activity appears to be nonessential for APC/C activation in mitosis (Lenart *et al.*, 2007).
-Prophase pathway: Removes cohesin from chromosome arms prior to anaphase (Sumara *et al.*, 2002; Hauf *et al.*, 2005).
-Chromosome condensation: Involved in DNA supercoiling (Kulukian *et al.*, 2009). Plk1 inhibition/depletion produces hyper-condensed chromosomes (LeMaire-Adkins *et al.*, 1997; Gimenez-Abian *et al.*, 2004; Lenart *et al.*, 2007).
-Mt-Kt attachment: Promotes the formation of stable Kt-Mt attachments (Lenart *et al.*, 2007), thus facilitating chromosome alignment, most probably through phosphorylation of BubR1 (Li and Zhang, 2004; Elowe *et al.*, 2007).
-Spindle elongation: Plk1 inhibition abrogates spindle elongation during anaphase B (Brennan *et al.*, 2007a).
-Cytokinesis: Plk1 activity is essential for the activation of RhoA, the upstream regulator of the contractile function (Brennan *et al.*, 2007a; Burkard *et al.*, 2007; Petronczki *et al.*, 2007; Santamaria *et al.*, 2007). [B adapted from (Lens *et al.*, 2010)].

(C) Schematic representation of mouse oocyte meiosis from Prophase I to MetII arrest indicating Plk1 localisation (green). In late prophase-arrest Plk1 is diffusely distributed throughout the ooplasm and enters the nucleus (GV) shortly prior to GVBD (Hoffmann *et al.*, 2011). In prometaphase and metaphase Plk1 becomes enriched at spindle poles and centromeres and also associates with spindle Mts. In anaphase Plk1 localises on the central spindle, then at the cleavage plane and finally accumulates on the midbody in telophase. During MetII arrest Plk1 is seen at spindle poles and along spindle Mts (Rieder *et al.*, 1994; Wianny *et al.*, 1998; Pahlavan *et al.*, 2000; Hassold and Hunt, 2009). Meiosis-specific functions of Plk1 remain largely elusive and are listed in gray boxes (red lettering) at the corresponding cell cycle stages:
- Cdk1 activation: Plk1 inhibition delays GVBD suggesting it is a positive regulator of meiotic resumption (Tong *et al.*, 2002; Vanderheyden *et al.*, 2009).
-Spindle formation: Plk1 inhibition abrogates spindle formation (Tong *et al.*, 2002).
-MII resumption: Induces the destruction of APC/C^{Cdc20} inhibitor Emi2 (Madgwick *et al.*; Lane *et al.*, 2012).

(Tong *et al.*, 2002) or by chemical means (Vanderheyden *et al.*, 2009) causes a delay in GVBD. In budding yeast, the Plk1 homologue, Cdc5, participates in the regulation of chromosome segregation during MI by being involved into the establishment of correct Kt-Mt attachments and removal of cohesin from chromosomes, through phosphorylation of Rec8 (Clyne *et al.*, 2003; Lee and Amon, 2003; Brar *et al.*, 2006). A previous study suggested that Plk1 phosphorylation is essential for Rec8 cleavage by separase *in vitro* (Kudo *et al.*, 2009), however, it is yet unknown whether Plk1 regulates these processes in mammalian oocytes.

1.6 Failure of meiotic division and associated repercussions

The process of cell division is of paramount importance for all organisms, with errors in chromosome segregation proving disastrous, either for the organism per se or its progeny. In most sexually reproducing species, meiosis is a highly accurate process and chromosome missegregation is a rare phenomenon. However, in humans more than 20% of all oocytes are regarded as being aneuploid, causing infertility, miscarriages and genetic birth defects, such as Down syndrome (trisomy 21), Turner syndrome (single X female) and Klinefelter's syndrome (XXY male) (Kuliev *et al.*, 2005; Rosenbusch and Schneider, 2006; Pacchierotti *et al.*, 2007). Approximately 2-3% of newborns are trisomic (Hassold and Jacobs, 1984) and most aneuploidies are non-viable; 35% of spontaneous abortions between 6th and 20th week of gestation and 4% of foetal deaths occurring during the second trimester of gestation are a consequence of aneuploid conceptions (Jacobs, 1992; Wells and Delhanty, 2000). Most of the errors leading to chromosome missegregation and aneuploidy may occur predominantly during the extended prophase I arrest of MI (Lister *et al.*) and are associated with the failure to establish, maintain or resolve chiasmata or with premature sister chromatid segregation (Jones, 2008).

Evidence from clinical genetic studies in cases of trisomy 21 provided valuable insight into the predisposition of oocytes to segregation errors during MI. The highest risk was associated with an absence of crossovers resulting to segregation of univalent rather than bivalent chromosomes. A single crossover in the subtelomeric or pericentromeric region was also associated with a high risk of trisomy (Lamb *et al.*, 1997). These data gave ground to the idea that bivalents with susceptible chiasmata configurations were predisposed to missegregation during MI (Lamb *et al.*, 1996; Lamb *et al.*, 1997; Warren and Gorringe, 2006). However, it was later found that this association is lost during maternal ageing (Lamb *et al.*, 2005) . This implied that age-related errors in female MI are due to defects occurring subsequent to crossover formation. Evidence from recent studies (Hodges *et al.*, 2005; Chiang *et al.*, 2010; Lister *et al.*, 2010; Revenkova *et al.*, 2010; Tachibana-Konwalski *et al.*, 2010) has established cohesin deficiency as a leading candidate for such a defect.

Although it had been known since the early 1930's that the occurrence of Down syndrome increases with maternal age (Penrose, 2009), it was only in the late 80's that the exact correlation between them was established (Morton *et al.*, 1988). Today we know that the probability of a pregnancy involving a trisomic fetus increases abruptly in women around the age of thirty-seven years old (Hassold and Hunt, 2001). Apart from this increasing risk, another thing that comes with ageing is a decrease in the chances of establishing a successful pregnancy due to the lack of oocytes. Maternal fecundity has a limit in time, with ovarian reserves being constantly reduced until the onset of menopause (Telfer and McLaughlin, 2007). The impact of this decline in oocyte numbers becomes more daunting when we consider the fact that instead of being stable it gradually accelerates at mid-thirties (Faddy *et al.*, 1992; Faddy, 2000). However, the reason why chromosomal instability becomes more prevalent as we reach the end of the oocyte pool remains unclear.

In the last fifty years birth patterns have markedly changed in developed societies. A variety of socioeconomic factors, influence contemporary human reproductive culture and ideology and as a result couples seek to have fewer children and they have them at older ages than before. For example, in the UK, between 1985 and 2001 there was a doubling (from 8% to 16%) in the number of first births for parents over the age of 35 years old (Rai and Regan, 2006). This trend to postpone childbirth combined with the increased risk of aneuploidies as women get older, have amplified the numbers of miscarriages and pregnancy terminations in recent years. As a reaction to these circumstances, there is an increasing focus on research in the field of female reproductive ageing. Not surprisingly, very little is still known about the molecular basis of this phenomenon in humans, a good reason being the ethical and physical limitations associated with human oocyte and embryo research. Our research employs the appropriate animal models that mimic human female ageing and aims to contribute to a further understanding of this inevitable physiological process.

1.7 Aims

The overall aim of this thesis is to investigate the mechanism of chromosome segregation in female mammalian meiosis in the context of reproductive ageing.

The specific aims were:

1. To further our understanding of female age-related meiotic segregation errors, I aim to investigate the effect of ageing on chromosome-associated cohesin and its protector Sgo2.

2. To advance knowledge of the mechanisms governing chromosome segregation in mammalian oocytes, I will characterise the functions of Plk1 during progression through MI using the small-molecule inhibitor BI 2536.

3. To establish whether oocyte chromosomal cohesin is removed by a mechanism analogous to the Plk1-dependent prophase pathway of somatic cells, I will measure the effect of Plk1 inhibition on levels of chromosome-associated cohesin using the transgenic *Rec-Myc* mouse strain.

Chapter 2 : Materials and Methods

2.1 Mouse Strains

C57BL/Icrfa^{t} mice were obtained from a long-established colony, which had been selected for use in studies of intrinsic ageing because it is free from specific age-associated pathologies and thus provides a good general model of ageing (Rowlatt *et al.*, 1976). *Smc1β*$^{+/+}$ and *Smc1β*$^{-/-}$ female mice were provided by Rolf Jessberger and their generation has been previously described (Revenkova *et al.*, 2004). The transgenic *Rec8-Myc* mouse strain was provided by Nobuaki Kudo and its generation has also been described previously (Kudo *et al.*, 2009). Finally, CD1 mice have also been used. The research was licensed by the UK Home Office.

2.2 Harvest, culture and drug treatment of mouse oocytes

Eight to twelve weeks old female CD1, eight to twelve weeks old female Smc1β$^{+/+}$ and Smc1β$^{-/-}$, eight to twelve weeks old and twelve month old Rec8-myc, and two month and fourteen month old C57BL/Icfra^{t} mice were killed by cervical dislocation and had their ovaries dissected out and briefly held in pre-warmed M2 medium (Sigma Aldrich, UK). C57BL/Icfra^{t} mice were injected with 7.5IU of pregnant mare serum gonadotrophin (PMSG; Sigma Aldrich, UK) approximately 48 hours prior to ovary collection. Oocytes were released from the excised ovaries by puncturing follicles with an insulin needle on a microscope stage in pre-warmed M2 medium supplemented with 0.022μg/ml 3-isobutyl-1-methylxanthine (IBMX; Sigma Aldrich, UK) to maintain oocytes at the germinal vesicle stage. After collection, only mature oocytes with a central GV were isolated for further experimentation and stored in 40μl droplets of pre-warmed M2 supplemented with IBMX overlaid with mineral oil (Sigma Aldrich, UK), until further use. Oocytes with peripheral GV were either discarded or used for optimising experimental techniques.

Oocytes to be *in vitro* matured were "washed" and transferred to 40µl drops of pre-equilibrated G-IVF™ medium (Vitrolife, Sweden), overlaid with pre-equilibrated mineral oil and incubated at 37°C in a humidified 7% CO_2 environment. In the absence of IBMX, MI resumption would occur, which is marked by GVBD. In order to be able to make timed and synchronous observations, the oocytes were scored for GVBD at 1, 1.5 and 2 hours after transfer to G-IVF, separated into groups accordingly and allowed to mature to the desired stage. Oocytes that had not undergone GVBD within 2 hours of G-IVF incubation were either discarded or used for optimising experimental methods.

Depending on the purpose of the experiment the "control" *in vitro* maturation medium would be either neat G-IVF or G-IVF supplemented with 1:500 (v/v) DMSO (Sigma Aldrich, UK).
The Plk1 inhibitor BI 2536 (Axon Medchem, The Netherlands) was reconstituted to a 5M solution in DMSO (as recommended by the manufacturer) and then diluted down and aliquoted to individual 1.5µM, 2µM, 3.125µM, 6.25µM and 12.5µM working solutions, which were stored at -20°C. To supplement G-IVF with IBMX, 1µl of the appropriate working solution was added to 500µl of G-IVF.
Nocodazole (Sigma Aldrich, UK) was reconstituted in a 5mg/ml solution in DMSO and stored at -20°C. Nocodazole treatments were carried out using G-IVF supplemented with 10µg/ml nocodazole, which allows the formation of the spindle assembly but causes microtubule instability, thus preventing chromosome congression and alignment.

2.3 Isolation of Oocytes from Pre-antral Follicles

Following puncture of antral follicles from excised ovaries, the remaining ovarian tissue was centrifuged at 700 rpm for 5 min. The supernatant was discarded and the pellet was washed twice in PBS pre-warmed at 37°C. After

the final wash, the pellet was resuspended in 4ml of 0.5 mg/ml collagenase type IV (Worthington Biochemical Corp., USA) and 2 IU TURBO™ DNase (Invitrogen, UK) in PBS and incubated at 37°C for 30-60min, on a shaker with occasional pipetting. Oocytes were manually isolated and transferred to M2 medium supplemented with 0.022 μg/ml IBMX.

2.4 Microinjection

Microinjections were performed on a Nikon TE-300 inverted diaphot microscope, fitted with an MMN-1 micromanipulator (Narishige, Japan) and an IM-300 Motor-Drive Microinjector (Narishige, Japan). Injection needles were made from thin-wall borosilicate glass capillaries with filament (BF 100-50-10; Intracel, UK) using a P-97 micropipette puller (Sutter Instruments Co, USA) programmed with the following settings: pressure, 200; heat, 518; pull, 70; velocity, 70; time, 150. Injection needle tips were angled to approximately 30° using a microforge device (Research Instruments, UK).

For mRNA microinjections, stock *in vitro*-transcribed mRNA was diluted to 500-1000ng/μl with injection buffer and 1.5μl of mRNA solution was loaded into a shortened glass capillary and mounted on a glass slide using beeswax. The glass slide with the capillary containing mRNA was placed on the microscope stage and the injection needle tip was broken open by gently tapping it to the edge of the glass capillary. The injection needle was then inserted into the mRNA solution and a negative pressure was applied to allow loading. mRNA loading columns were kept at 4°C during experiments, to avoid evaporation in case re-loading was required.

Mature GV stage oocytes to be microinjected were transferred to appropriate culture dishes containing 5μl droplets of IBMX-supplemented M2 medium, covered with mineral oil. Five to ten oocytes were transferred in each droplet and the dishes were kept at 37°C. During microinjections, the oocytes were

immobilised by gentle suction using a holding pipette (Hunter Scientific, UK) and the injection needle was inserted through the zona pellucida and oolemma, into the ooplasm, taking care to avoid the GV. Injections producing a cytoplasmic disturbance of approximately the size of the GV (~5% of oocyte volume) were administered. Injection pressure and balance pressure had to be adjusted constantly throughout a microinjection session to avoid intake of culture medium and deliver equal injection volumes. Following injections, oocytes were allowed to recover for 1-2 hours at 37^{o}C, before being used for further experimentation.

2.5 Oocyte immuno-fluorescence staining

2.5.1 Whole oocyte Ca^{2+}-buffer treatment and fixation

Maturing oocytes were collected from *in vitro* culture and washed with pre-warmed PBS at 37^{o}C. Oocytes were then transferred in a drop of pre-warmed Ca^{2+}-buffer for 90 sec on a stage heated at 37^{o}C. Following Ca^{2} treatment, oocytes were fixed in Ca^{2+}-buffer supplemented with 1% formaldehyde for 30 min at room temperature. After fixation, the oocytes were washed three times (5min/wash) with PBT (PBS supplemented with 0.1% Triton X-100) and were stored in PBS at 4^{o}C for a maximum of three weeks.

2.5.2 Indirect immuno-fluorescence staining of whole oocytes

Fixed oocytes were blocked with 4% BSA in PBT (block solution) overnight at 4^{o}C or for 1h at room temperature. Primary antibody incubations were performed in block solution overnight at 4^{o}C, using the antibodies and the concentrations shown in table 2.1. After washing three times (5min/10min/10min) in PBT, the oocytes were incubated with the appropriate secondary antibodies (shown in table 2.1) diluted in block solution, in dark at room temperature for 1h on a shaker at a very low rpm setting. After washing three times (10min/15min/20min) in PBT and once (2min) in PBS, the oocytes were transferred into droplets of Vectashield with DAPI (Vector Labs, UK)

diluted 1:10 with PBS, in glass bottom dishes, and covered with mineral oil. Imaging was performed as described in section 2.9.3.

Primary Antibody	Source	Dilution	Secondary Antobody	Source	Dilution
human AutoAb CREST	Cellon HCT-0100	1:50	goat-anti-human Cy5	Jackson Immuno 109-175-003	1:400
human AutoAb CREST	Europa Bioproducts FZ90C-CS1058	1:100	goat-anti-human Cy5 or goat-anti-human AlexaFluor 555	Jackson Immuno 109-175-003 or Invitrogen A-21433	1:400 or 1:800
rabbit-anti-human Sgo2	Gift from Yoshinori Watanabe, The University of Tokyo, Tokyo	1:50	donkey-anti-rabbit AlexaFluor 488	Invitrogen A-21206	1:800
mouse-anti Myc Tag clone 4A6	Millipore 05-724	1:100	goat-anti-mouse AlexaFluor 488	Invitrogen A-11001	1:800
mouse-anti-PP2A monoclonal clone 106	Millipore 05-421	1:50	donkey-anti-mouse AlexaFluor 555	A-31570	1:800
mouse-anti Plk1 monoclonal clone F-8	Santa Cruz 17783	1:100	goat-anti-mouse AlexaFluor 488	Invitrogen A-11001	1:800
mouse-anti-a-Tubulin (DM1A)	Sigma Aldrich T6199	1:100	goat-anti-mouse AlexaFluor 488	Invitrogen A-11001	1:800

Table 2.1 Antibodies used for immunofluorescence staining

2.6 Chromosome Spreads that preserve chromosome-associated proteins

The protocol for chromosome spreads was modified from Patricia Hunt (Scott, 2009).

2.6.1 Paraformaldehyde and slide preparation

0.25g of paraformaldehyde (PFA) and 4µl of 10M NaOH were added in 22.5ml of Milli-Q H_2O (Millipore, UK) in a 50ml universal tube. The solution was incubated at 60°C with occasional vortexing until it turned clear. Once cooled to room temperature pH was adjusted to 9.2 using 50mM boric acid. Finally, 175µl of 20% (v/v) Triton X-100 and 150µl of 0.5M DTT were added shortly prior to use.

In order to have a reference point that would assist in locating the chromosome spreads, a line was drawn on the back of the poly-L-Lysine coated glass microscope slides (Polysine® Slides; Fisher Scientific, UK) to be used, using a permanent marker.

2.6.2 Removal of zona pellucida, fixation and spreading

The zona pellucida was dissolved by brief exposure to a drop of acid Tyrode's solution pre-warmed at 37°C. The oocytes were then moved through two successive drops of M2 medium, also pre-warmed at 37°C, to remove Tyrode's solution, and were then incubated for 2 minutes in a drop of hypotonic 0.5% (w/v) solution of tri-sodium citrate. While waiting for the incubation, a slide was dipped in the PFA solution and excess fixative was removed by gentle tapping in a paper towel. The oocytes were then transferred on the slide, along the length of the drawn line under an SMZ-2T (Nikon, Japan) stereomicroscope. Finally, the slide was placed inside a humid chamber and allowed to dry overnight at room temperature.

Following overnight incubation, a rectangular region was drawn around the area containing the spreads using an ImmEdge™ hydrophobic barrier pen (Vector Laboratories, UK), to create a "chamber" to hold media drops for subsequent immunostaining procedures. After drying, slides were washed twice (2x2min) in 0.4% (v/v) Kodak Photo-Flo (Silverprint, UK) in dH_2O solution, then twice (2x2min) in PBS and they were finally stored in PBS at 4°C, until further use.

2.6.3 Indirect immunofluorescence staining of chromosome spreads

Slides containing chromosome spreads were blocked in either 10% (v/v) goat serum (Sigma Aldrich, UK) in PBTT (0.1% Triton-X and Tween in PBS) or 10% (v/v) donkey serum (Sigma Aldrich, UK) in PBTT, depending in which animal the secondary antibodies to be used were raised in (i.e. if secondary antibodies

were raised in goat, then the goat block was used). After 1 hour of blocking at room temperature, primary antibody incubations were performed in block solution overnight at 4°C, using the antibodies and the concentrations shown in table 2.1. Following incubation with primary antibody slides were washed as follows: once (1x10min) in 0.4% (v/v) Photo-Flo in PBS; twice (2x10min) in 0.01% (v/v) Triton-X in PBS; once (1x10min) 0.4% (v/v) Photo-Flo in PBS; once (1x2min) in PBS. All washes were performed at RT on a shaker at 100rpm. The Spreads were then incubated with the appropriate secondary antibodies (shown in table 2.1) diluted in block solution, in dark at room temperature for 1h, before repeating the aforementioned wash steps. Chromosome spreads were covered using Vectashield with DAPI and glass coverslips (#1.5; VWR International, UK), and sealed with rubber solution to prevent evaporation (Halfords, UK). Imaging was performed as described in section 2.9.2.

2.7 Fluorescent Constructs

All constructs used in this thesis were manufactured by Lisa Lister or were gifts from collaborators.

For the generation of constructs and the production of mRNA the pRN3 vector was used (Fig 2.1) (Lemaire *et al.*, 1995). The coding sequence for a fluorescent protein was inserted between the cloning site for the gene of interest and the 3'-UTR for most fluorescent constructs used. The gene of interest was either sub-cloned or amplified using a polymerase chain reaction (PCR) from a mouse oocyte cDNA library, constructed using the SMART PCR cDNA Synthesis Kit (Clontech, USA), and inserted into the plasmid by restriction digest and ligation. The cloning was confirmed by sequencing (The Sequencing Service, Dundee).

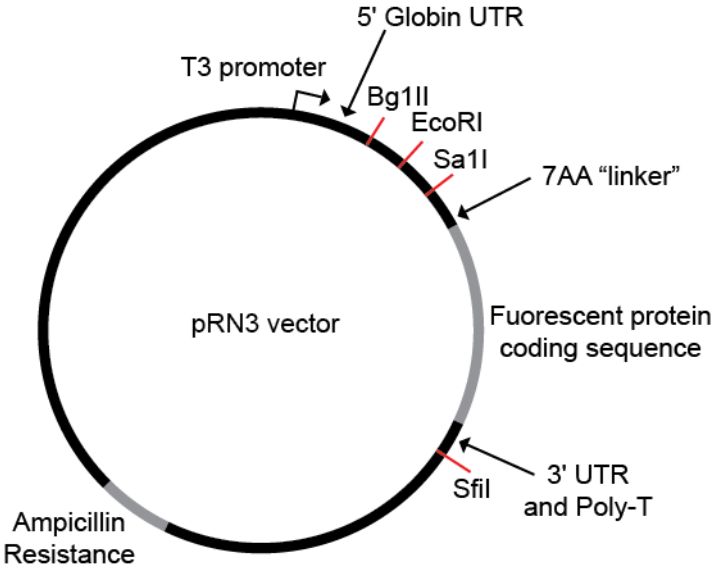

Figure 2.1 Schematic representation of the constructs made using a pRN3 vector backbone

The pRN3 vector contains a T3 promoter, an upstream 5′ globin untranslated region (UTR), which conferees stability of RNA transcripts and a downstream globin 3′ UTR and a poly-A encoding sequence, to enhance translation. A series of restriction sites (red lines) allow the insertion of the desired gene and fluorescent protein coding sequences. The ampicillin resistance insert allows the identification of successfully transfected microbial colonies.

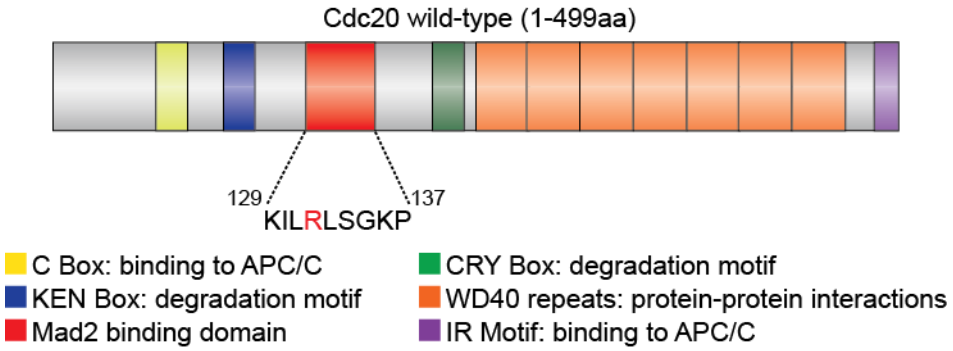

Figure 2.2 Conserved domains and motifs of Cdc20

A schematic representation of human wild-type Cdc20. Cdc20 contains a C-box, required to interact with APC/C core subunits (Schwab *et al.*, 2001; Thornton *et al.*, 2006); a KEN-box, a degradation motif (Pfleger and Kirschner, 2000); the Mad2-binding motif (Zhang and Lees, 2001); a CRY-box, another degradation motif (Reis *et al.*, 2006b); seven WD40 repeats, forming a scaffold for protein-protein interactions [reviewed in (Yu, 2007)]; an IR motif at the C-terminal, which contributes to binding to the core APC/C subunits, as well as to its activity (Passmore *et al.*, 2003; Vodermaier *et al.*, 2003; Thornton *et al.*, 2006). The R132A mutation allows robust binding to APC/C, but reduces the binding to Mad2 (Zhang and Lees, 2001; Ge *et al.*, 2009).

2.8 Preparation of mRNAs

Capped mRNA constructs with a 30 poly-A tail were made using an mMESSAGE mMACHINE kit (T3, T7, or SP6 kit, depending on the RNA polymerase promoter site on the plasmid; Ambion, UK) from plasmid cDNA encoding histone H2B-RFP (a gift from Z. Polanski), cyclin B1-GFP (a gift from M. Levasseur), securin-YFP (a gift from K. Wassmann), $Cdc20^{WT}$ (a gift from A. Rattani) and $Cdc20^{R132A}$ (a gift from A. Rattani; Fig 2.2).

2.9 Microscopic Methods

2.9.1 Time-lapse (4D) Microscopy

Oocytes injected with fluorescent mRNA constructs (as described in 2.4) were transferred into a drop of pre-equilibrated G-IVF, covered with mineral oil, in a glass bottom dish (Ibidi μ-Dish; Thistle Scientific, UK). In experiments involving the use of BI 2536, a 40μl drop was made, as it was observed that smaller volumes (e.g. 2μl, as in controls) would weaken the effect of the inhibitor, probably because the latter is moderately oil soluble. The dish was fitted in a custom made CO_2 chamber (Medical Physics Department, Newcastle University) which was securely placed on the microscope stage and would allow imaging while maintaining a 7% CO_2 atmosphere.

Time-lapse imaging was performed on a Nikon Eclipse TE-2000-U inverted microscope using a 20x/0.75 n.a. Plan Fluor oil immersion objective and a Photometrics Cool- SnapHQ interline cooled charge-coupled device (CCD) camera (Roper Scientific, USA). The microscope was fitted with an incubator (Solent, UK) to maintain a stable temperature of 37°C. For fluorescence imaging, illumination was provided by a Xenon short arc XBO® 100W OFR lamp (Osram, Germany) and the following filter settings (Chroma, Germany) were available:

Fluorescent Taq / Stain	Excitation Filter	Dichroic	Emission Filter
DAPI	355±25	400	420 Longpass
GFP/AlexaFluor 488	480±10	500	510±10
YFP	500±10	CYR Multi Bandpass	535±15
RFP	580±10	GFP/RFP Multi Bandpass	630±30
Rhodamine/AlexaFluor 555	535±25	565	590 Longpass
Cy5	620±30	660	700±37

Filter wheels, shutters, Z-focus motor (Prior Scientific, UK) and camera were driven by Metamorph Image Acquisition software (Universal Imaging, USA) via a ProScan™ Controller (Prior Scientific, UK).

Oocytes were imaged for 14–16 hours with bright-field or DIC and fluorescence images acquired every 20 min on 5 x 0.75 μm Z planes.

2.9.2 Epifluorescence Imaging of Chromosome Spreads

The microscope used for time-lapse imaging was also utilised for acquisition of fluorescence images of chromosome spreads, prepared as described in 2.6.3, using a 100x/1.3 n.a Plan Fluor oil immersion objective.

IF stained chromosome spreads were also imaged on a Zeiss Axio Imager Z1 microscope fitted with a Zeiss ApoTome 2. Images were captured using an EC Plan Apochromat 63x/1.4 Oil DIC objective and a Zeiss AxioCam HRm Rev3 camera in combination with the Axiovision 4.8 software package. Excitation source was a Mercury short arc HBO® 100 W/2 lamp (Osram, Germany).
The filter sets that were utilised were:

Filter Number	Fluorophore	Excitation Filter (nm)	Dichroic Mirror cut off (nm)	Emission Filter (nm)
Zeiss 49	DAPI	335-385	395	420-470
Zeiss 38HE	Alexa 488	450-490	495	500-550
Zeiss 20HE	Alexa 555 Rhodamine	534-558	560	567-647
Zeiss 50	Cy5	610-670	660	665-715

Image acquisition of mature GV-stage and immature pre-antral-follicle oocytes, described in 3.2, was performed by Anna Kouznetsova, on a Leica DMRXA microscope equipped with a Hamamatsu C4880-40 CCD camera.

2.9.3 Confocal Imaging

Oocytes prepared as described in 2.5 were imaged using a Nikon A1R confocal microscope, using a Plan Apo VC 100x/1.40 Oil DIC N2 objective. Sequential (Channel series ON)/Simultaneous (Channel series OFF) excitation at 405nm, 488nm, 561nm and 642nm was provided by the 405nm Cube Laser (Coherent Inc., USA), 488nm Argon Laser (Melles Griot, USA), Sapphire 561nm Laser (Coherent Inc., USA) and Red Diode 642nm Laser (Melles Griot, USA), respectively.

Emission filters BP 425-475nm, BP 525-555nm, 570-620nm and 662-737nm were used to collect DAPI, Alexa 488, Alexa 555 and Cy5 signal respectively. Images, with a frame size of 1024x1024 pixels and a 2x line average, were captured using the Nikon Elements AR software package. The entire spindle was imaged with Z-confocal sections every 0.5 μm, in total covering at least 15.91μm x 15.91μm x 12.5μm volume.

2.10 Image Processing and Quantification

All figures and images in this thesis were designed and produced using Adobe Photoshop (Adobe Systems), Adobe Illustrator (Adobe Systems) and PowerPoint (Microsoft), unless otherwise indicated.

2.10.1 Time-lapse

Processing and analysis of time-lapse acquisitions was performed using MetaMorph software. Best focus images were identified for each timepoint and used for further analysis. To analyse the dynamics of a particular fluorophore, a region of interest has been drawn inside the oocyte and the average fluorescence intensity (FI) minus background FI was measured at each timepoint. The values were normalised relative to that of GVBD and were plotted against time in Excel (Microsoft).

2.10.2 Chromosome spreads

Images were acquired as raw 12-bit (Zeis Axio Imager) or 16-bit (Nikon Eclipse) images using identical exposure times within each experiment. Pseudo-colouring, brightness/contrast adjustments and general image processing were done using ImageJ software (http://rsb.info.nih.gov/ij/). For quantification of antibody staining fluorescence intensities (FI), six to eight cells or chromosome spreads were randomly selected. Prior to quantification, background subtraction was performed using the "subtract background" function in ImageJ, which removes uneven background from images using a "rolling ball" algorithm (Sternberg, 1983). In order to determine the appropriate "rolling ball radius", different settings were used and average CREST FI of individual centromeres was measured at each setting. Then average CREST FI of the same centromeres was measured again, but this time local background was subtracted using the method described by Hoffman et al. (Hoffman *et al.*, 2001). Briefly, an "inner" square region of interest (ROI) was drawn manually around a centromere and integrated FI was measured using MetaMorph software. This ROI was then expanded to create an "outer" region. The integrated FI of the "outer" ROI was subtracted from the "inner" ROI, after scaling values for differences in area, as described previously (Hoffman *et al.*, 2001; Waters, 2009). Finally, the background-subtracted CREST integrated FI was divided by the

area of the "inner" ROI. The average CREST FI values obtained by utilizing the two different methods were statistically compared in Excel and the "rolling ball radius" setting that gave a correlation coefficient of approximately 1 (R^2= 0.9895) was chosen for further application. For calculating centromeric Rec8:CREST fluorescence intensity ratios (Fig 5.4), following background FI subtraction, a square region of fixed area was centered on the centromere to be measured and the Rec8 and CREST intensities were measured in the same region.

3D surface plots of FI were produced using the "Interactive 3D Surface plot" plug-in in ImageJ (Barthel K.U.; Internationale Medieninformatik Berlin, Germany).

Inter-centromere distances were measured as described in 4.5.1. Briefly, "linear" ROI were drawn manually through sister-centromere CREST foci and their FI/length profiles were measured and logged using the "Plot Profile" function in ImageJ. Inter-centromeric distance (Δx) values were calculated using the in-house developed software Extrema™ (Glenis V.; School of civil engineering and geosciences, Newcastle University).

2.10.3 Confocal

With confocal images the "background subtraction" function of the Nikon Elements AR software was used to optimise image quality. 3D rendering of Z-stacks and subsequent distance measurements were performed using Nikon Elements AR software. Z-projections of maximum intensity and general image processing were done using ImageJ software.

2.11 Statistical Analysis

All statistical calculations and relevant data plotting were performed using Minitab (Minitab Inc., USA) or GraphPad Prism (GraphPad Software, Inc.,

USA) software. For numerical values the normality of the distribution of the data was firstly assessed using the either the Kolgomorov-Smirnov test or the D'Agostino and Pearson omnibus normality test. When normal distribution was confirmed, the appropriate parametric test was carried out. If normality was rejected, the appropriate non-parametric tests were performed.

The most commonly used tests for parametric data in this thesis were the unpaired t-test and one-way Anova, followed by a post hoc Tukey's multiple comparison test. The most commonly used non-parametric tests were the Mann Whitney test and the Kruskal-Wallis test, followed by a post hoc Dunn's multiple comparison test. In case a different test was used it will be specified alongside the relevant group of data throughout this thesis.

2.12 Reagents

All chemicals mentioned in this chapter were purchased from Sigma unless otherwise specified.

Ca^{2+}-buffer: 100mM PIPES pH 7.0, 1mM $MgCl_2$, 0.1mM $CaCl_2$, 0.1% Triton X-100

Tyrode's solution: 0.8g NaCl, 0.02g KCl, 0.024g $CaCl_2.2H_2O$, 0.01g MgCl2.6H2O, 0.1g Glucose, 0.4g Polyvinylpyrrolidone. Added to 100ml Milli-Q water and pH adjusted to 2.5 with 5M HCl Aliquoted and stored at -20°C.

0.5M DTT: 77.1g/ml DTT in Milli-Q water. Aliquoted and stored at -20°C

50mM Boric Acid: 0.15g in 50ml of Milli-Q water

0.5% tri-Sodium Citrate: 0.25g $Na_3C_6H_5O_7$ in 50ml Milli-Q water

PBS: Diluted from 10x to 1x with Milli-Q water

Injection Buffer: 1M Tris HCl pH 7.5, 1M KCL in sterile Milli-Q water

Chapter 3 . The effect of female ageing on chromosomal cohesin in oocytes

3.1 Introduction

In mammals, cohesion is established during the S-phase in the foetal ovary and its resolution to allow chromosome segregation may actually take place months (e.g. in mice) or even decades (e.g. in humans) later. This prolonged meiotic arrest, combined with the early establishment of cohesion has given rise to the notion that the maternal ageing effect could be caused by a gradual depletion of cohesin levels. Initial key findings came from *Drosophila melanogaster*, where age-related meiotic nondisjunction errors in oocytes were associated with defects in cohesion (Jeffreys *et al.*, 2003). Since then, various groups including ours have studied a variety of mouse models and have provided evidence that depletion of cohesin during ageing can lead to chromosome missegregation and aneuploidy (Hodges *et al.*, 2005; Liu and Keefe, 2008; Chiang *et al.*, 2010; Lister *et al.*, 2010).

The experiments described in this chapter involve the use of oocytes from C57BL/Icfra^{t} mice, unless otherwise stated. Previous research in our lab has established that the C57BL/Icfra^{t} mouse strain exhibits a distinct maternal age effect with aged oocytes appearing to have lower levels of chromosome-associated cohesin that younger ones. In particular, oocytes from 14-month-old mice exhibited a clear depletion of cohesin on chromosome arms and at centromeres when compared to 2-month-old oocytes at late prometaphase I (Lister *et al.*, 2010). However, given that female ageing is characterised by a prolonged prophase arrest, a key question is whether cohesin depletion occurs during this prophase arrest. Here, the experiments aiming to answer this question are described.

3.2 Cohesin is depleted in oocytes of aged mice

In order to determine whether cohesin is depleted during the extended prophase arrest, I have compared the levels of the cohesin subunit Rec8 in the nuclei of GV-stage oocytes from 2-month and 14-month-aged mice using immunofluorescence (IF) labelling. Fully grown GV-stage oocytes from pre-ovulatory follicles were isolated, spread on PFA-coated slides and stained for Rec8 and CREST. The results show reduction of cohesin levels in oocytes of aged mice (Fig 3.1.A). These results tempted us to investigate even earlier stages of oocyte maturation. Therefore, oocytes from pre-antral follicles were isolated and similarly spread and stained (Staining and image acquisition was performed by Anna Kouznetsova). As with fully-grown GV-stage oocytes, cohesin levels were reduced in immature oocytes of aged mice, showing that cohesin depletion may occur at all the stages of oocyte development (Fig 3.1.B). These findings indicate that cohesin depletion during the protracted prophase arrest of aged oocytes may be a major causative factor in age-related chromosome missegregation during anaphase I of meiosis.

3.3 Cohesin depletion in aged oocytes is linked with disruption of bivalent chromosome structure

In previous immunofluorescence staining experiments we noticed from the CREST staining that sister centromeres are further apart during late prometaphase of MI (GVBD+5hr) in oocytes from 14-month-aged mice compared to oocytes from 2-month-old mice. This observation prompted a more detailed examination aiming to characterise and quantify these variations in sister-centromere apposition.

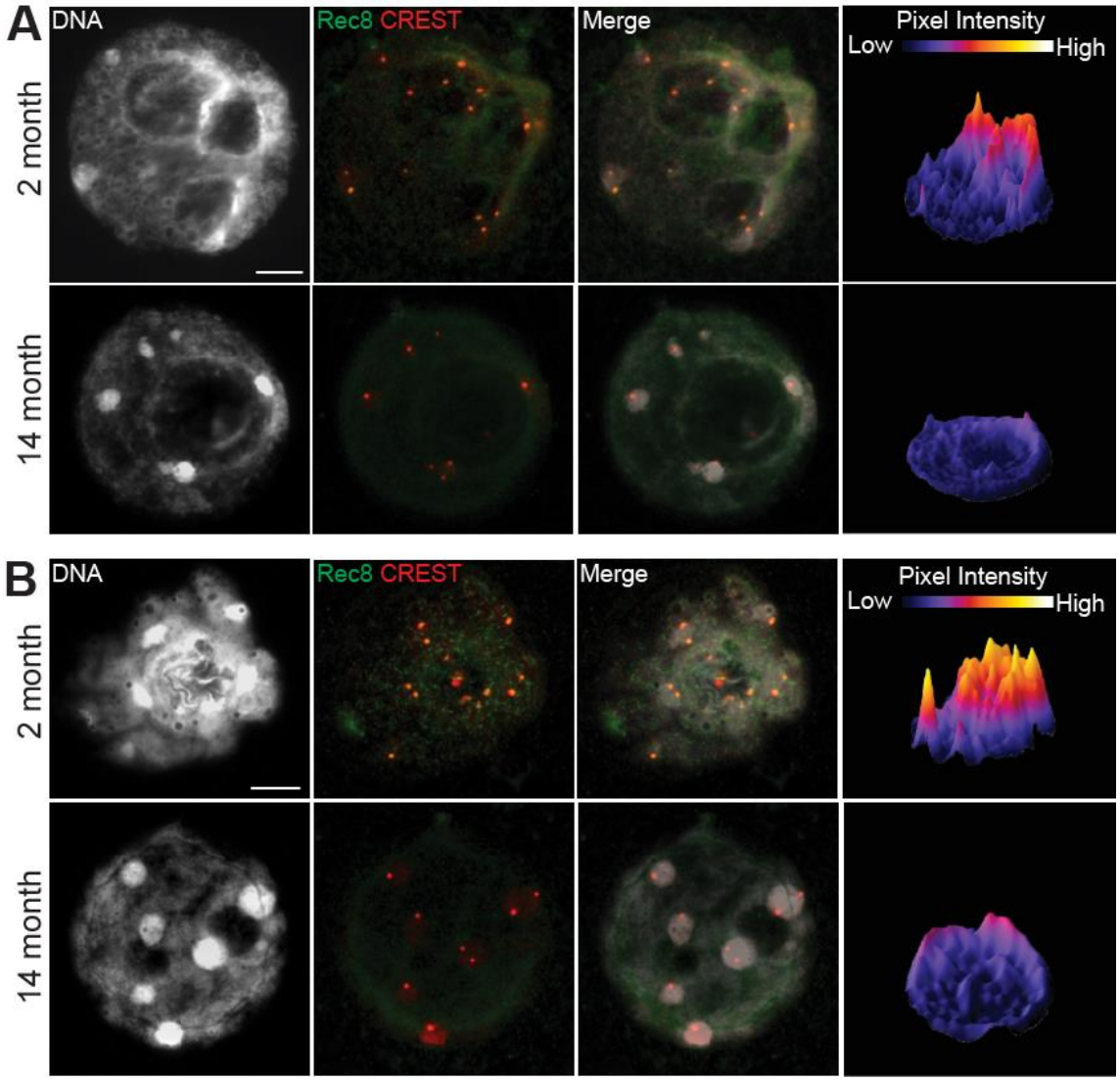

Figure 3.1 Cohesin depletion in oocytes of aged mice.

(A) Representative images showing DNA, Rec8, and CREST immunofluorescence (IF) staining in the nuclei of a fully-grown GV oocyte from 2-month-old (n = 18 oocytes from three mice) and 14-month-old (n = 16 from six mice) mice. Scale bar represents 10μm. Corresponding 3D surface plots show higher Rec8 fluorescence intensity in the 2-month-old compared with 14-month-old GV oocytes. **(B)** Images show DNA, Rec8, and CREST IF staining in the nuclei of oocytes isolated from pre-antral follicles, from 2-month-old (n = 21 from three mice) and 14-month-old (n = 12 from six mice) mice. Scale bar represents 10μm. Corresponding 3D surface plots show higher Rec8 pixel fluorescence intensity in the 2-month-old compared to 14-month- old oocytes. This experiment was performed in collaboration with Anna Kouznetsova.

Oocytes from young and old mice were used to prepare chromosome spreads at late prometaphase of MI (GVBD+5hr) and stained for CREST (Chromosome spreads were prepared by Lisa Lister). CREST antiserum binds to the centromeric proteins CENP-A, CENP-B and CENP-C (Earnshaw and Cooke, 1989) and subsequent staining with a secondary fluorescent probe produces clearly visible and well-defined centromere foci. Sister centromeres were categorized into three groups; sister centromeres that almost overlap each other and appear as single foci, others that are slightly separated and show as adjacent foci and finally some that appear as two well separated foci (Fig 3.2.A). Classification of numerous sister centromere pairs showed that there were significant (P<0.001) differences between young and old mice in all three sister centromere configurations (Fig. 3.2.B), with inter-centromere distance increasing with age. For example, in young oocytes 90% of MI centromeres appeared as "unified", whereas the respective proportion in old oocytes was just 32%.

In order to eliminate any bias that might have entered the sister centromere classification analysis, I have also measured the distances between sister centromeres. Distances were measured from the outer extremities of the pairs, because sister centromeres were often overlapping. Consistent with our previous observation, I have found that inter-centromere distances significantly (P<0.001) increased in old oocytes compared to young oocytes (Fig 3.2.C). Based on these results it could be argued that weakened centromeric cohesion results in loss of the tightly apposed structure of sister centromeres required to promote monopolar attachment of sister centromeres (Hauf and Watanabe, 2004). This is consistent with the finding that monopolar attachment in fission yeast requires Rec8 at the core centromere (Yokobayashi and Watanabe, 2005). Thus, it could be proposed that depletion of cohesin at centromeres creates a bias against monopolar attachment by inducing splitting of sister centromeres.

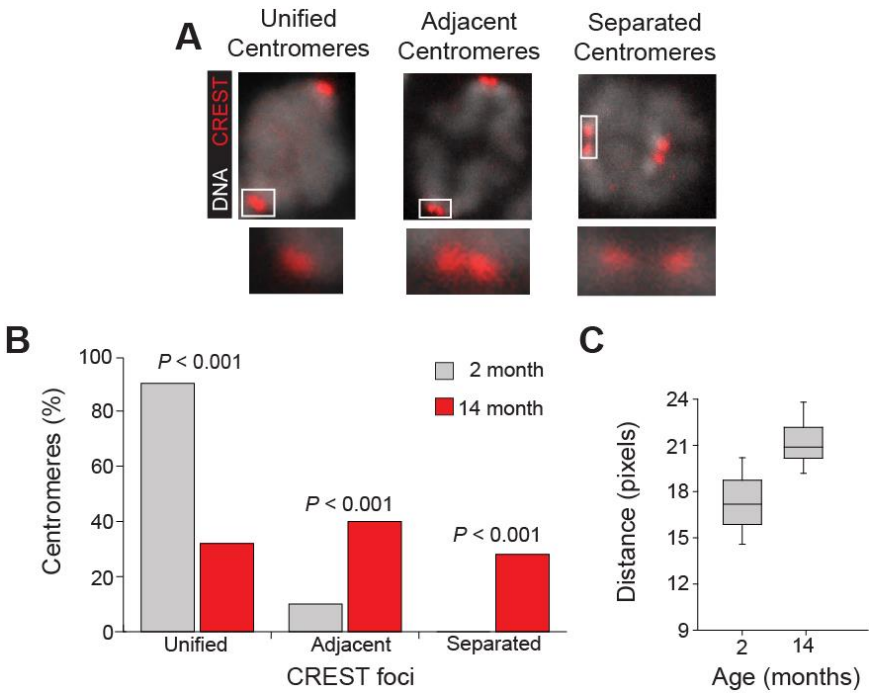

Figure 3.2 Reduced cohesin is associated with splitting of sister centromeres

(A) Representative images of sister centromeres at late prometaphase of M I (GVBD+5h) stained with CREST appearing as unified, adjacent and separated foci. Crest foci surrounded by white boxes are shown in the enlarged images. **(B)** Graph shows the proportions of centromeres in 2-month-old (n = 360 centromeres; 10 oocytes from four mice) and 14-month-old (n = 293 centromeres; 8 oocytes from six mice) oocytes showing unified, adjacent, and separated sister centromeres. The proportion of unified sister centromeres was significantly ($P < 0.001$) reduced in 14-month-old oocytes, whereas the proportion of adjacent and separated foci was significantly ($P < 0.001$) higher compared to 2-month-old oocytes. **(C)** Graph shows the distance between the outer extremities of CREST signals in 2-month-old (n = 218 centromeres; 10 oocytes from one mouse), and 14-month-old (n = 199 centromeres; nine oocytes from four mice) oocytes. The distance was significantly higher in the 14-month-old compared oocytes ($P < 0.001$). The calibrated pixel size for the microscope objective is 66.89 nm. This experiment was performed in collaboration with Lisa Lister.

3.4 Mechanisms of cohesin depletion and the role of Sgo2

During anaphase I, cohesin is removed from chromosome arms by separase-mediated cleavage, which is activated by the APC/C pathway (Buonomo *et al.*, 2000; Kudo *et al.*, 2006). Throughout this process, centromeric cohesin is protected from cleavage by shugoshin (Sgo1 in yeast and Sgo2 in mice) (Kitajima *et al.*, 2004). Sgo2 together with PP2A protects centromeric cohesin throughout anaphase I until metaphase II, thus allowing proper bivalent segregation to occur (Riedel *et al.*, 2006; Lee *et al.*, 2008). Upon fertilization and release into anaphase II, centromeric cohesin is removed by separase allowing sister chromatid segregation to occur.

Having established that Rec8 is significantly depleted in aged MI oocytes the next question was whether this might be the result of a "defective" shugoshin protection mechanism. In particular, we decided to focus on Sgo2, which is known to protect centromeric cohesion in mouse oocytes during anaphase I (Llano *et al.*, 2008) and investigate for differences in its levels between young and aged mice.

3.4.1 Sgo2 levels are reduced in aged mouse oocytes

Mature oocytes from 2-month and 14-month old mice were harvested at the GV stage and were allowed to undergo MI. Chromosome spreads were produced at late prometaphase (GVBD+5h) and chromosome-associated Sgo2 and CREST were detected by immunofluorescence (IF) (Chromosome spreads were prepared by Lisa Lister). Subsequent fluorescence analysis showed that Sgo2 levels were reduced on chromosomes of older oocytes (Fig 3.3.A/B). Interestingly, we found that Sgo2 localises to chromosome arms in young oocytes during prometaphase of MI (Fig 3.3A). As this had not been previously reported, we confirmed specificity of arm staining by performing siRNA-mediated depletion of Sgo2 (Lister *et al.*, 2010). Recruitment of Sgo2 to chromosome arms as well as centromeres raises the possibility that Sgo2 also

functions to protect arm cohesin until the onset of anaphase I. In support of this, data from our lab also indicates that Sgo2 recruits the phosphatase PP2A to arms as well as to centromeres (Lisa Lister, PhD thesis). These results suggest that Sgo2 might protect cohesin even before the onset of anaphase I in mouse oocytes.

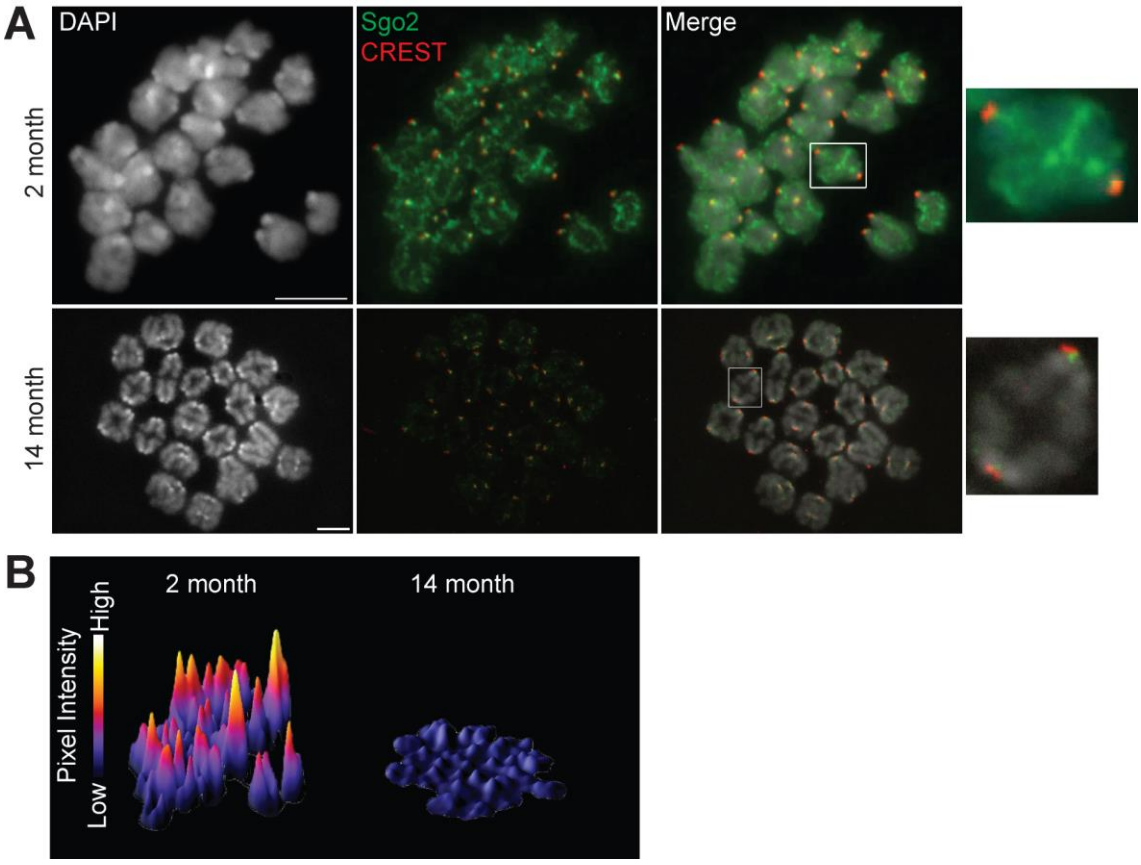

Figure 3.3 Age-related decline in chromosome-associated Sgo2 levels
(A) Representative images of chromosome spreads of oocytes at late prometaphase of MI (GVBD+5h) from 2-month-old mice (n = 20 from three mice) and 14-month-old mice (n = 10 from four mice) stained (IF) for Sgo2 and CREST. Sgo2 levels on chromosomes of oocytes from 14-month-old mice appear reduced. Chromosomes surrounded by white boxes are shown in the enlarged images. Scale bar represents 10 μm. (B) 3D surface plots of images in (A) showing higher Sgo2 fluorescence intensity on chromosomes of 2-month-old compared to 14-month-old oocytes. This experiment was performed in collaboration with Lisa Lister.

3.4.2 Sgo2 becomes enriched on chromosomes during the transition from prophase to metaphase of MI

In view of the results presented above, it was of particular interest to investigate the relationship between cohesin and Sgo2 depletion. Therefore, we asked

whether Sgo2 is recruited on the chromosomes during prophase arrest of oocytes. To address this question, chromosome spreads from fully-grown prophase-arrested oocytes were prepared and stained for Sgo2 and CREST, using the same techniques as for prometaphase oocytes. The findings indicate that at this stage most of Sgo2 is localised into the nucleolus and only a small fraction appears to colocalise with DNA (Fig 3.4). For the time being, although it is still unclear at which stage during the oocyte's development Sgo2 is recruited on the chromosomes, it could positively be argue that Sgo2 localisation on the chromosomes is gradually increased during transition from late prophase to metaphase of MI. Thus, Sgo2 might not be playing its putative protective role during the prolonged prophase-arrest.

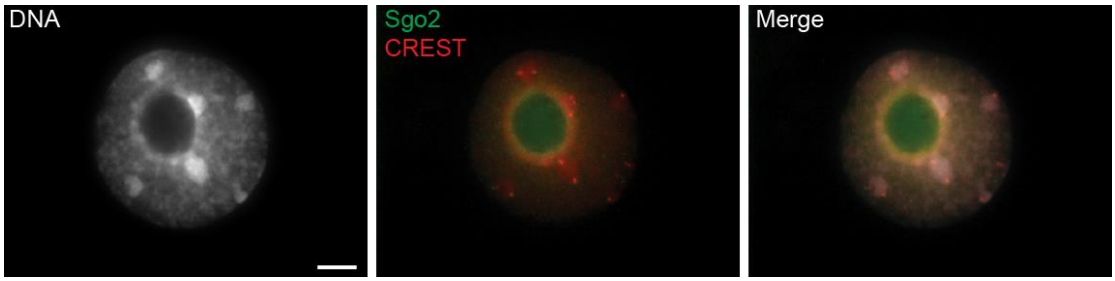

Figure 3.4 Localisation of Sgo2 in GV-stage mouse oocytes
Image of the nucleus of a fully-grown prophase I-arrested oocyte stained (IF) for Sgo2 and CREST, using the same techniques as for prometaphase oocytes. It appears that at this stage most of Sgo2 is localized into the nucleolus with only a small fraction colocalised with DNA.

3.4.3 Sgo2 levels are reduced in Smc1β$^{-/-}$ mouse oocytes

The next step was to investigate the possibility that the observed recruitment of Sgo2 in oocytes from aged females might as well be a consequence and not exclusively a putative causative factor of cohesin depletion. To assess that, we have used the *Smc1β* knockout mouse (Revenkova *et al.*, 2004). In mouse meiocytes, Smc1β is involved in maintenance of sister chromatid cohesion, and in *Smc1β*$^{-/-}$ oocytes defective sister chromatid cohesion has been shown to lead to a massive increase in aneuploidy (Revenkova *et al.*, 2004), which is further amplified by age (Hodges *et al.*, 2005). If Sgo2 levels in Smc1β depleted oocytes are equal with that of Smc1β wild type oocytes, it would imply that levels of

chromosome-associated Sgo2 are independent of the levels of the established chromosome-associated cohesin.

Chromosome spreads from *Smc1β*$^{+/+}$ and *Smc1β*$^{-/-}$ late prometaphase (GVBD+5h) oocytes were prepared and immunolabeled (IF) for Sgo2 and CREST (Chromosome spreads were prepared by Lisa Lister). Analysis of the IF signal has shown that *Smc1β*$^{-/-}$ oocytes exhibit lower levels of chromosome associated Sgo2 (Fig 3.5.A/B). This indicates that in mouse oocytes, cohesin is either directly or indirectly required for recruitment of Sgo2. This is consistent with results from studies on maze meiosis (Hamant *et al.*, 2005).

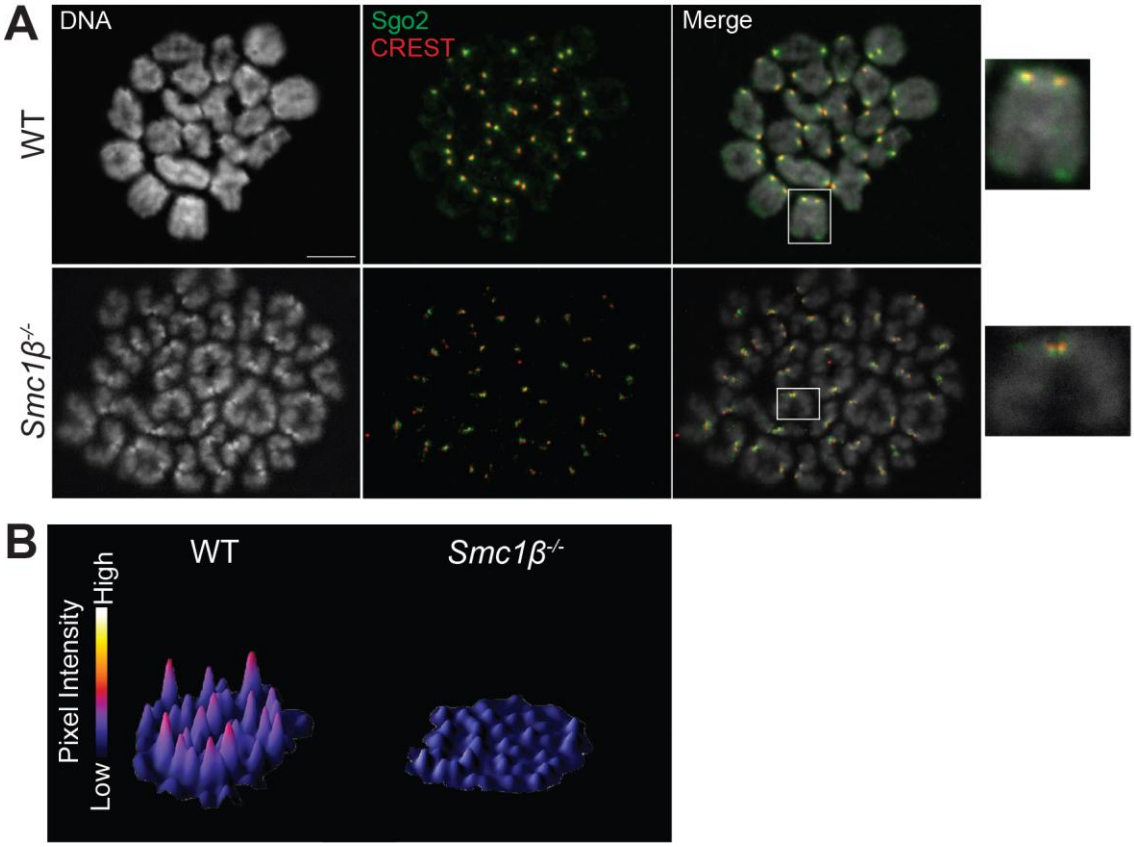

Figure 3.5 Reduced levels of chromosome-associated Sgo2 in *Smc1β*$^{-/-}$ mouse oocytes

(A) Representative images of chromosome spreads of oocytes at late prometaphase (GVBD+5h) from *Smc1β*$^{+/+}$ mice (n = 32 from three mice) and *Smc1β*$^{-/-}$ mice (n = 20 from three mice), stained (IF) for Sgo2 and CREST. Sgo2 levels on chromosomes of *Smc1β*$^{-/-}$ mice appear reduced. Note loss of bivalent association *Smc1β*$^{-/}$ oocytes due to depleted cohesin levels. Chromosomes surrounded by white boxes are shown in the enlarged images. Scale bar represents 10 μm. (B) 3D surface plots of images in (C) showing reduced Sgo2 fluorescence intensity on chromosomes of *Smc1β*$^{-/-}$ oocytes compared with wild-type oocytes. This experiment was performed in collaboration with Lisa Lister.

3.5 Discussion

This chapter represents an investigation of the hypothesis that cohesin loss during the protracted arrest of oocytes at prophase I is a leading causative factor of age-related aneuploidy. Overall, I have presented evidence that chromosome-associated Rec8 is reduced in growing and fully grown prophase arrested oocytes of aged mice (Fig 3.1) and this decrease correlates with an increase in the distance between sister chromatid centromere during late prometaphase (Fig 3.2). Moreover, we found that Sgo2 becomes enriched on chromosomes during the transition from prophase to metaphase of MI (Fig 3.4) and that this is markedly reduced in oocytes of aged mice (Fig 3.3). Finally, we have shown that Sgo2 is reduced in oocytes of *Smc1β*$^{-/-}$ mice (Fig 3.5).

3.5.1 Cohesin depletion in oocytes of aged mice

Previous studies investigating the effect of cohesin depletion in vertebrate meiocytes has depended on the introduction of genetic perturbations. Mouse strains deficient for SMC1β and REC8 have been generated, giving rise to sterile female and male mice (Bannister *et al.*, 2004; Revenkova *et al.*, 2004). *Rec8*$^{-/-}$ spermatocytes exhibited abnormal synapsis and deficiency in sister chromatid cohesion, and in *Rec8*$^{-/-}$ females the oocyte pool disappeared during embryonic development, thus precluding the use of this strain for research into oocyte ageing (Bannister *et al.*, 2004; Xu *et al.*, 2005). *Smc1β* KO mice, although they are also sterile, provided evidence that cohesin is a prime candidate for the molecular link between female age and oocyte aneuploidy. This strain exhibits an accelerated age-related loss of oocytes, which almost disappeared after 8 months of age and even young mice exhibit premature loss of sister chromatid cohesion along chromosome arms and at centromeres (Revenkova *et al.*, 2004; Hodges *et al.*, 2005). Importantly, SMC1β deficient oocytes show a striking age-depended destabilisation of chiasmata, resulting in an accumulation of distally associated and separated homologues during metaphase I (Hodges *et al.*, 2005). In a study investigating cohesin behaviour outside the context of genetically

engineered mice, it has been reported that premature sister chromatid separation strongly correlated with reduced levels of chromosome associated REC8, SMC1β and STAG3 in oocytes from older females (Liu and Keefe, 2008). However, the latter study utilized a senescence-accelerated wild-type mouse strain, and since the molecular basis for ageing-acceleration is yet unknown, the conclusion might not describe accurately the mechanisms involved in age-associated loss of cohesion.

Unlike the experimental systems described above, here we have used oocytes of a long-lived, non-mutant mouse model, which we have shown to exhibit age-related loss of cohesin amongst other meiotic defects in oocytes (Lister *et al.*, 2010). The conclusion that oocyte chromosomal cohesin was depleted during female ageing was based on analysis of prometaphase of MI chromosomes (Lister *et al.*, 2010), however, as ageing is characterised by prolonged prophase arrest, a key question was whether cohesin is already depleted during prophase arrest. To test this I have measured colocalisation of Rec8 and DNA in fully grown and growing prophase-arrested oocytes. Compared with prometaphase of MI chromosomes, the chromatin of prophase-arrested oocytes is diffuse and is enclosed in the nucleus (GV). Moreover, the chromatin configuration appeared to vary widely and is probably influenced by transcriptional activity in the growing oocyte. Furthermore, the centromeric CREST signal used to normalize cohesin levels on prometaphase of MI chromosomes, were not distinct in many oocytes. This made it difficult to perform a quantitative assessment of chromosome –associated cohesin levels. To address this problem, I have employed the use of fluorescence intensity 3D surface plots.

My findings (Fig 3.1) indicate that loss of cohesion takes place during the growing phase of prophase-arrested oocytes. What mechanisms could be responsible for this loss? Is cohesin being actively replenished in growing prophase-arrested oocytes or does the oocyte rely just on the cohesin that is

loaded on meiotic chromosomes during fetal development? If the former is true then the observed cohesin loss in aged oocytes would imply a decline in this putative cohesin-reloading process and/or a decrease of cohesin reserves, likely due to impaired expression. Two recent mouse studies have elegantly addressed these questions and have surprisingly shown that cohesin loaded onto chromosomes during fetal development is sufficient to maintain cohesion even in aged oocytes (Revenkova *et al.*, 2010) and that there is little or no cohesin replenishment on meiotic chromosomes during postnatal prophase I arrest (Tachibana-Konwalski *et al.*, 2010). So, considering that low levels of Smc1β transcripts have been detected in growing oocytes (Hodges *et al.*, 2005; Revenkova *et al.*, 2010), and that Rec8 protein levels appear to be similar between young and aged mice (Chiang *et al.*, 2010) the data I present here suggest that *de novo* cohesin synthesis is insufficient and probably not used for counteracting the depletion of chromosomal cohesion during ageing.

Various assumptions could be made regarding the mechanism(s) responsible for cohesin loss during prophase arrest. It is likely that the observed age-related depletion of cohesin could be due to degeneration of cohesin subunits, for example by oxidative stress. Alternatively, a mechanism that protects cohesin might be in place during prophase arrest and its gradual deterioration during ageing could lead to premature removal of cohesin from chromosomes. It is also conceivable that cohesin removal might be caused by a low background activity of either separase or a meiotic equivalent of the mitotic "prophase pathway". Prolonged exposure to such a "cohesin-hostile" environment could provide a simple explanation for the cohesion depletion phenomenon in aged oocytes.

The next crucial step in this work is to establish whether cohesin loss is confined to the oocyte growth phase, or whether it is also a feature of primordial oocytes, which represents a relatively quiescent state, in which

oocytes remain for the vast majority of their lifespan. This question is the subject of ongoing research in the lab.

3.5.2 Female ageing is associated with loss of the closely apposed structure of sister kinetochores required for their monopolar attachment

Apart from maintaining the integrity of bivalent and dyad chromosomes until anaphase I and anaphase II, respectively, (Watanabe, 2005) cohesin plays another important role during MI. Studies in fission yeast indicate that cohesin at the core centromere promotes the establishment of monopolar attachment of sister kinetochores on the MI spindle, by keeping sister centromeres closely apposed (Watanabe and Nurse, 1999; Sakuno and Watanabe, 2009). Studies in plants have also provided similar evidence supporting the role of centromeric cohesin in the establishment of correct Kt-Mt attachments during MI (Chelysheva *et al.*, 2005; Li and Dawe, 2009).

The depletion of cohesin in aged mouse oocytes (Lister *et al.*, 2010) prompted us to investigate whether sister centromeres have lost their tight association. Indeed, based on centromere staining, I have shown here that the majority of sister centromeres in aged oocytes appear as two distinct foci, whereas in young oocytes they are predominantly merged into a single focus (Fig 3.2.A/B). By measuring the distance between the extremities of the CREST signals at sister centromeres, I found that the inter-centromeric distance is increased in aged oocytes compared to young ones (Fig 3.2.C). These results are consistent with findings in another naturally aged mouse strain (Chiang *et al.*, 2010) and indicate that reduced centromeric cohesin levels at MI are associated with a failure of sister centromeres to maintain their tightly apposed structure. Given the importance of centromeric cohesion for correct Kt-Mt attachments in other organisms, it is likely that separation of sister Kts during prometaphase of MI creates a bias against monopolar attachment of sisters. In support of this, live-cell imaging of oocyte chromosomes during progression through MI, revealed

that the majority of oocytes from aged mice showed anaphase defects ranging in severity, from a single lagging chromosome, to large clumps of chromatin trapped in the spindle mid zone (Lister *et al.*, 2010). These defects are considered to be the hallmark of erroneous Kt-Mt attachments (Sakuno *et al.*, 2011). Thus, splitting of sister centromeres may be a major contributor to age-related missegregation during MI, by creating unpropitious prospects for stable biorientation and segregation of homologous chromosomes.

3.5.3 The role of Sgo2 in cohesin depletion

Mouse Sgo2 has been shown to be essential for protecting centromeric cohesin during anaphase I (Lee *et al.*, 2008; Llano *et al.*, 2008). Several lines of evidence indicate that cohesin is lost from centromeres in oocytes from aged mice. First, immunofluorescence labeling revealed reduced levels of centromeric Rec8 in oocytes of aged mice (Lister *et al.*, 2010). Second, complete loss of centromeric cohesion leading to premature separation of sisters was prevalent in MII oocytes from aged mice (Lister *et al.*, 2010). Moreover, the increased distance between sister centromeres discussed above is likely linked to cohesin depletion at centromeres. Together these findings raise the possibility that the mechanisms responsible for protecting cohesin at centromeres are compromised during female ageing. To address this we have measured and compared the levels of chromosome associated Sgo2, between young and aged oocytes. Our findings indicate that Sgo2 is actually massively reduced in aged oocytes (Fig 3.3).

Interestingly, we found that Sgo2 localises to chromosome arms in young oocytes during prometaphase of MI (Fig 3.3A). Unpublished live-cell imaging data (Ahmed Rattani; Nasmyth Lab) also suggest that Sgo2 localises along the entire chromosome during prometaphase I and is gradually restricted to the centromere prior to anaphase I. It is conceivable that Sgo2 and its partner PP2A

might be protecting arm cohesin to ensure timely removal by separase during exit from MI. Possible mechanisms by which cohesin might be removed before the onset of anaphase I, could involve phosphorylation of cohesin subunits promoting its dissociation in a prophase pathway-like manner.

The above data raised the possibility that Sgo2 might be protecting cohesin prior to anaphase I. However, my findings indicate that Sgo2 becomes enriched on chromosomes during the transition from prophase to metaphase of MI (Fig 3.4), indicating that it is recruited at this stage. Therefore, although we cannot exclude the possibility that Sgo2 might move on and off the chromosomes during prophase arrest, the data suggest Sgo2 is unlikely to be guarding cohesin's integrity during prophase arrest.

Finally, in this chapter we have shown that the level of chromosome-associated Sgo2 was reduced in oocytes of *Smc1β*$^{-/-}$ mice (Fig 3.5). This observation, consistent with findings in maize meiosis (Hamant *et al.*, 2005), suggests that Sgo2 depletion could be a consequence of cohesin loss. Therefore, we propose a model where cohesin loss during prophase arrest impairs recruitment/retention of Sgo2 during prometaphase I, thereby amplifying further cohesin depletion during prometaphase I. This could subsequently lead to cohesin depletion below the 10% threshold (Chiang *et al.*, 2010), thus promoting chromosome missegregation. Given that recruitment of Sgo2 to centromeres appears to be regulated by various factors, including Bub1 (Kitajima *et al.*, 2004; Huang *et al.*, 2007) and Aurora B (Huang *et al.*, 2007) kinase activities, and that recently MAD2 was identified to interact with SGO2 in human and *X. laevis* (Orth *et al.*, 2011), our observation that Sgo2 is depleted in aged oocytes actually raises many questions regarding its etiology and possible repercussions.

Chapter 4 . Characterisation of Plk1 mediating chromosome segregation during Meiosis I of the mouse oocyte

4.1 Introduction

Mammalian oocytes arrest at prophase of meiosis I (MI) during embryonic development and only resume meiosis when they receive the appropriate ovulatory cues. Meiotic resumption leads to a reductional chromosome segregation followed by an immediate entry into meiosis II (MII), without an intervening round of DNA replication, and a subsequent arrest at metaphase. Upon fertilisation MII resumes leading to an equatorial chromosome segregation, after which the zygote enters interphase. Meiotic resumption and passage through the two rounds of chromosome segregation of meiosis demands a high level of coordination of cellular processes to ensure accurate chromosome segregation and to prevent aneuploidy. Synchronization of meiotic events is achieved through an intrinsically complex interplay of interconnected regulatory pathways, where kinases and phosphatases play central roles. Cyclin-dependent kinases (Cdks), Aurora kinases and Polo-like kinases (Plks) are key to regulating various meiotic processes including meiotic arrest/progression, chromosome dynamics and spindle assembly/disassembly. This chapter focuses on the role of Plk1 during MI.

A significant step in uncovering the roles of Plk1 during mitosis has been the recent development and application of specific small-molecule inhibitors allowing acute inactivation of Plk1. The dihydropteridinone BI 2536, an ATP-competitive drug, is currently the best-established small-molecule inhibitor of Plk1 (Lenart *et al.*, 2007; Steegmaier *et al.*, 2007). It exhibits a potent and highly selective function as it can inhibit Plk1 *in vitro* with an IC50 of 0.83nM, while showing negligible activity against a panel of 63 other kinases (Steegmaier *et al.*, 2007). There are several advantages in the use of BI 2536 to study Plk1 function during meiosis. Firstly, it is highly penetrant and acts fast, thus allowing precise

temporal control of Plk1 inhibition at any desired stage. Moreover, it can be combined with other treatments, its effect is reversible and by varying the applied dose, various phenotypes could be revealed. Importantly, although it inhibits the enzymatic function of Plk1, it still allows the kinase to function as a scaffold for protein-protein interactions, which would not be feasible if other methods of inactivation, such as RNA interference or genetic modification, were applied (Taylor and Peters, 2008).

Previous studies have shown that the activity of Plk1 increases during meiotic maturation, but little is known about its function in oocytes. This chapter aims to perform a functional analysis of Plk1 in mammalian oocytes. To achieve that the chemical inhibitor of Plk1, BI 2536 has been used in combination with indirect immuno-fluorescence (IF) staining and live-cell imaging of oocytes injected with mRNAs encoding fluorescent proteins.

4.2 Plk1 is recruited to the kinetochore after release from prophase I arrest

Enzymes do not just wander aimlessly inside the cell. Their localisation is directly associated and indicative of their function and vice versa. Therefore, a first step in investigating the role of Plk1 during meiotic maturation was to identify its localisation. To achieve that, fully-grown oocytes from CD1 mice were harvested at the GV stage and were allowed to undergo MI. Chromosome spreads were produced using oocytes at the GV-stage, early prometaphase I, late prometaphase I and Met-II arrest (Fig 4.1).

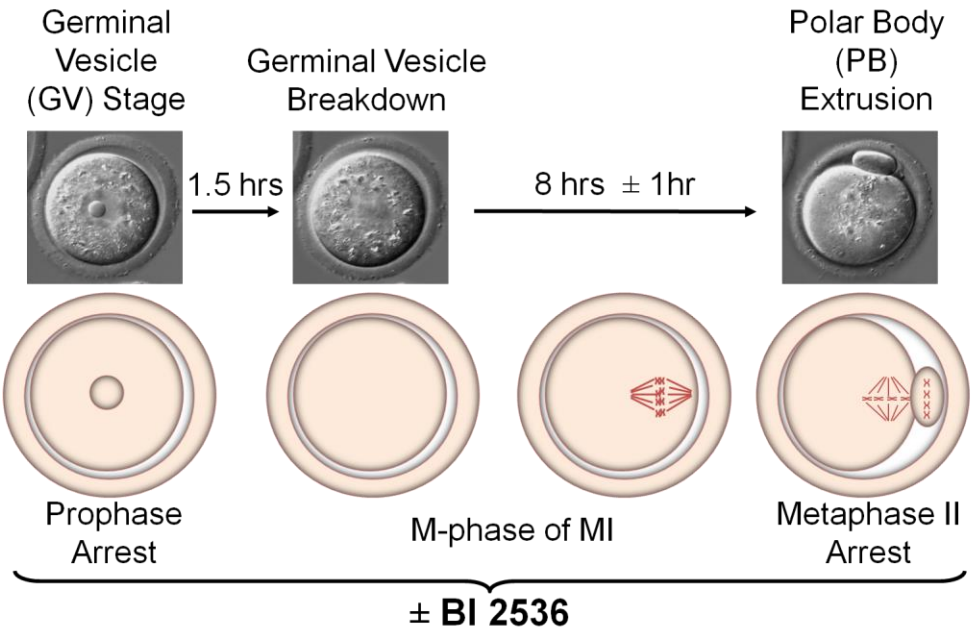

Figure 4.1 Experimental design.

Diagrammatic representation of the experimental methodology. Mature prophase arrested oocytes were harvested from CD1 mice and were allowed to undergo MI in media with or without BI 2536.

IF staining against Plk1 and CREST revealed that Plk1 is localised near the CREST foci at the GV-stage (Fig 4.2A), to the centromere of prometaphase I chromosomes (Fig 4.2B,C) and to the centromere of Met-II arrested chromosomes (Fig 4.2D), albeit at much lower levels compared to centromeric prometaphase I levels. A first look of the chromosome spreads at prometaphase I gives the impression that Plk1 shows both inner- and outer-centromere localisation. However, upon closer inspection Plk1 foci actually appear to have a common orientation on each individual chromosome spread (e.g. in Fig 4.2B they all "look" south, whereas in Fig 4.2C they all "look" west). This orientation suggests that Plk1 is localised to the kinetochore, which during the process of chromosome spreading may collapse on either side of the centromeric CREST foci, thus giving the wrong impression of being at the inner-centromere region of chromosomes. Similar observations were made for Met-II stage chromosome spreads, suggesting that during that stage of meiosis Plk1 is also localised to the kinetochore region of chromosomes.

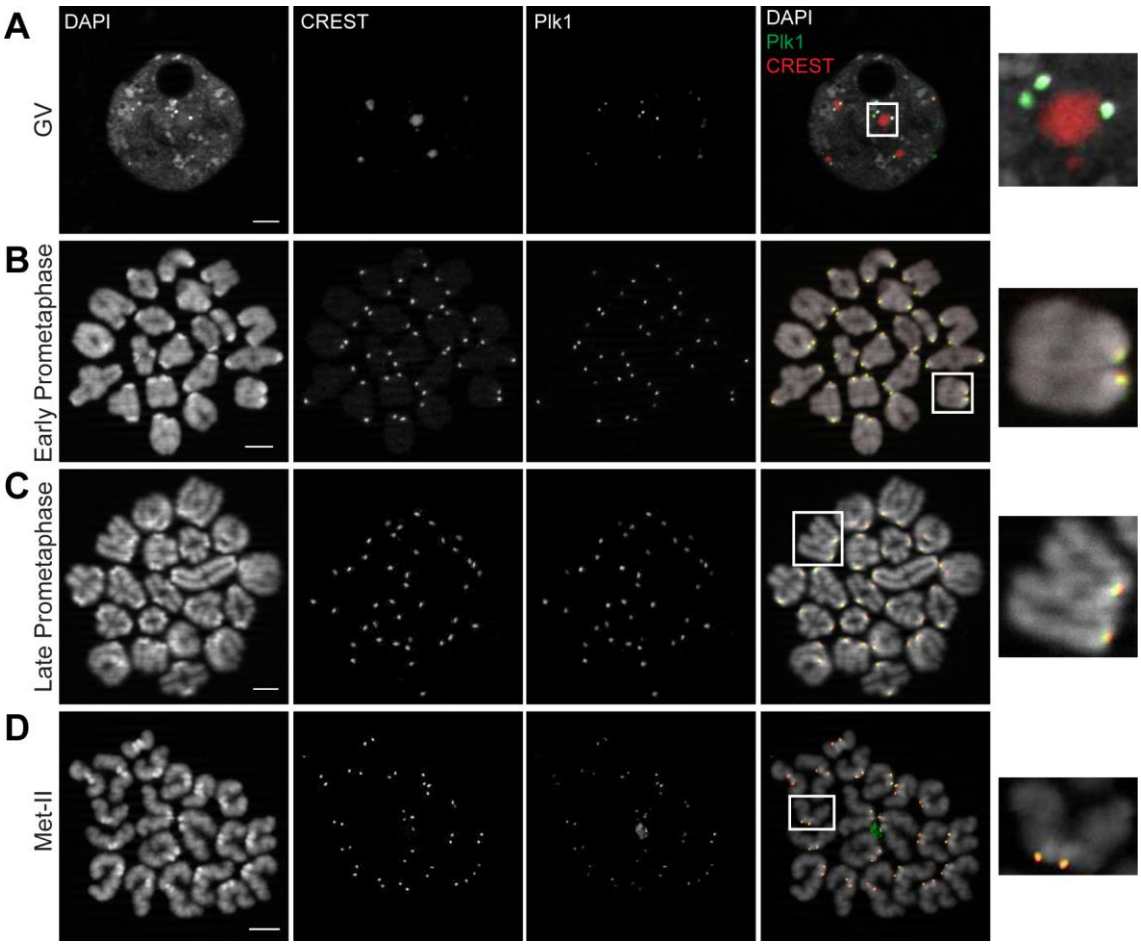

Figure 4.2 Plk1 is enriched at the centromere upon meiotic resumption.
(A) Images show the nucleus of a prophase-arrested (GV-stage) oocyte. Representative images show DNA, Plk1, and CREST staining in the nucleus of a fully-grown GV-stage oocyte (n = 7 oocytes from three mice). **(B)** Representative images showing DNA, Plk1, and CREST staining of chromosome spreads prepared during early prometaphase of MI (GVBD + 2 hr). **(C)** Representative images showing DNA, Plk1, and CREST staining of chromosome spreads prepared during late prometaphase of MI (GVBD + 5 hr). **(D)** Representative images showing DNA, Plk1, and CREST staining of chromosome spreads prepared at the MetII-arrest stage. Notably, samples had to be exposed to the appropriate excitation wavelength for longer compared to (B) and (C) in order to "visualise" the Plk1 signal at the centromere of Met-II oocytes. Plk1 and CREST foci (A) and chromosomes (B, C, D) surrounded by white boxes are shown in the enlarged images. Scale bars represent 10 μm.

4.3 BI 2536 does not prevent recruitment of Plk1 to the kinetochore during MI

Next step was to assess the effect of BI 2536 on chromosome localisation of Plk1. Fully-grown oocytes from CD1 mice were harvested at the GV stage and were allowed to undergo MI in media supplemented with 6.25nM BI 2536 (Fig 4.1). Chromosome spreads were prepared using oocytes at early and late prometaphase of MI. Staining against Plk1 and CREST revealed that Plk1 localised to the kinetochore of prometaphase I chromosomes (Fig 4.3). These results suggest that the concentration of BI 2536 used here does not prevent recruitment of Plk1 to the kinetochore during meiotic resumption. Interestingly, the chromosomes of BI 2536-treated oocytes were characterised by extremely short chromosome arms (e.g. Fig 4.3.B/enlarged image). As it will be shown in later images (Fig 4.6), this hyper-condensation effect became more severe as the concentration of BI 2536 increased. This observation is consistent with previous studies describing chromosome condensation defects when Plk1 function was perturbed (Losada *et al.*, 2002; Gimenez-Abian *et al.*, 2004; Jeong *et al.*, 2010). These results suggest that Plk1 kinase activity is required to curtail chromosome condensation.

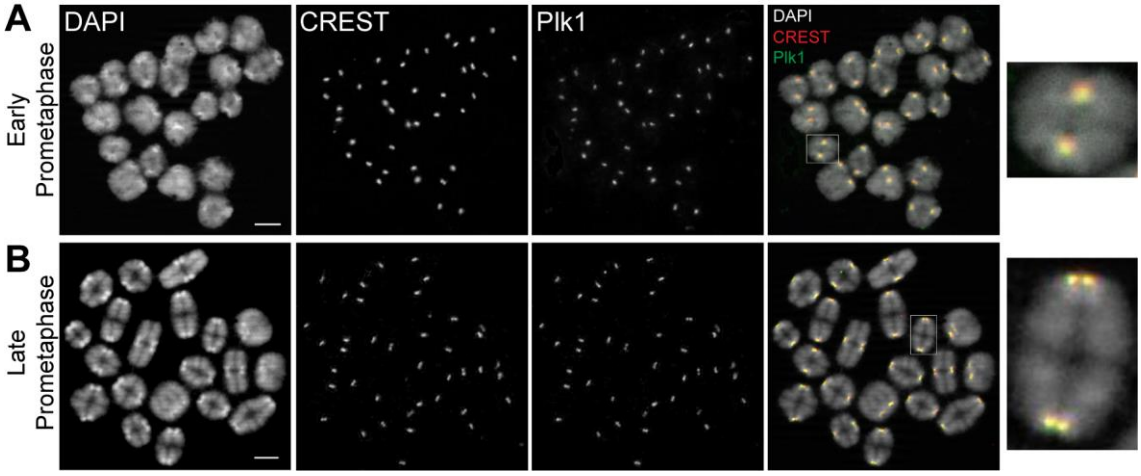

Figure 4.3 BI 2536 does not prevent recruitment of Plk1 to the kinetochore during MI.

Representative images showing DNA, Plk1, and CREST staining of chromosome spreads prepared using oocytes cultured in media supplemented with 6.25nM BI 2536 (A) during early prometaphase (GVBD + 2 hr) and (B) late prometaphase (GVBD + 5 hr) of MI. Chromosomes surrounded by white boxes are shown in the enlarged images. Scale bars represent 10 μm.

4.4 BI 2536 does not affect the timing of entry into prometaphase of MI in mouse oocytes

Previous studies on somatic cells have reported that BI 2536 causes a significant delay in Nuclear Envelope Breakdown (NEB) during mitosis. In order to assess if BI 2536 has a similar effect on GVBD (entry into prometaphase) during oocyte MI, I performed a series of *in vitro* dose-response experiments.

4.4.1 Effect on the timing of GVBD with short exposure to BI 2536

Fully-grown oocytes from CD1 mice were harvested at the GV stage and were allowed to undergo MI in control medium and medium supplemented with 3/4/6.25/12.5 and 25nM BI 2536. Under control conditions, GVBD normally occurs within 1h of removal from IBMX, which maintains arrest at the GV stage by inhibiting cAMP phosphodiesterases and maintaining high cAMP levels inside the oocyte (Schultz *et al.*, 1983). Moreover, based on empirical observations, oocytes that undergo GVBD within 1 to 2 hours of removal from IBMX are competent to successfully reach the MetII arrest stage.

In this set of experiments the percentage of oocytes in each group that underwent GVBD within 1.5-2h varied in the range of 75-100% (Fig 4.4A) and statistical analysis showed that the concentrations of BI 2536 used had no significant effect on the timing of GVBD ($P>0.05$).

Thus, consistent with what has been observed previously (Vanderheyden *et al.*, 2009), the tested BI 2536 concentrations do not cause a delay in GVBD in oocyte meiosis.

4.4.2 Effect on the timing of GVBD with prolonged exposure to BI 2536

Small molecule chemical inhibitors such as BI 2536 are generally highly penetrant and exhibit a rapid biochemical effect even at low concentrations

(Steegmaier *et al.*, 2007). In order to eliminate the possibility that absence of an effect on GVBD timing might be due to delayed action of BI 2536, I decided to prolong the exposure to BI 2536 to 48h, prior to releasing the oocytes from prophase arrest.

Fully-grown prophase arrested oocytes were harvested from CD1 mice and were cultured in control medium and medium supplemented with 6.25nM BI 2536. Both media were also supplemented with IBMX in order to keep oocytes arrested at prophase of MI. After 48h of incubation oocytes were transferred to control medium and medium supplemented with 6.25nM BI 2536, and were allowed to resume MI. The average percentage of oocytes in each group that underwent GVBD within 1.5-2h varied between 80% and 100% (Fig 4.4B). Statistical analysis of these results showed that prolonged incubation at 6.25nM BI 2536 did not impede the transition from prophase-arrest (GV) to prometaphase of MI compared to control (P=0.5).

Moreover, comparing these results with the previous relevant results (i.e. Control, 6.25nM BI 2536) from short exposure to BI 2536, leads to the conclusion that GVBD timing remains unaffected with either short or prolonged exposure to 6.25nM BI 2536 ($P>0.05$).

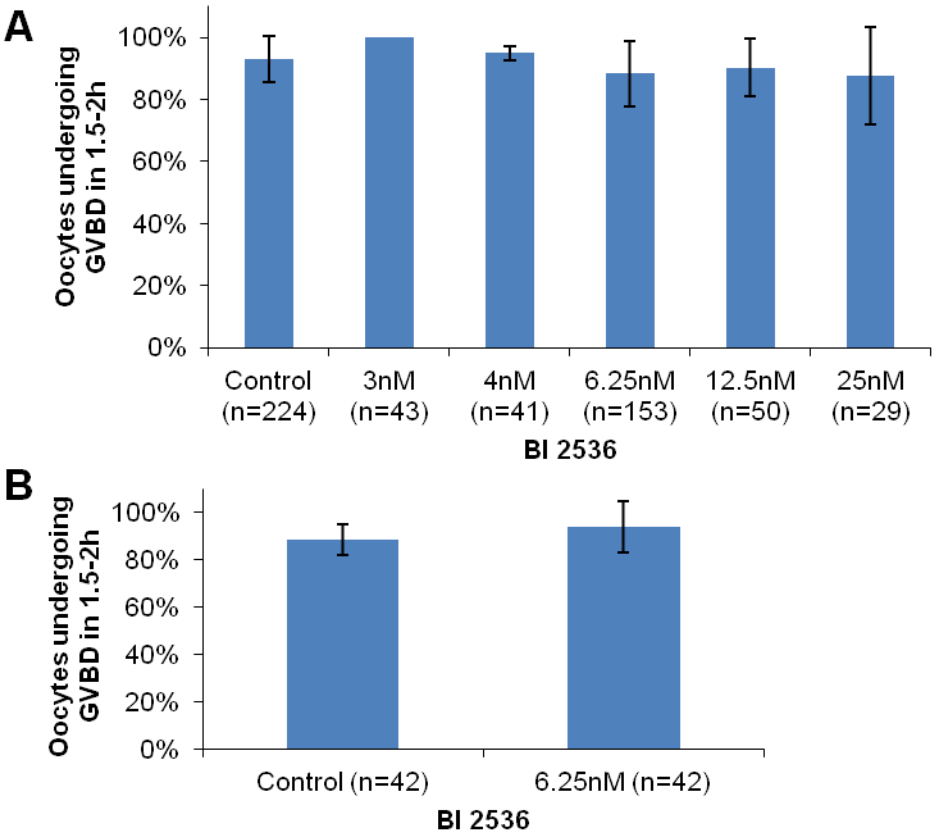

Figure 4.4 BI 2536 does not affect the timing of entry into prometaphase of MI
(A) Average percentage of oocytes undergoing GVBD in 1.5-2h at various BI 2536 concentrations: Control, 92.87% (±7.47% SD); 3nM BI2536, 100% (±0% SD), 4nM BI 2536, 94.88% (±2.19% SD); 6.25nM BI 2536, 88.33% (±10.57% SD); 12.5nM BI 2536, 90.26% (±9.22% SD); 25nM BI 2536, 87.79% (±15.75% SD). No significant difference was observed between the different groups (P>0.05). **(B)** Average percentage of oocytes undergoing GVBD in 1.5-2h after exposure to 6.25nM BI 2536 for 48h: Control, 88.33% (±6.41% SD); 6.25nM BI 2536, 93.75% (±10.82 SD). No significant difference was observed between the two groups (P=0.5). Errors bars indicate ±SD.

4.5 BI 2536 inhibits exit from MI in a dose-dependent manner

Once I established that prolonged exposure to BI 2536 was not necessary to exert its effect, the next step was to investigate for possible effects on the ability of oocytes to exit MI and extrude their first PB. As previously, fully grown, prophase arrested oocytes from CD1 mice were harvested and were allowed to progress through MI in control medium and medium supplemented with 3/4/6.25/12.5 and 25nM BI 2536. After 20h of culture, oocytes that had completed MI, as assessed by the presence of the first PB, were scored in each group. I also prepared chromosome spreads to verify the scored numbers and avoid mistakes due to oocytes retracting their PBs. Under normal conditions, the first PB extrusion occurs 10-12h after release from prophase arrest.

In this set of experiments, concentration as low as 3nM and 4nM BI2536 did not have an effect on the ability of oocytes to exit MI, compared with control oocytes ($P>0.05$) (Fig 4.5). However, at higher concentrations the proportion of oocytes in each group that did not exit MI increased in a dose-dependent manner, ranging from 54.76% (±16.84% SD) in 6.25nM to 100% in 25nM BI 2536 ($P<0.05$) (Fig 4.5).

Overall, these results indicate that BI 2536 inhibits exit from MI in a dose-dependent manner, with 25nM producing a fully penetrant phenotype.

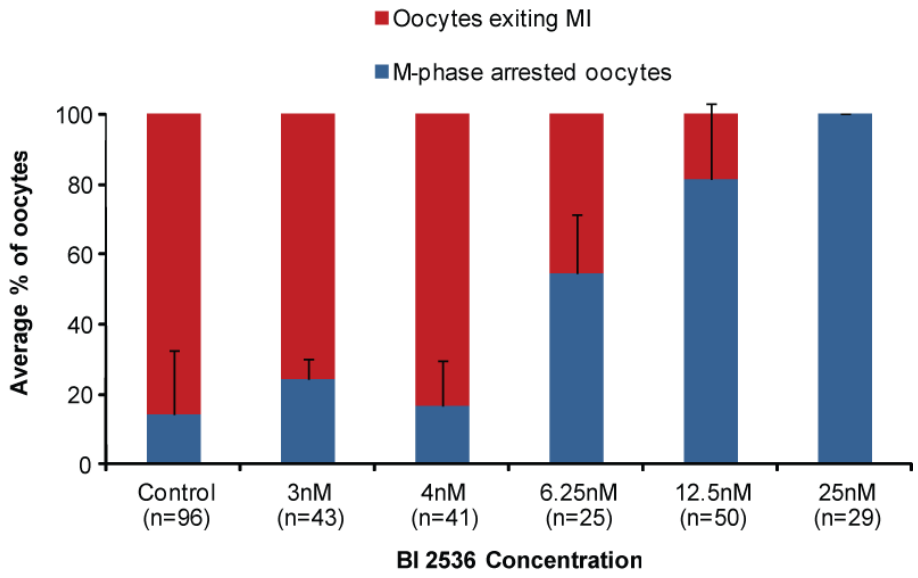

Figure 4.5 BI 2536 inhibits exit from MI in a dose-dependent manner

The graph shows the average percentages of oocytes that exit MI and arrest at MI with increasing concentrations of BI 2536: Control, 14.09% (±18.64% SD); 3nM BI2536, 24.29% (±6.06% SD), 4nM BI 2536, 16.53% (±13.28% SD); 6.25nM BI 2536, 54.76% (±16.84% SD); 12.5nM BI 2536, 81.62% (±21.24% SD); 25nM BI 2536, 100% (±0% SD). Statistical analysis of these results showed a significant difference between the following groups: Control vs. 6.25/12.5/25nM; 3/4nM vs. 12.5/25nM; 6.25nM vs.25nM (P<0.05). Notably, 25nM of BI 2536 are adequate to produce a fully penetrant phenotype. Error bars indicate +SD.

4.5 Oocytes arrested in MI in the presence of BI 2536 do not undergo anaphase.

Previous studies have shown that BI 2536 can inhibit mitotic M-phase at different stages depending on the timing of application; early application could inhibit anaphase, whereas late application may allow anaphase and inhibit cytokinesis (Taylor and Peters, 2008). Could a mixture of these phenotypes arise in the subset of oocytes that arrest in MI? In other words, a visual microscopic assessment was not sufficient to classify an MI arrested oocyte, as anaphase might have occurred, but without being followed by cytokinesis and subsequent polar body extrusion. In order to assess at which stage of MI the BI 2536-treated oocytes were arrested, I produced chromosome spreads and IF stained them against CREST. The results revealed the presence of intact bivalents (Fig 4.6) in MI arrested oocytes in all tested BI 2536 concentrations. This clearly suggests that in this particular subset of oocytes, which arrest in MI in the presence of BI 2536, the mechanism of anaphase is inhibited.

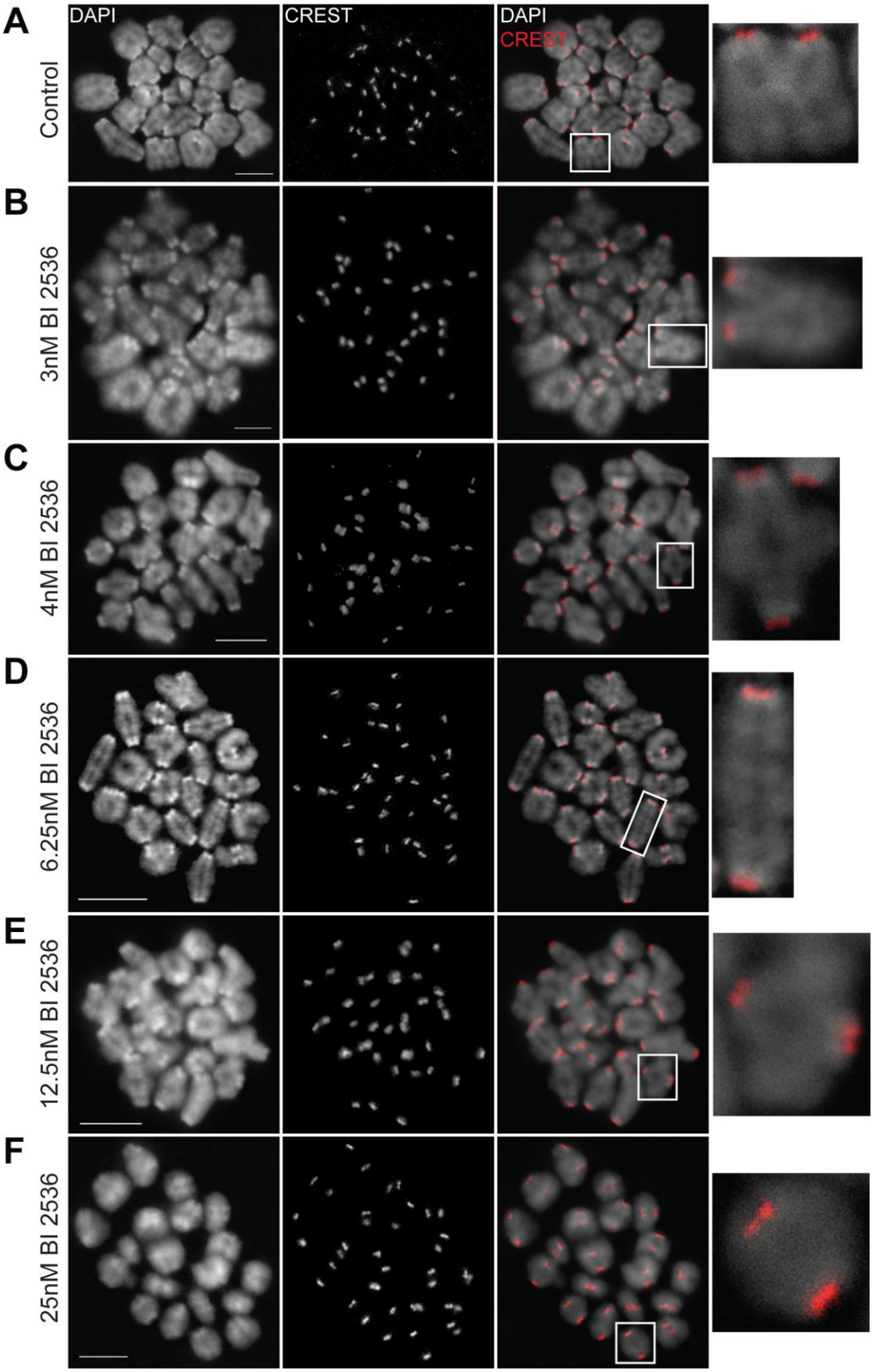

Figure 4.6 BI 2536 inhibits anaphase I

(See legend on next page)

Figure 4.6 BI 2536 inhibits anaphase I

Representative images showing DNA and CREST staining of chromosome spreads prepared from oocytes arrested in MI after overnight incubation in increasing BI 2536 concentrations; A, control; B, 3nM; C, 4nM; D, 6.25nM; E, 12.5nM; F, 25nM. Chromosomes surrounded by white boxes are shown in the enlarged images. Scale bars represent 10 μm.

4.5.1 BI 2536 increases inter-centromere distance during prometaphase of MI

In previous immunofluorescence staining experiments I noticed from the CREST staining that sister centromeres appear to be further apart during late prometaphase of MI (GVBD+5hr) in oocytes treated with BI 2536 compared to control oocytes (Fig 4.3). This observation suggested that centromeric cohesion, which is required to closely appose sister kinetochores for accurate monopolar sister kinetochore-spindle attachment to be established (Sakuno and Watanabe, 2009) might be weakened in BI 2536-treated oocytes. However, as it will be shown in the next chapter this does not appear to be the case. Nevertheless, such disrupted sister centromere configurations could lead to erroneous Kt-Mt attachments, which might be the underlying cause of the observed prometaphase I arrest.

In order to examine for a possible disruption in sister centromere integrity, the inter-centromeric distances were measured and compared between late prometaphase I (GVBD+5h) control oocytes and oocytes matured in media supplemented with 6.25nM BI 2536 (Fig 4.7.A). Distances between sister centromeres were measured by identifying the peaks of CREST fluorescence (Fig 4.7.B; each peak represents the center of a sister centromere) and calculating the distance between them. Consistent with our previous observation, it was found that inter-centromere distances significantly (P<0.05) increased in BI 2536 treated oocytes compared to control oocytes (Fig 4.7.C). These results indicate that the close apposition of sister centromeres, which is required for the establishment of monopolar sister kinetochore-microtubule attachment (Hauf and Watanabe, 2004; Brar and Amon, 2008), is affected in oocytes in the presence of BI 2536.

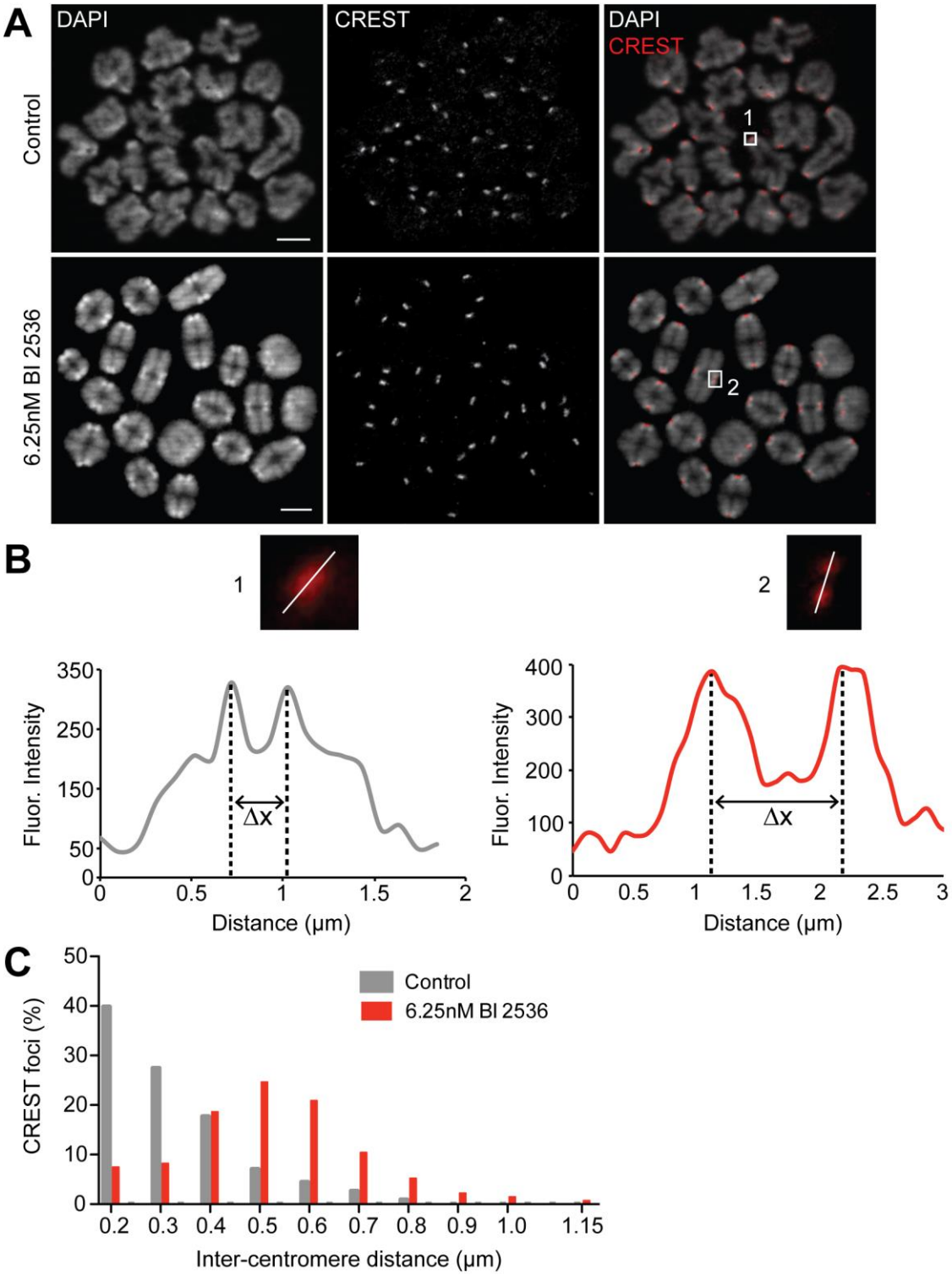

Figure 4.7 BI 2536 increases inter-centromere distance in prometaphase of MI

(A) Representative images showing DNA and CREST staining of chromosome spreads prepared from control and 6.25nM BI2536-treated oocytes, at late prometaphase I (GVBD+5h). Scale bars represent 10μm. **(B)** The outlined regions in **A** enlarged with DNA omitted. Plotted is the intensity profile of the CREST (red) signal measured along a line (white) drawn across the centromere. Δx represents inter-centromere distance. **(C)** Frequency distribution of the distance between sister centromeres (Δx), measured from the CREST signals in control (n = 113 centromeres; 4 oocytes from three mice) and BI 2536-treated (n = 134 centromeres; four oocytes from three mice) oocytes, showing a significantly greater mean distance in the 6.25nM BI 2536-treared compared with control oocytes ($P < 0.05$).

4.5.2 BI 2536 increases the number of erroneous Kt-Mt attachments at prometaphase of MI

In view of the increased distance between sister centromeres, I next asked whether the establishment of Kt-MT attachments is disrupted in BI 2536-treated oocytes. To address this question, control oocytes and oocytes cultured in medium supplemented with 6.25nM or 25nM BI 2536 were briefly treated with Ca^{2+}-buffer and fixed shortly prior to anaphase (GVBD+6h). As kinetochore microtubules (K-fibers) are differentially stable to Ca^{2+}-buffer treatment in comparison to non-kinetochore microtubules, a short treatment allows an easier assessment of Kt-Mt attachments. Following IF staining against CREST and α-Tubulin, images of the whole spindle were acquired by means of scanning confocal microscopy.

One of the first observations was that in contrast to findings in mitosis, where BI 2536 induces the formation of monopolar spindles (Lenart *et al.*, 2007), the meiotic spindle geometry appears to remain overall unaffected at the BI 2536 concentrations used in this study (Fig 4.8.A/B).

Next step was to determine the effect of BI 2536 on chromosome congression/alignment. To achieve this, bivalents were individually assessed for congression, by measuring the distance of their kinetochores from the spindle equator. Bivalents with both pairs of sister kinetochores situated further than 4μm of the spindle equator were classified as non-aligned, and those with both pairs of kinetochores inside this radius were classified as aligned (Fig. 4A). Results indicate that maturation in 25nM BI 2536-supplemented medium leads to significant congression defects at late prometaphase of MI ($P<0.05$; Fig 4.8.C).

Further analysis of the oocytes cultured in 25nM BI 2536 revealed that almost 57% of them exhibited severe bivalent misalignment (Fig 4.8.D), having at least

one bivalent with all four centromeres attached to a single pole (Fig 4.8.E/"Failed"). In addition, the increased distance between sister centromeres in the presence of BI 2536 (Fig 4.8.F/25nMBI2536/"Monopolar"2, 3) was also evident from these whole mount preparations, consistent with the data obtained previously from chromosome spreads (Fig 4.7).

Overall, these data indicate a dose-dependent effect of BI 2536 on the establishment of correct Kt-Mt attachments indicating the Plk1 kinase activity is required to promote bipolar attachment of bivalents. This raises the possibility that inhibition of anaphase by BI 2536 might be due to activation of the SAC.

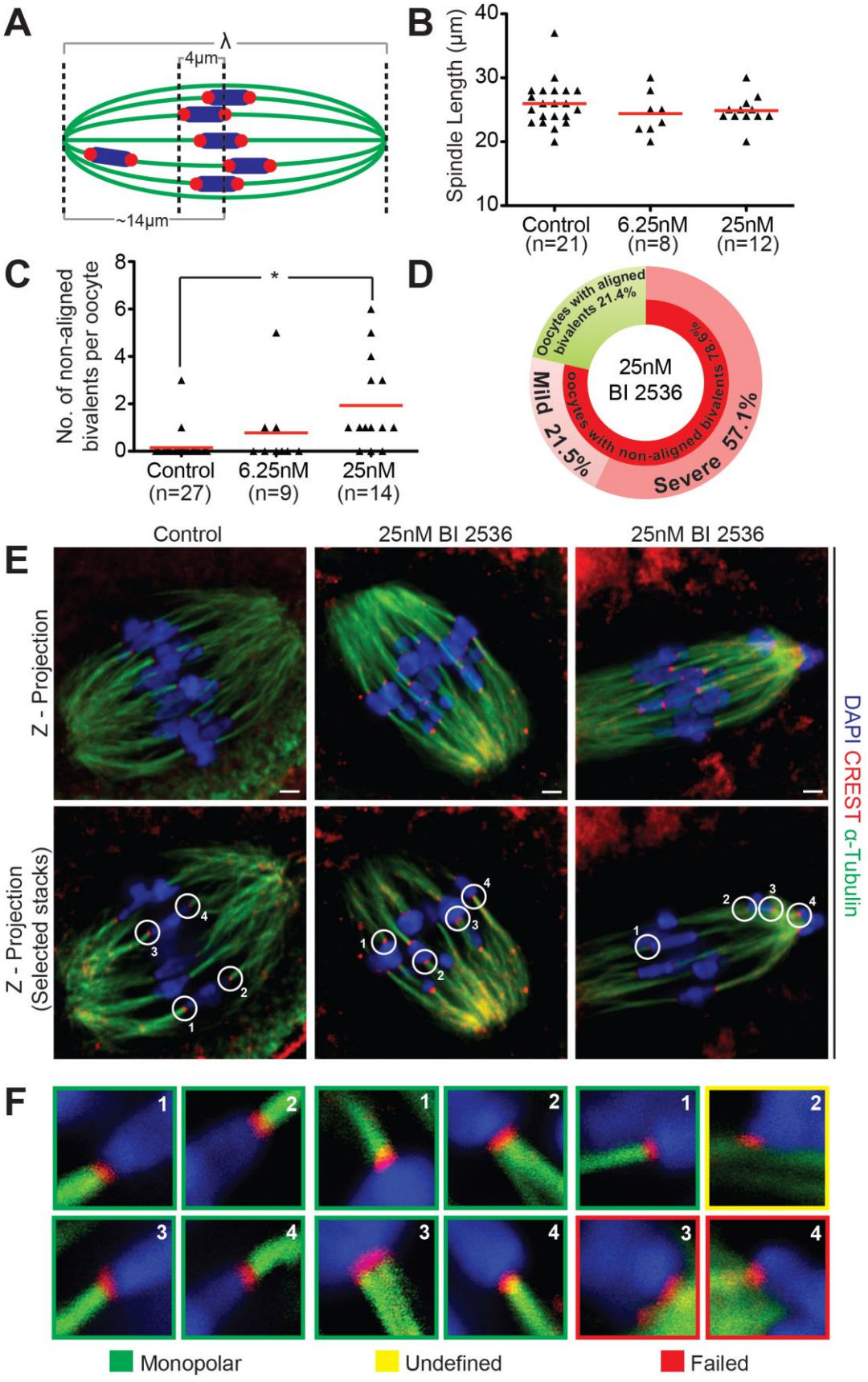

Figure 4.8 BI 2536 increases the frequency of erroneous Kt-Mt attachments at late prometaphase of MI.

(See legend on next page)

Figure 4.7 BI 2536 increases the frequency of erroneous Kt-Mt attachments at late prometaphase of MI

(A) Schematic representation of a meiotic spindle in late prometaphase of MI. Bivalents with all kinetochores being further than 4μm from the spindle equator were classified as non-aligned; λ indicates the measured spindle length. **(B)** Graph showing spindle length at late prometaphase of MI (GVBD+6h) in control oocytes and oocytes cultured in media supplemented with 6.25/25nM BI 2536: Control, 25.95μm (±3.5μm SD); 6.25nM, 24.38μm (±3.3μm SD); 25nM, 24.83μm (±2.3μm SD). No significant differences were observed between analysed groups ($P \geq 0.05$); red lines indicate individual mean values. **(C)** Graph showing number of non-aligned bivalents at late prometaphase of MI (GVBD+6h) in control oocytes and oocytes cultured in media supplemented with 6.25 or 25nM BI 2536: Control, 0.12(±0.6 SD); 6.25nM, 0.78 (±1.6 SD);25nM, 1.9 (±1.9 SD). Asterisk indicates groups exhibiting significant difference from one another ($P<0.05$); red lines indicate individual mean values. **(D)** Graph showing the percentages of oocytes with aligned and non-aligned bivalents in the 25nM BI 2536 group from (C). Oocytes with non-aligned bivalents are further categorized into "Mild" and "Severe" misalignment groups. Oocytes with a bivalent attached to a single pole (e.g. Failed in (F)) were classified as exhibiting "Severe" misalignment. **(E)** Representative images showing DNA, CREST and α-Tubulin staining of oocytes at late prometaphase (GVBD+6h) after maturation in control media or media supplemented with 25nM BI 2536. Prior to fixation, oocytes were briefly treated with Ca^{2+}-buffer. The top row shows maximum intensity Z projection images across the whole spindle, whereas the bottom row shows Z projection images of four selected sections from the same oocytes. Numbered circled regions indicate the kinetochores magnified in (E). Scale bars represent 1μm. **(F)** Enlarged images showing examples of kinetochore-microtubule attachments in the oocytes shown in (D). Kinetochore-microtubule attachments are classified into three categories: Monopolar (green), Undefined (yellow) and Failed (red). The images are colour-coded according to these categories. Note the increased inter-centromeric distance in BI 2536-treated oocytes (Monopolar-2, 3), where the 2 K-fibers can be distinguished from one another, compared to control oocytes, where the 2 K-fibers appear as one.

4.6 Plk1 is required for efficient activation of APC/C^{Cdc20} during exit from MI.

4.6.1 BI 2536 inhibits securin degradation in MI.

In mitotic cells the SAC acts as a surveillance mechanism to ensure that the onset of anaphase is delayed until all chromosomes establish stable bipolar kinetochore microtubule attachments (Peters, 2006). The wait-anaphase signal generated from unattached Kts inhibits APC/C-mediated degradation of cyclin B and securin, thereby inhibiting activation of separase-mediated cleavage of cohesin (Musacchio and Salmon, 2007). Studies in oocytes indicate that the timing of cyclin B and securin degradation required for the onset of anaphase of MI (Herbert *et al.*, 2003), is regulated by the SAC (Homer *et al.*, 2005b; McGuinness *et al.*, 2009).

Having established that BI 2536 severely compromises chromosome attachment and alignment, the next step was to investigate whether inhibition of anaphase in the presence of 25nM BI 2536 was a consequence of sustained activation of the SAC in the presence of erroneous Kt-Mt attachments. To address this question, fully-grown prophase-arrested CD1 oocytes were co-injected with mRNA encoding securin-YFP and H2B-RFP and were imaged by time-lapse microscopy during maturation in control or 25nM BI 2536-supplemented media, for approximately 16h (Fig 4.9.A). For these experiments, I used 25nM of BI 2536, because this concentration produced a single phenotype, where all oocytes arrest at prometaphase of MI (Fig 4.5). Analysis of the time-lapse movies showed that in control oocytes securin-YFP fluorescence declines about 6h post-GVBD (Fig 4.9.B/C), prior to anaphase and subsequent polar body extrusion (PBE) at 8.3h (±1.15h SD) post-GVBD (Fig 4.9.C). In contrast, in BI 2536-treated oocytes, securin-YFP FI does not decline (Fig 4.9.B/D) indicating that BI 2536 inhibits degradation of securin and subsequently the onset of anaphase and PBE (Fig 4.9.D). However, in contrast to control oocytes, securin-YFP did not accumulate during progression through prometaphase I. This could be due either to a low level of degradation or to suppression of translation of securin-YFP mRNA.

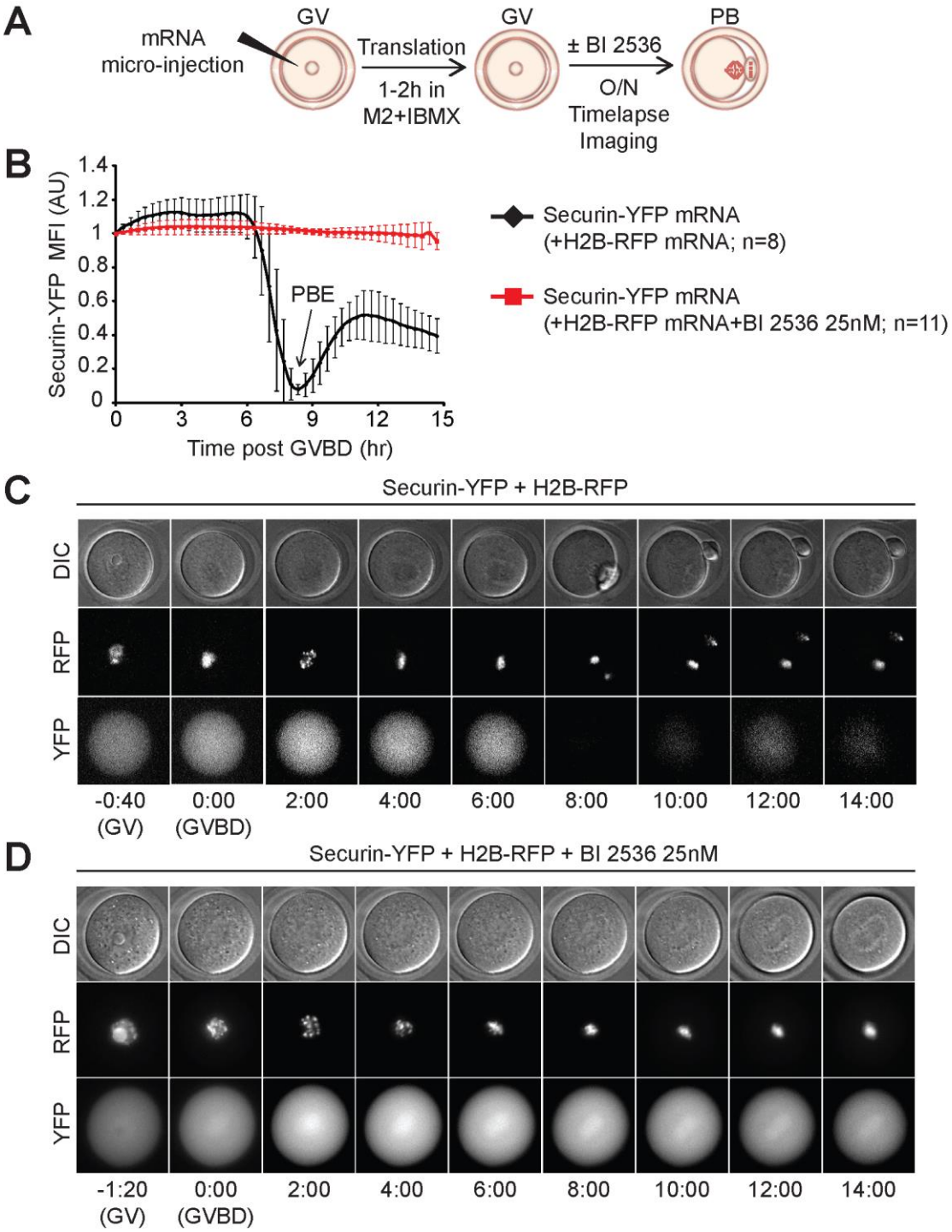

Figure 4.9 BI 2536 inhibits the degradation of securin in late metaphase of MI

(A) Schematic representation of experimental design: CD1 oocytes were co-injected with mRNA encoding securin-YFP and H2B-RFP. Following recovery oocytes were examined by time-lapse microscopy during progression through MI in control or BI 2536-supplemented medium, for approximately 16h. **(B)** Securin-YFP average fluorescence intensity (FI) in control (black) and 25nM BI 2536-treated (red) oocytes was measured at each time-point and background FI was subtracted. The values were normalised relative to that of GVBD (0h), and their mean values at each time-point were plotted against time. Securin-YFP degradation is inhibited in the presence of BI 2536. Errors bars indicate ±SD; AU, arbitrary units; PBE, polar body extrusion; n, oocyte number. **(C)** Selected DIC, RFP and YFP time-lapse images of a representative control oocyte at the indicated time-points. **(D)** Selected DIC, RFP and YFP time-lapse images of a representative 25nM BI 2536-treated oocyte at the indicated time-points. Note the absence of efficient securin degradation and PBE.

4.6.1 BI 2536 inhibits the activation of APC/C^{Cdc20} in MI.

According to the latter results BI 2536 inhibits the degradation of securin in late metaphase of MI, indicating that the APC/C is not efficiently activated. However, they do not provide proof that this is mediated by sustained activation of the SAC. Could BI 2536 have a SAC-independent inhibitory effect on the APC/C? To answer that, it was necessary to find a way to bypass the SAC and that was achieved by employing a mutant form of the APC/C activator Cdc20, known as Cdc20^{R132A} (Fig 2.2). According to the currently prevalent model of SAC activation, unattached kinetochores cause the formation of the mitotic checkpoint complex, a complex comprising the checkpoint proteins Mad2, Bub3, BubR1 and Cdc20, which sequesters Cdc20, thus inhibiting APC/C from targeting cyclin B and securin for degradation (Musacchio and Salmon, 2007). Recent studies have identified the binding domain of Cdc20 on Mad2 and a point mutation in that domain (R132A) has been shown to allow robust binding to APC/C, but prevent binding with Mad2 (Zhang and Lees, 2001; Ge *et al.*, 2009). In other words, Cdc20^{R132A} can activate the APC/C and promote anaphase without being given the "ok" signal from the SAC.

To test the ability of Cdc20^{R132A} to bypass the SAC in oocytes, I asked whether it could degrade securin the presence of the drug nocodazole, which activates the oocyte SAC by depolymerising microtubules (Wassmann *et al.*, 2003). Fully-grown prophase-arrested CD1 oocytes were co-injected with mRNA encoding securin-YFP, H2B-RFP and wild type Cdc20 (control group) or Cdc20^{R132A} (test group) and were imaged by time-lapse microscopy during maturation in nocodazole-supplemented media, for approximately 16h (Fig 4.10). Analysis of the time-lapse movies showed that, in control oocytes exogenous securin is accumulated (Fig 4.10.A/B). This is consistent with sustained activation of the oocyte SAC in the presence of nocodazole (Wassmann *et al.*, 2003). In contrast, in Cdc20^{R132A}-injected oocytes, exogenous securin is degraded (Fig 4.10.A/C).

Considering that in oocytes injected with $Cdc20^{R132A}$-encoding mRNA, the timing of APC/C activation is unregulated, it would be reasonable to expect differences in the kinetics of securin degradation between individual oocytes as it could initiate any time during prometaphase of MI. Nevertheless, the results indicate that $Cdc20^{R132A}$ is capable of bypassing the SAC to activate APC/C in mouse oocytes.

The next step was to use $Cdc20^{R132A}$ to determine whether inhibition of APC/C during exit from MI in the presence of BI 2536 was due to sustained activation of the SAC. Therefore, fully-grown prophase-arrested CD1 oocytes were co-injected with mRNA encoding securin-YFP, H2B-RFP and wild-type Cdc20 or $Cdc20^{R132A}$ and were monitored by time-lapse microscopy in the presence of nocodazole and 25nM BI2536 supplemented medium, for approximately 16h (Fig 4.11). As expected, oocytes injected with wild-type Cdc20 accumulated exogenous securin (Fig 4.11.A/B) in the presence of nocodazole. Surprisingly, in $Cdc20^{R132A}$-injected oocytes, exogenous securin was also stable, despite the ability of $Cdc20^{R132A}$ to override the SAC and activate the APC/C (Fig 4.11.A/C). These results indicate that the SAC is not the sole cause of prometaphase arrest in the presence of BI 2536. Although we cannot rule out the SAC, it is clear that another mechanism, which involves inhibition of the APC/C is in play.

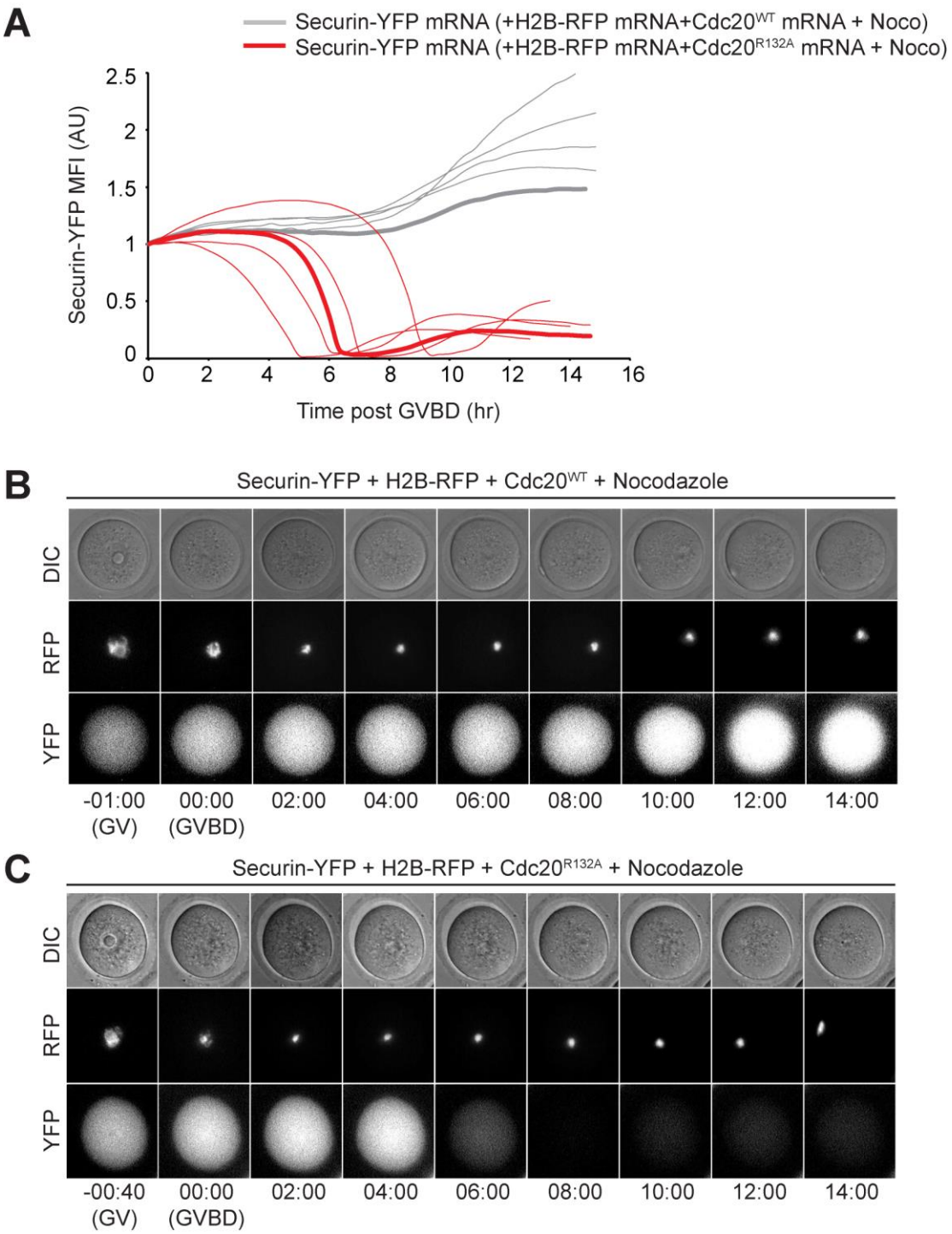

Figure 4.10 Cdc20^{R132A} allows degradation of securin in the presence of nocodazole.

(A) Securin-YFP levels of representative oocytes (5 per group) co-injected with mRNA encoding securin-YFP, H2B-RFP and Cdc20^{WT} (grey, n=8) or securin-YFP, H2B-RFP and Cdc20^{R132A} (red, n=7) and examined by time-lapse microscopy during progression through MI, in nocodazole-supplemented media. Securin-YFP mean fluorescence intensity (MFI) in oocytes was measured at each time-point and background FI was subtracted. The values were normalised relative to that of GVBD (0h), and plotted against time. Securin-YFP degradation is inhibited in oocytes injected with Cdc20^{WT} in the presence of nocodazole, whereas it is allowed in Cdc20^{R132A}-injected oocytes. Bold curves indicate oocytes shown in (B) and (C). AU, arbitrary units. **(B, C)** Selected DIC, RFP and YFP time-lapse images of the oocytes whose securin-YFP levels are illustrated by bold curves in (A), at the indicated time-points before and after GVBD in hours. Note securin-YFP degradation in (C).

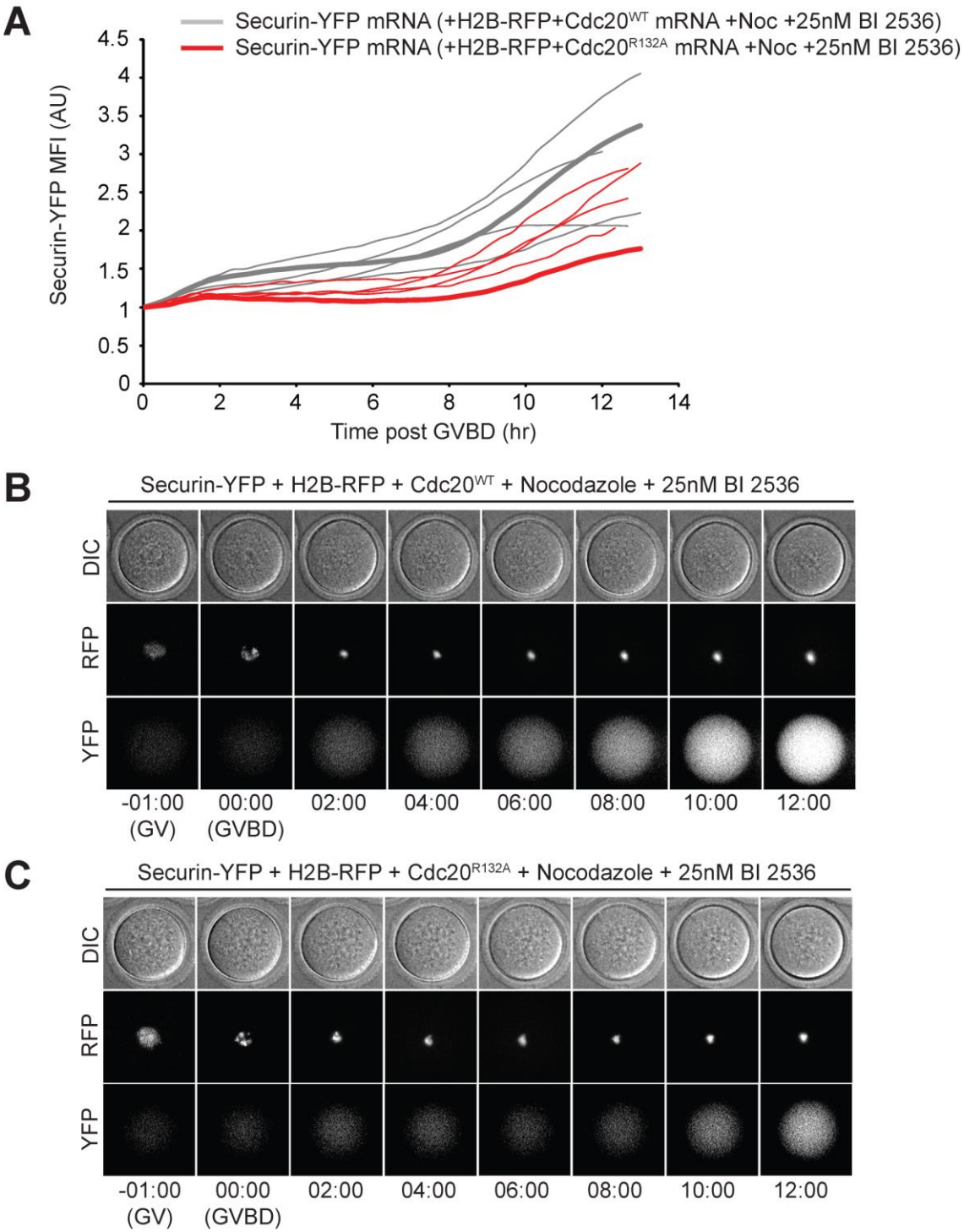

Figure 4.11 BI 2536 inhibits degradation of securin in Cdc20^{R132A}-injected oocytes in the presence of nocodazole.

(A) Securin-YFP levels of representative oocytes (5 per group) co-injected with mRNA encoding securin-YFP, H2B-RFP and Cdc20^{WT} (grey, n=6) or securin-YFP, H2B-RFP and Cdc20^{R132A} (red, n=7) and examined by time-lapse microscopy during progression through MI, in medium supplemented with nocodazole and 25nM BI 2536. Securin-YFP mean fluorescence intensity (MFI) in oocytes was measured at each time-point and background FI was subtracted. The values were normalised relative to that of GVBD (0h), and plotted against time. Securin-YFP degradation is inhibited even in oocytes injected with Cdc20^{R132A}. Bold curves indicate oocytes shown in (B) and (C). AU, arbitrary units. **(B, C)** Selected DIC, RFP and YFP time-lapse images of the oocytes whose securin-YFP levels are illustrated by bold curves in (A), at the indicated time-points before and after GVBD in hours.

4.6.2 Exogenous cyclin B1 relieves inhibition of securin degradation in the presence of BI 2536.

Based on the latter observations, the effect of Plk1 inhibition on the APC/C is not mediated solely by the SAC. To determine whether this is a securin-specific effect or if BI 2536-treatment also affects the degradation of other APC/C^{Cdc20} substrates, we monitored the kinetics of ectopically expressed RFP-tagged cyclin B1 during progression through MI in the presence of BI 2536.

Fully-grown prophase-arrested CD1 oocytes were co-injected with mRNA encoding cyclin B1-RFP and securin-YFP and were monitored by time-lapse microscopy during maturation in control medium or medium supplemented with 25nM BI 2536 (Fig 4.12). Analysis of the time-lapse movies showed that in control oocytes degradation of exogenous securin and cyclin B1 is initiated at 4.8h (±1.5h SD) post-GVBD and continues until PBE, which is followed by reaccumulation of exogenous securin and cyclin B1 (Fig 4.12.A/B/C). Rather expectedly, in BI 2536-treated oocytes, exogenous securin and cyclin B1 do not accumulate as much as in controls and their degradation is initiated earlier, at 2.9h (±1h SD) post-GVBD (Fig 4.12.A/B/D). Moreover, degradation appears less abrupt, compared to controls, and continues until it reaches a baseline level (about 9h post-GVBD), without leading to anaphase or PBE during the experimental time-frame (Fig 4.12.A/B/D). Finally, in contrast to controls, no reaccumulation of exogenous securin and cyclin B1 is observed (Fig 4.12.A/B.D). These data indicate that overexpression of exogenous cyclin B1 partially relieves inhibition of APC/C^{Cdc20} in the presence of BI 2536.

Additional experiments involving microinjection of exogenous mRNA encoding a mutant cyclin B1, which does not bind to Cdk1 [namely, cyclin $B1^{Y170A}$ (Bentley *et al.*, 2007)], would allow us to test the hypothesis that the partial rescue was due to increased Cdk1 activity associated with overexpression of cyclin B1.

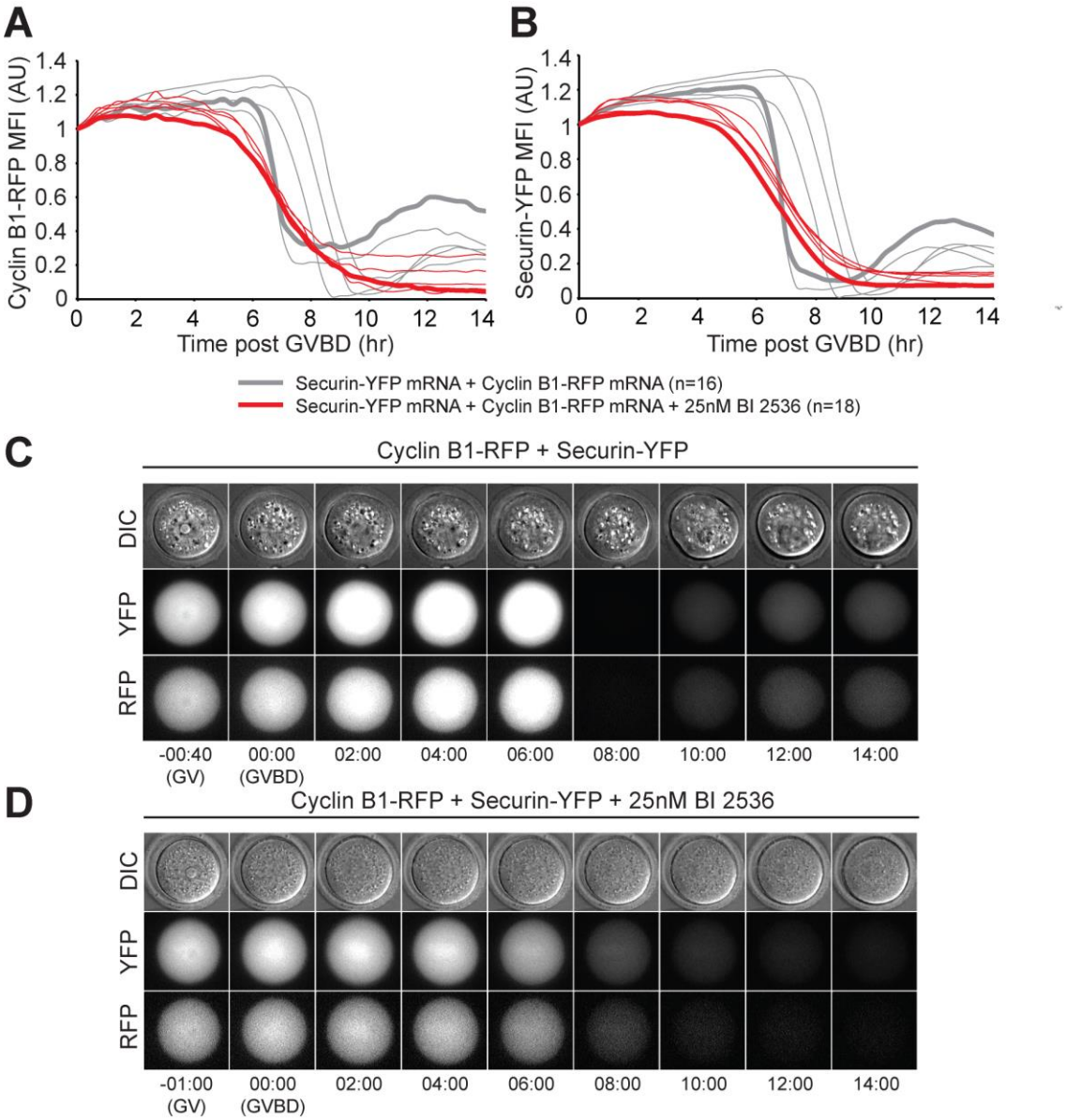

Figure 4.12 Exogenous cyclin B1 relieves inhibition of securin degradation in the presence of BI 2536.

(A) Cyclin B1-RFP and **(B)** securin-YFP levels of representative oocytes (5 per group) co-injected with mRNA encoding cyclin B1-RFP and securin-YFP and examined by time-lapse microscopy during progression through MI in control medium (grey) or medium supplemented with 25nM BI 2536 (red). Cyclin B1-RFP and securin-YFP mean fluorescence intensities (MFI) in oocytes were measured at each time-point and background FI was subtracted. The values were normalised relative to that of GVBD (0h), and plotted against time. Securin-YFP degradation is rescued in oocytes co-injected with cyclin B1-RFP in the presence of BI 2536. Bold curves indicate oocytes shown in (C) and (D). AU, arbitrary units; n, number of oocytes. **(B, C)** Selected DIC, RFP and YFP time-lapse images of the oocytes whose cyclin B1-RFP and securin-YFP levels are illustrated by bold curves in (A) and (B), at the indicated time-points before and after GVBD in hours.

4.7 Discussion

In this chapter I have aimed to perform a functional analysis of Plk1 in mammalian oocytes. To achieve that I have used BI 2536, a chemical inhibitor of Plk1, in various concentrations and in combination with indirect immuno-fluorescence staining and live-cell imaging of oocytes injected with mRNAs encoding fluorescent proteins. I have provided evidence that Plk1 is recruited to the kinetochore region upon release into prometaphase and its recruitment is unaffected by a low dose of BI 2536. Inhibition of Plk1 kinase activity by BI 2536 did not affect the timing of entry into prometaphase of MI, but prevented initiation of anaphase of MI in a dose-dependent manner. Oocytes that were arrested in prometaphase of MI in the presence of BI 2536 did not undergo anaphase, were characterised by increased distance between sister centromeres and exhibited severe chromosome misalignment defects. Finally, I have shown that BI 2536 inhibits securin degradation and the data indicate that this occurs by a SAC-independent mechanism.

4.7.1 Plk1 is recruited to the kinetochore of meiotic chromosomes

The association of Plk1 with chromosomes has not received much attention in published studies of the subcellular localisation of the protein during meiosis. Based on my knowledge, currently only a single publication has provided evidence that Plk1 localises to the kinetochore of mouse oocytes during prometaphase of MI (Kouznetsova *et al.*, 2007). The localisation of Plk1 described here on the meiotic chromosomes suggests that it is associated with the kinetochore region during meiotic maturation, where it persists until late prometaphase of MI (Fig 4.2). I have also found that Plk1 localised on kinetochores of Met II arrested oocytes, albeit at significantly reduced levels compared to MI. The Kt-localisation of Plk1 described here is consistent with previous findings in somatic cells (Arnaud *et al.*, 1998; Sumara *et al.*, 2004; Lenart *et al.*, 2007). The presence of Plk1 on this region of the chromosome

during meiotic maturation suggests that it is required for accurate kinetochore function as in mitosis [reviewed by (Petronczki *et al.*, 2008)].
Furthermore, the data presented here indicate that inhibition of Plk1 kinase activity by BI 2536 did not prevent its kinetochore recruitment during MI when the concentrations of 6.25nM (Fig 4.3) and 25nM (data not shown) were applied. This contradicts findings in mitosis where Plk1 activity is required for its accumulation at kinetochores (Lenart *et al.*, 2007; Santamaria *et al.*, 2007), suggesting that this mechanism may not be essential in meiosis. However, we cannot exclude the possibility of residual Plk1 activity as previous mitotic studies have applied a 100nM concentration of BI 2536 to reach their conclusions (Lenart *et al.*, 2007). Further experimentation with higher concentrations of BI 2536 could provide an answer regarding the necessity of Plk1 activity for the enzyme's kinetochore recruitment in meiosis. However, considering the greater volume of an oocyte (~ $4x10^5$ μm^3) compared with that of a HeLa cell (~ $2x10^3$ μm^3) it is conceivable that a concentration of BI 2536 higher than 100nM might be required to achieve total Plk1-inhibition, thereby posing the risk of inhibiting other Plks with unpredictable effects.

4.7.2 BI 2536 does not affect the timing of entry into prometaphase of MI, but prevents initiation of anaphase of MI in a dose-dependent manner

A number of studies have implicated Plk1 in promoting mitotic entry in vertebrate cells by activating Cdk1-cyclin B (Toyoshima-Morimoto *et al.*, 2001; Toyoshima-Morimoto *et al.*, 2002; Jackman *et al.*, 2003; Watanabe *et al.*, 2004). However, Plk1 activity does not appear to be essential for mitotic entry, as its inhibition will only delay prophase and nuclear envelope breakdown (NEBD) (Lenart *et al.*, 2007). Similar observations have been made in mouse and rat oocyte studies; inhibition of Plk1 activity either by Plk1 antibody microinjection (Tong *et al.*, 2002; Fan *et al.*, 2003) or by BI 2536 (Vanderheyden *et al.*, 2009) caused a delay in resumption of meiosis I and GVBD onset and prevented the

extrusion of the first polar body. To determine the efficiency of different BI 2536 concentrations on oocyte maturation I have examined GVBD timing and PB extrusion. The results show that none of the tested BI 2536 concentrations causes a significant delay in GVBD (Fig 4.4A), consistent with previous observations, where concentrations of BI 2536 below 100nM had no effect on meiosis I resumption (Vanderheyden *et al.*, 2009). Prolonged exposure to BI 2536 in order to eliminate the possibility of a delayed action also had no effect on GVBD timings (Fig 4.4B). However, BI 2536 has a dose-dependent effect on the ability of oocytes to exit MI; the extrusion of the first PB is abrogated by 25nM of BI 2536, while significant inhibition is observed even at a 6.25nM concentration (Fig 4.5). Overall these results indicate that in mouse oocytes, Plk1 activity is not essential for meiosis resumption, but is essential for MI completion and BI 2536 can effectively and rapidly inhibit it.

4.7.3 BI 2536 inhibits anaphase of MI, disrupts sister-centromere integrity and promotes misalignment of bivalents.

Analysis of chromosome spreads of oocytes arrested during prometaphase of MI in the presence of BI 2536 revealed the presence of intact bivalents (Fig 4.6) indicating that BI 2536 treatment induces arrest in prometaphase. Previous studies in somatic cells have shown that BI 2536 leads to arrest in prometaphase due to activation of the SAC (Lenart *et al.*, 2007) and that Plk1 is involved in the establishment of correct Kt-Mt attachments [reviewed in (Petronczki *et al.*, 2008)]. Could BI 2536-treated oocytes arrest in prometaphase I due to failure to establish monopolar Kt-Mt attachments of sister centromeres? Indeed, I have shown here that sister centromeres in BI 2536-treated oocytes lose their tight apposition (Fig 4.7), which has been proposed to facilitate the establishment of monopolar Kt-Mt attachments of sister chromatids (Hauf and Watanabe, 2004; Brar and Amon, 2008; Sakuno and Watanabe, 2009). Moreover, at 25nM of BI 2536 the majority (~78% - Fig 4.8C/D) of oocytes exhibited bivalent misalignment and more than half (~57% - Fig 4.8D) had at least one mono-

oriented bivalent (Fig 4.8.E/"Failed"). Finally, although I saw no convincing evidence of bipolar attachment of sisters, it is impossible to rule it out based on the immuno-labeling experiments shown here. Overall, these results demonstrate that bivalents do not congress in the presence of BI 2536, indicating that Plk1 kinase activity is required for congression in MI.

Taken together, our data suggest that Plk1 activity is essential for the establishment of stable microtubule- kinetochore attachments in MI. This is consistent with previous observations in somatic cells [reviewed in (Petronczki *et al.*, 2008)]. It is possible that kinetochores can be captured by microtubules in the absence of Plk1 activity, but these attachments may not be stable and proper K-fibers may therefore not be formed. Previous studies in mammalian somatic cells (Ditchfield *et al.*, 2003; Lampson and Kapoor, 2005) and oocytes (Homer *et al.*, 2009b) have shown that depletion of BubR1 also causes defects in microtubule-kinetochore attachments. BubR1 phosphorylation is essential for the stability of Kt-Mt interactions and it is Plk1-dependent (Elowe *et al.*, 2007; Suijkerbuijk *et al.*, 2012). Moreover, BI 2536-treated cells have been shown to lack the hyper-phosphorylated form of BubR1 (Lenart *et al.*, 2007). Thus, as in mitosis, meiotic Plk1 activity might contribute to K-fiber formation by phosphorylation of BubR1 at kinetochores during MI.

On the basis of these findings, we propose that BI 2536 impairs the ability to establish and maintain monopolar sister kinetochore-microtubule attachments.

4.7.4 Plk1 prevents degradation of exogenous securin and is required for efficient activation of APC/C^{cdc20} in MI

Previous studies in mouse oocytes have shown that the target of the SAC is APC/C^{cdc20} activation and subsequent degradation of securin and cyclin B1, which are essential for completion of MI. Here, we have shown that BI 2536-

treated oocytes arrest in late prometaphase of MI (Fig 4.6) and that exogenous securin is not efficiently degraded in these oocytes (Fig 4.9). These data suggested the possibility that BI 2536-treated oocytes arrest in prometaphase I because of SAC activation.

To further test this possibility, we employed mRNA encoding $Cdc20^{R132A}$, which can over-ride the SAC (Fig 4.10A/C). When we filmed oocytes expressing exogenous $Cdc20^{WT}$ and securin-YFP incubated in the presence of BI 2536 and nocodazole, which causes sustained activation of the SAC in oocytes (Brunet *et al.*, 2003; Wassmann *et al.*, 2003; Homer *et al.*, 2005a; Kudo *et al.*, 2006), all oocytes arrested in prometaphase I and exhibited accumulation of exogenous securin (Fig 4.11A/B). Similarly, we observed prometaphase I arrest and exogenous securin accumulation in oocytes expressing exogenous $Cdc20^{R132A}$ and incubated in nocodazole and BI 2536 (Fig 4.11A/C). These data indicate that inhibition of APC/C in the presence of BI 2536 is SAC –independent. This stands in contrast to what has been recently shown in mammalian mitosis (Lenart *et al.*, 2007), but is consistent with older reports that in the absence of Plx1 activity some APC/C targets are not degraded by the proteasome (Descombes and Nigg, 1998).

By what mechanism might Plk1 inhibit the APC/C? In support of a direct effect on core APC/C subunits, it has been reported that mouse Plk1 phosphorylates subunits of the APC/C (Kotani *et al.*, 1998). Also, the finding that overexpression of cyclin B1 partly relieves inhibition of APC/C^{Cdc20} in the presence of BI 2536 (Fig 4.12), suggests that Cdk1 and Plk1 may act synergistically to promote efficient activation of the APC/C during exit form MI. In support of this, subsequent experiments in the lab have shown that a mutant cyclin B1 (Y170A), which does not bind to Cdk1 (Bentley *et al.*, 2007), does not rescue the inhibitory effect of Plk1 on securin degradation (data not shown), indicating that

activation of Cdk1 is necessary for rescuing the APC/C inhibition in the presence of BI 2536.

An alternative or additional possibility is that Plk1 is also required to deactivate an inhibitor of the APC/C in oocytes. This scenario might actually involve Emi1, which is known to inhibit APC/C in both mitosis (Reimann *et al.*, 2001a; Reimann *et al.*, 2001b) and meiosis (Marangos *et al.*, 2007) . During mitotic prometaphase, Plk1 phosphorylates Emi1, thereby leading to its recognition by the SCF ubiquitin ligase and its subsequent degradation by the proteasome (Guardavaccaro *et al.*, 2003; Margottin-Goguet *et al.*, 2003; Hansen *et al.*, 2004; Moshe *et al.*, 2004). Similarly, in meiosis Emi1 is degraded soon after GVBD (Marangos *et al.*, 2007) presumably to allow APC^{Cdc20} activation, once the SAC has been satisfied, which is necessary to coordinate the destruction of securin and cyclin B and allow exit from MI. Although the idea that Emi1 inhibits APC/C^{cdc20} has been previously contended (Di Fiore and Pines, 2007), a recent study has re-ignited the debate (Moshe *et al.*, 2011). Based on the above, I propose that the observed APC/C^{Cdc20} inactivation/inhibition during MI in the presence of BI 2536 is probably due to insufficient phosphorylation/activation of APC/C subunits, combined with insufficient degradation or accumulation of Emi1. Additional experimentation involving microinjection of oocytes with fluorescently-tagged Emi1 mRNA, to assess Emi1 kinetics in the presence of BI 2536, and non-degradable Emi1, to assess its effect on APC/C^{cdc20}, would allow further evaluation of this hypothesis.

In summary, the findings presented in this chapter indicate that Plk1 is required for activation of the APC/C during exit from prometaphase of MI. Inhibition of Plk1 also induced congression defects, and it is possible that severely misaligned bivalents induce sustained activation of the SAC. However, the findings indicate that inhibition of the APC/C in the presence of BI 2536 is not solely due to SAC and raise the possibility that phosphorylation of APC/C core

subunits by Plk1 is required for its efficient activation. To assess SAC activation in the presence of BI 2536 future experimentation should examine for the presence of Mad2 at the centromere of metaphase I arrested oocytes, which is a clear indication of Kt-Mt attachment defects (Wassmann *et al.*, 2003; Homer *et al.*, 2005a). Finally, the experiments described in section 4.6.1 should also be repeated in the absence of nocodazole as an additional control to further strengthen our conclusion that inhibition of APC/C in the presence of BI 2536 is SAC –independent.

Chapter 5 . Plk1 is required for stepwise removal of cohesin in mouse meiosis

5.1 Introduction

The findings of the previous chapter indicate that Plk1 is required for efficient activation of the APC/C during exit from MI. However, a proportion of oocytes did produce polar bodies in lower concentrations (≤12.5nM) of BI 2536. This provided an assay to investigate possible functions of Plk1 in mediating chromosome segregation during MI.

In budding yeast, the Plk1 homolog, Cdc5, phosphorylates and primes Rec8 for cleavage by separase and is required for proper kinetochore orientation during MI (Clyne *et al.*, 2003; Lee and Amon, 2003; Brar *et al.*, 2006). However, a recent study suggests that Cdc5 has little, if any, role in promoting Rec8 cleavage and attributes this role to Casein Kinase 1 (Katis *et al.*, 2010; Rumpf *et al.*, 2010). It is not currently known if Plk1 regulates these processes in mouse oocytes. However, a previous study suggested that Plk1 phosphorylation is essential for Rec8 cleavage by separase *in vitro* (Kudo *et al.*, 2009).

While the requirement for Plk1-mediated phosphorylation to prime Rec8 for cleavage by separase is controversial, Plk1 has a well-established function in removing the bulk of arm cohesin during prophase and prometaphase of vertebrate somatic cells, via a process known as the "prophase pathway"(Losada *et al.*, 1998; Sumara *et al.*, 2002). This process does not require the cleavage of cohesin by separase, as cohesin dissociation is achieved through its phosphorylation by Plk1, mediated by Aurora B (Hauf *et al.*, 2005). My hypothesis was that a similar process might also occur during meiotic prophase. In other words, Plk1 could be involved in cohesin removal through a mechanism that would be the meiotic equivalent of the prophase pathway. Given that mammalian oocytes remain arrested in prophase of MI for an extended time period, prior to being released into prometaphase I, it is

conceivable that prolonged exposure to such a mechanism could be another factor contributing to the observed depletion of chromosome-associated cohesin in old oocytes.

In this chapter, I investigate the interplay between Plk1 activity and cohesin in mammalian oocytes during MI. I also investigate the role of Plk1 on chromosome segregation in mouse oocytes by analyzing oocytes that formed polar bodies in the presence of BI 2536. To achieve accurate observations I have used oocytes from the transgenic *Rec8*-myc mouse strain (Kudo *et al.*, 2006) where cohesin-related measurements were necessary.

5.2 Securin profile of oocytes that exit MI in the precence of BI 2536

As described in the previous chapter BI 2536 inhibits anaphase of MI in a dose-dependent manner (Section 4.5). At low concentrations (6.25 and 12.5 nM) a subset of oocytes exit MI and extrude the first polar body. Having established that BI 2536 leads to prometaphase I arrest by inhibiting securin degradation , I hypothesised that in the case of oocytes that exit MI, securin degradation ,and therefore anaphase, would most probably be delayed compared to control conditions. To test this hypothesis, fully-grown prophase-arrested CD1 oocytes were co-injected with mRNA encoding securin-YFP and H2B-RFP and were monitored by time-lapse microscopy during incubation in control or 6.25nM BI 2536-supplemented medium, for approximately 16h (Fig 5.1.A). Analysis of the time-lapse movies showed that in control oocytes exogenous securin starts being degraded about 6h post-GVBD and anaphase and subsequent polar body extrusion (PBE) occur at 8.3h (±1.15h SD) post-GVBD, followed by reaccumulation of securin (Fig 5.1.A/B). In contrast, in BI 2536-treated oocytes, exogenous securin degradation is delayed (Fig 5.1.A/C), and the onset of anaphase and PBE occur at 9.7h (±0.78h SD) post-GVBD (Fig 5.1.C). As in control oocytes, securin-YFP reaccumulated after PBE (Fig 5.1.C).

Interestingly, polar body formation was perturbed in BI 2536-treated oocytes. Abnormalities included production of large polar bodies (observed in 25% of oocytes), suggesting improper positioning of the meiotic spindle at the oocyte cortex. In addtion, a proportion of oocytes (58%) showed polar body fragmentation, and failed abscission (17%). The latter phenotypes may reflect a requirement for Plk1 kinase activity for correct cytokinesis, which is consistent with previous observations in somatic cells (Brennan *et al.*; Burkard *et al.*, 2007; Petronczki *et al.*, 2007; Santamaria *et al.*, 2007).

Overall, these results indicate that Plk1 kinase activity is required for timely degradation of securin and successful cytokinesis in MI.

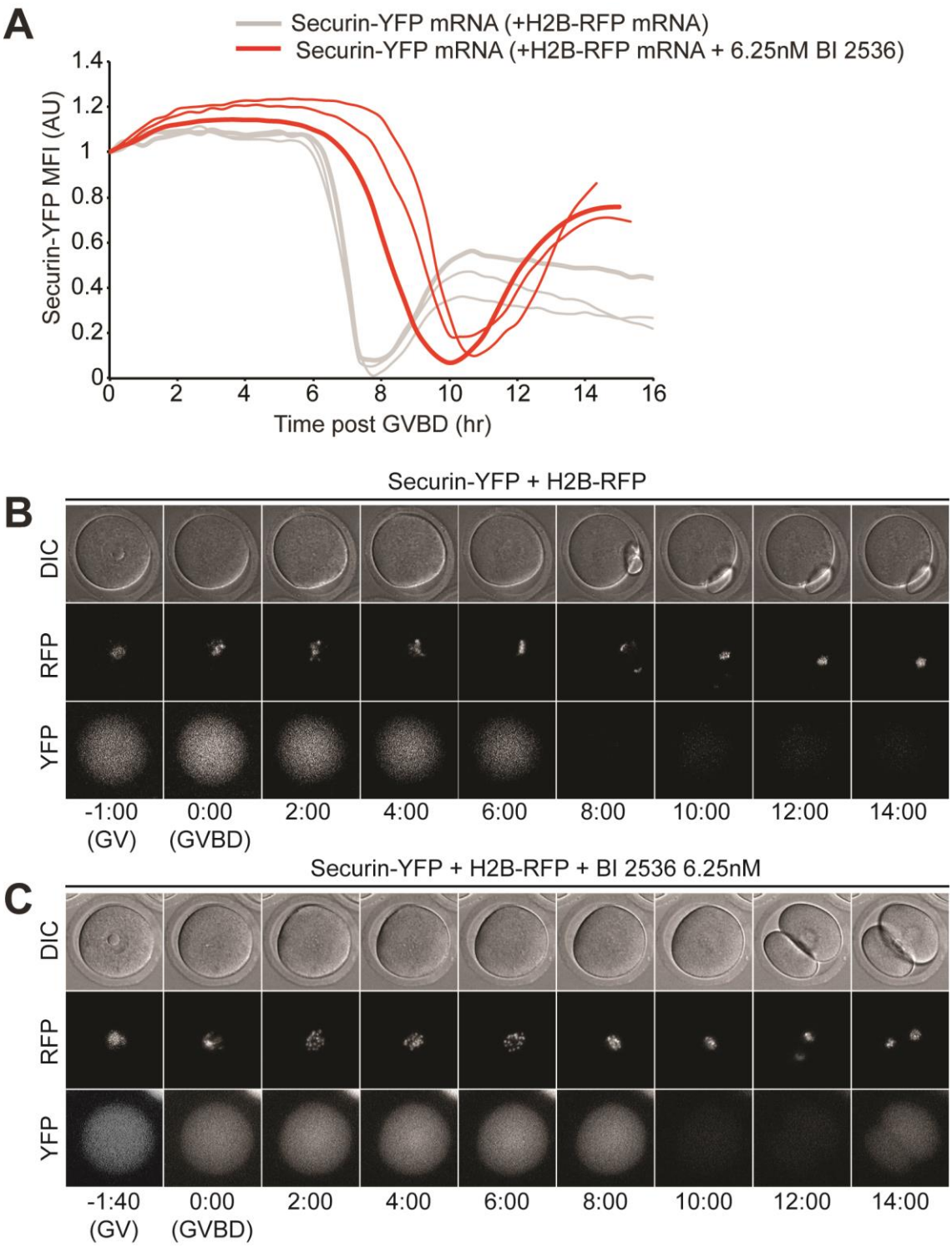

Figure 5.1 Degradation of securin-YFP during exit from MI in the presence of low concentrations (6.25 nM) of BI 2536

(A) Securin-YFP levels of representative oocytes (3 per group) co-injected with mRNA encoding securin-YFP and H2B-RFP and examined by time-lapse microscopy during incubation in control medium (grey, n=15) or in medium supplemented with 6.25nM BI 2536 (red, n=12). Securin-YFP mean fluorescence intensity (MFI) in oocytes was measured at each time-point and background FI was subtracted. The values were normalised relative to that of GVBD (0hr), and plotted against time. Securin-YFP degradation is delayed in the presence of BI 2536. Bold curves indicate oocytes shown in (B) and (C). AU, arbitrary units. **(B, C)** Selected DIC, RFP and YFP time-lapse images of the oocytes whose securin-YFP levels are illustrated by bold curves in (A), at the indicated time-points before and after GVBD in hours. Note the large polar body in (C)

5.3 BI 2536 promotes separation sister chromatids in a dose-dependent manner

The next step was to identify any possible effects that BI 2536 might have on chromosome segregation during meiosis I. To do that I prepared chromosome spreads of the oocytes that produced polar bodies and immunolabelled the centromeres for CREST.

Surprisingly, I found that BI 2536 induced premature separation of sisters (Fig 5.2). Concentration as low as 3nM BI2536 resulted in precocious separaton of sisters in the majority (90%) of oocytes compared with 8% of control oocytes (P<0.05) (Fig 5.2.B). The proportion of dyads showing premature separation of sisters increased in a dose-dependent manner, ranging from 9.3% (± 7.2%) in 3nM to 100% in 6.25nM and 12.5 nM (Fig 5.2.C).

Overall, these data indicate that Plk1 kinase activity is required to protect centromeric cohesion and that this function is highly sensitive to inhibition by BI 2536.

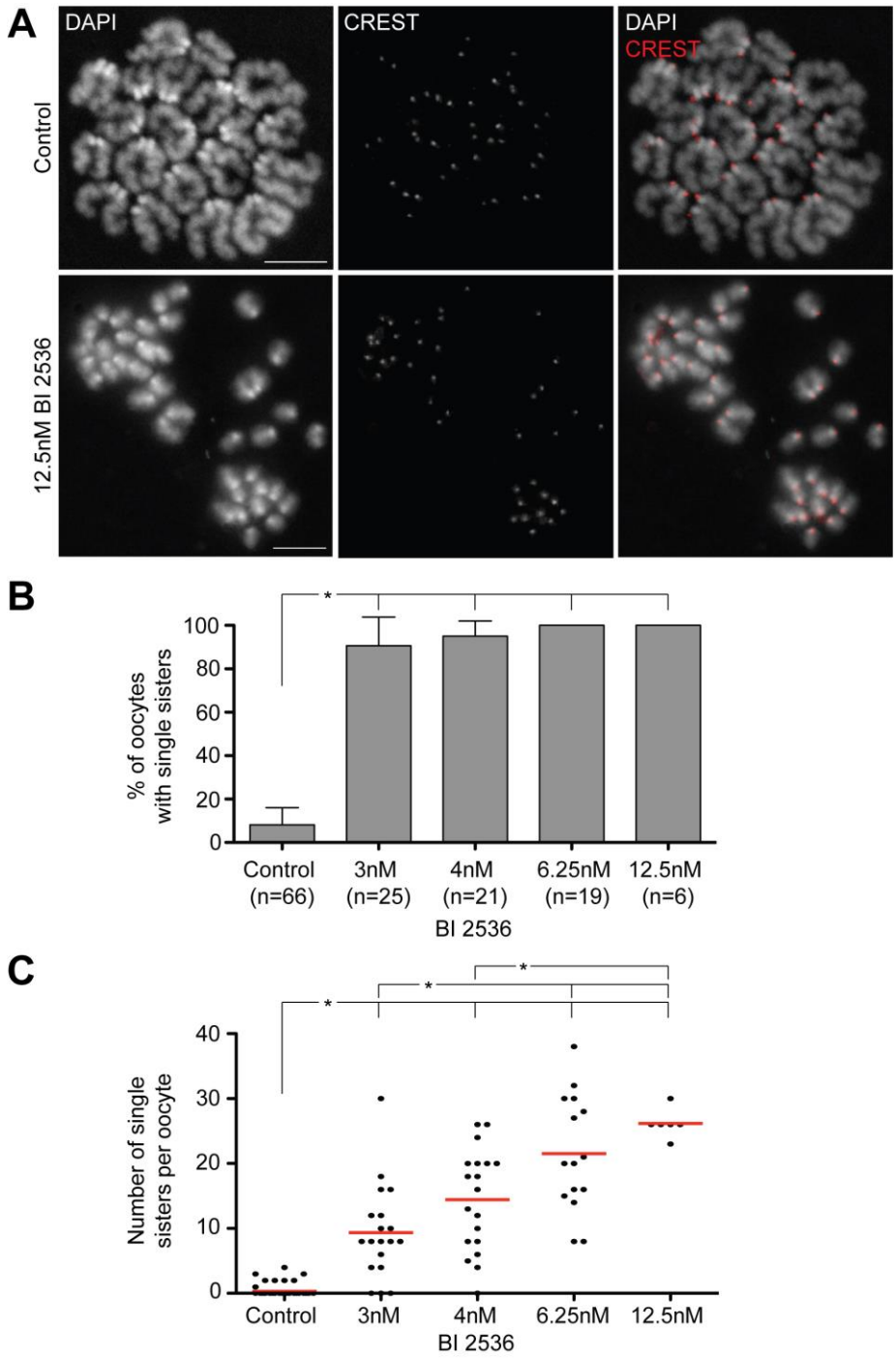

Figure 5.2 Sister chromatid separation in the presence of BI 2536

(A) Representative images showing DNA and CREST staining of chromosome spreads prepared from control and 12.5nM BI2536-treated oocytes, after exit from MI. Scale bars represent 10μm. Notice the separation of sister chromatids in BI 2536-treated oocytes. **(B)** The graph shows the percentages of oocytes exhibit premature sister-chromatid separation, following MI exit, after incubation in increasing concentrations of BI 2536: Control, 8% (±8% SD); 3nM BI2536, 90% (±13% SD), 4nM BI 2536, 95% (±7% SD); 6.25nM BI 2536, 100% (±0% SD); 12.5nM BI 2536, 100% (±0% SD). Notably, 6.25nM of BI 2536 are adequate to produce a fully penetrant effect. **(C)** The graph shows the number of separated sister chromatids in oocytes that exit MI, after incubation in increasing concentrations of BI 2536: Control, 0.3% (±0.87% SD); 3nM BI2536, 9.3% (±7.2% SD), 4nM BI 2536, 14.4% (±7.8% SD); 6.25nM BI 2536, 21.5% (±9% SD); 12.5nM BI 2536, 26.2% (±2.2% SD). BI 2536 appears to promote premature separation of sisters in a dose-dependent manner. Red lines indicate mean values and asterisks (*) indicate groups whose mean values show significant difference (P<0.05).

5.4 Post-PBE treatment with BI 2536 does induce premature separation of sister chromatids

In order to investigate whether the observed premature separation of sister chromatids caused by BI 2536 is due to an effect that occurs prior to metaphase II (MetII) arrest, I decided to expose oocytes to BI 2536 after the extrusion of the first polar body. Fully-grown prophase-arrested oocytes from CD1 mice were harvested and were cultured in control medium; those that had undergone GVBD within two hours were selected for further maturation. From the latter group, those that had successfully arrested at MetII after nine hours were transferred into medium supplemented with 6.25nM or 12.5nM of BI 2536. The oocytes were cultured for a further 10-12 hours in the presence of the inhibitor, before being used to produce chromosome spreads, which were immunolabeled for CREST.

In contrast to MI oocytes, exposure of MetII-stage oocytes to BI 2536 did not result in an increased incidence of single sisters (Fig 5.3). In particular, concentrations of 6.25nM and 12.5nM of BI 2536 did not have a significant effect either on the number of oocytes with separated sisters ($P>0.05$) or on the number of dyads showing premature separation of sisters per oocyte ($P>0.05$) compared with control oocytes .

These results indicate that PLK1 is likely to be involved in preventing separation of sisters during anaphase of MI.

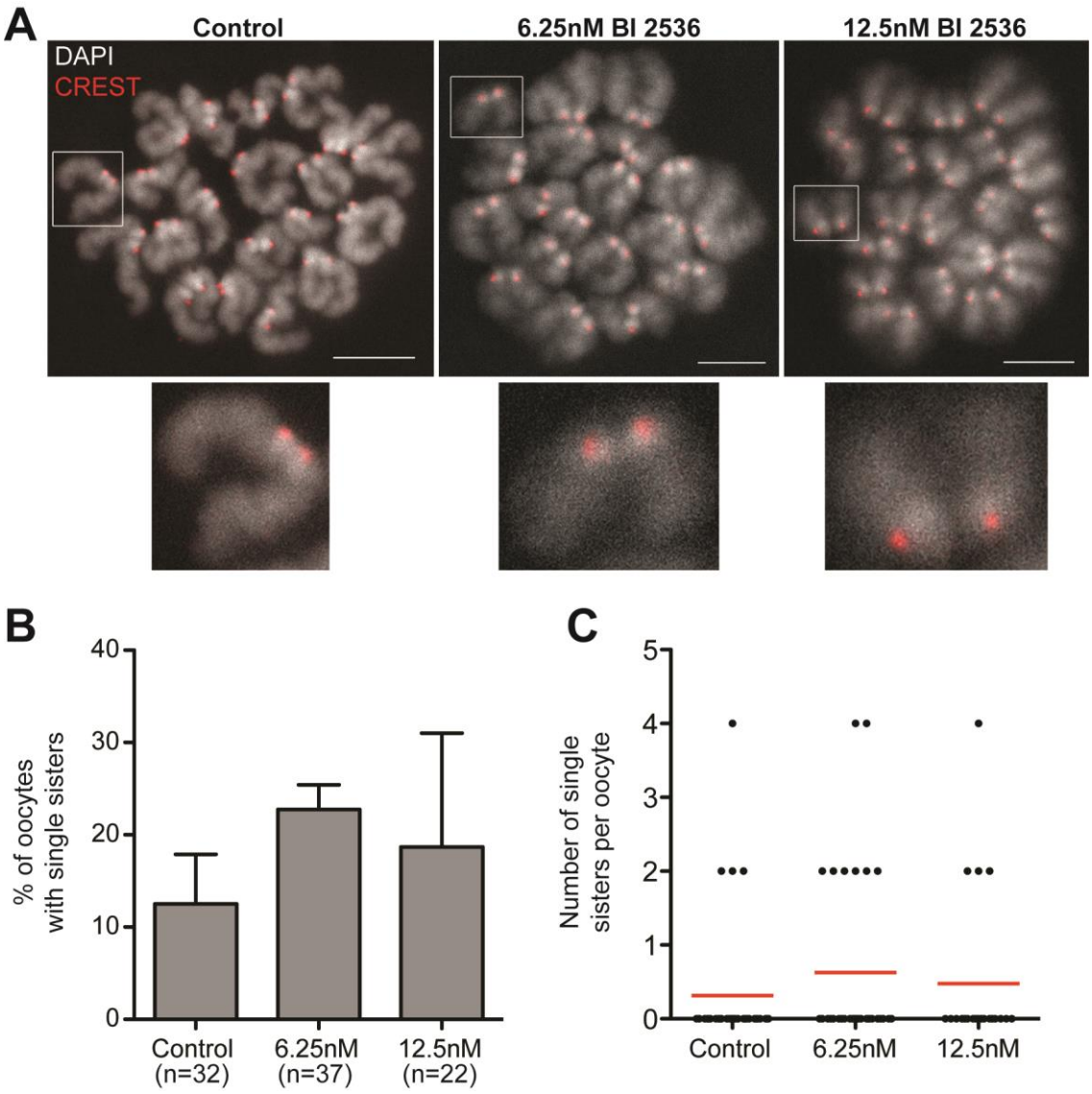

Figure 5.3 BI 2536 does not induce premature separation of sisters during MetII arrest

(A) Representative images showing DNA and CREST staining of chromosome spreads prepared from control and 6.25nM or 12.5nM BI2536-treated oocytes. BI 2536 was applied after PBE (MetII-arrest). Chromosomes surrounded by white boxes are shown in the enlarged images. Scale bars represent 10µm. **(B)** The graph shows the percentages of oocytes that exhibit premature sister-chromatid separation at MetII-arrest, after post-PBE incubation in increasing concentrations of BI 2536: Control, 12% (±10% SD); 6.25nM BI 2536, 22% (±5% SD); 12.5nM BI 2536, 19% (±8.9% SD). BI 2536 did not have a significant effect on the number of oocytes with separated sisters (P>0.05) **(C)** The graph shows the number of separated sister chromatids in oocytes exposed to increasing concentrations of BI 2536 after PBE: Control, 0.31 (±0.89 SD); 6.25nM BI 2536, 0.63 (±1.19 SD); 12.5nM BI 2536, 0.5 (±1.08 SD). BI 2536 does not appear to compromise sister chromatid integrity at the concentrations used (P>0.05). Red lines indicate mean values.

5.5 Centromeric cohesin is not depleted during in BI 2536-treated oocytes.

The presence of single sisters in oocytes which exit MI in the presence of BI 2536, gave ground to the hypothesis that centromeric cohesin might become depleted before the onset of anaphase I. To test this idea, I used the transgenic *Rec8-myc* mouse strain, where wild-type Rec8 has been replaced by a C-terminally 9x Myc-tagged wild-type Rec8 (Rec8-Myc), which can be specifically immunolabeled with an anti-myc antibody (Kudo *et al.*, 2009). In order to examine for a possible disruption in sister centromere integrity, the inter-centromeric distances and the levels of centromeric cohesin were measured and compared between late prometaphase (GVBD+6h) control oocytes and oocytes matured in medium supplemented with 6.25nM or 12.5nM BI 2536 (Fig 5.4). Consistent with my previous observation in oocytes from the CD1 mouse strain (Section 4.5.1), I found that inter-centromere distances significantly ($P < 0.0001$) increased in BI 2536 treated oocytes compared to control oocytes (Fig 5.4.D). For calculating centromeric Rec8:CREST fluorescence intensity ratios, following background FI subtraction, a square region of fixed area (5.4.Ea) was centred on the centromere to be measured and the Rec8 and CREST intensities were measured in the same region. Surprisingly, statistical analysis of the results showed a significant increase in the levels of centromeric Rec8-Myc in the presence of BI 2536.

These results indicate that premature sister separation in the presence of BI 2536 is not due to depletion of centromeric cohesin during progression through prometaphase I.

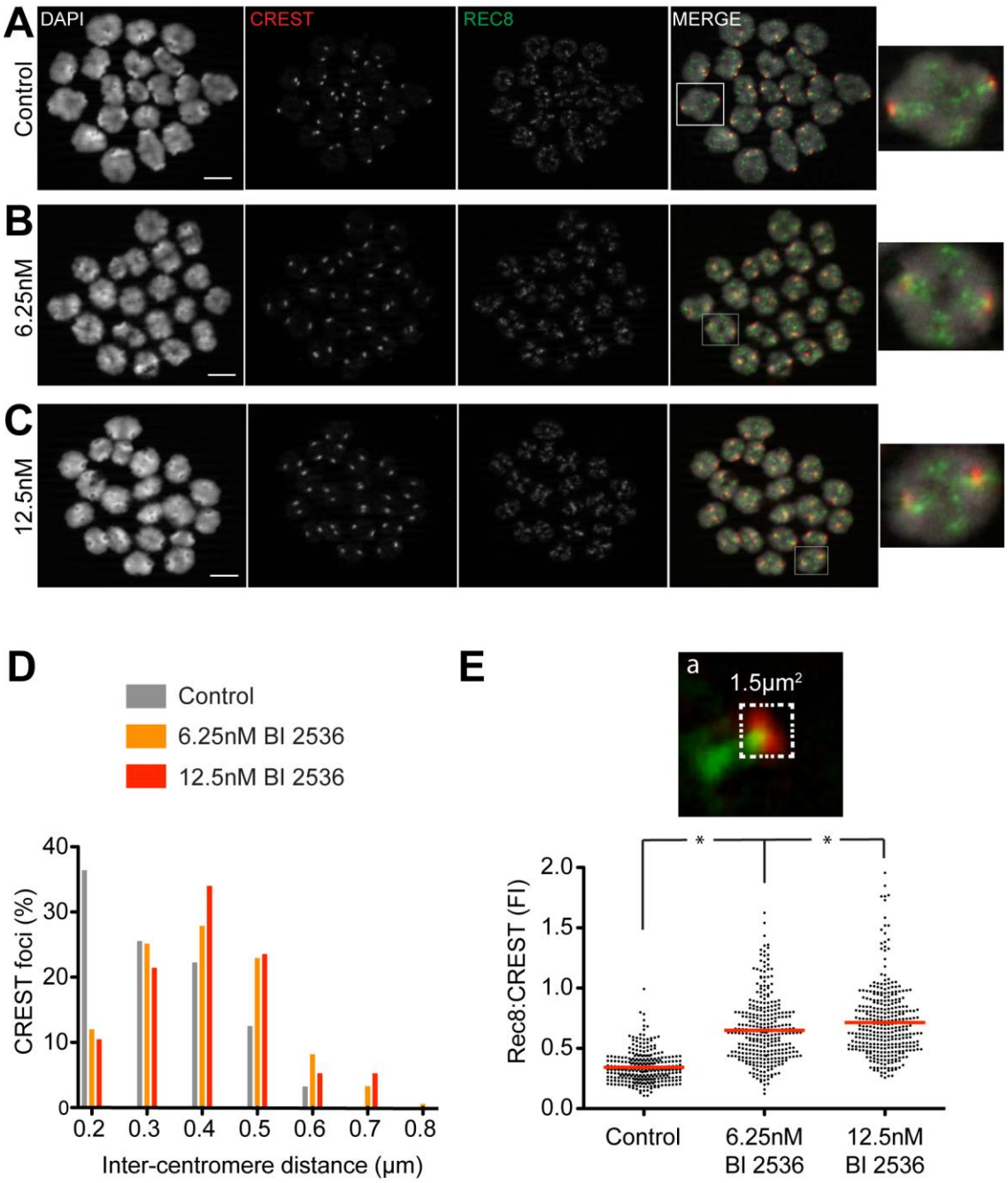

Figure 5.4 Effect of BI 2536 on inter-centromere distance and centromeric cohesin in Rec8-myc oocytes

Representative images showing DNA, Rec8, and CREST staining of chromosome spreads prepared during late prometaphase (GVBD + 6 hr) of MI oocytes from Rec8-myc mice incubated in **(A)** control media and media supplemented with **(B)** 6.25nM or **(C)** 12.5nM BI 2536. Chromosomes surrounded by white boxes are shown in the enlarged images. Scale bars represent 10µm. **(D)** Frequency distribution of the distance between sister centromeres, measured from the CREST foci in control (mean= 0.33±0.12µm; n = 184 centromeres; six oocytes from three mice), 6.25nM BI 2536-treated (mean= 0.41±0.13µm; n = 183 centromeres; six oocytes from three mice) and 12.5nM BI 2536-treated (mean= 0.42±0.13µm; n= 191 centromeres; six oocytes from three mice) oocytes, showing a significantly greater mean distance in the BI 2536-treared compared to control oocytes ($P < 0.0001$). **(E)** Graph showing Rec8: CREST fluorescence intensity (FI) ratios at the centromeres (a) of oocytes in (A) (n = 302 centromeres; eight oocytes from three mice), in (B) (n = 307 centromeres; eight oocytes from three mice) and in (C) (n = 333 centromeres; eight oocytes from three mice). Red lines indicate mean values and asterisks (*) indicate groups whose mean values show significant difference ($P<0.0001$).

5.6 BI 2536 compromises the centromeric localisation of Sgo2-PP2A at late prometaphase of MI

In light of the finding that centromeric cohesin is not depleted before the onset of anaphase I, I next asked whether premature separation of sisters might be due to disruption of the mechanisms responsible for protecting centromeric cohesin during anaphase of MI. As discussed previously, Sgo2 and PP2A are known to protect centromeric cohesion in mouse oocytes during anaphase of MI (Riedel *et al.*, 2006; Lee *et al.*, 2008; Llano *et al.*, 2008). I therefore investigated whether recruitment of these proteins to centromeres is disrupted in the presence of BI 2536.

Fully-grown prophase-arrested oocytes from CD1 mice were harvested and were allowed to mature in control medium or medium supplemented with 6.25nM BI 2536. Chromosome spreads were produced using oocytes at late prometaphase of MI (GVBD+7h) and were immunolabeled for CREST, Sgo2 and PP2A. Subsequent image analysis revealed what could be described as a diffused and "off-centred" localisation of both Sgo2 and PP2A on the sister centromeres of BI 2536-treated oocytes (Fig 5.5.B) compared to control oocytes (Fig 5.5.A). In addition, BI 2536-treated oocytes also appear to have higher levels of chromosome-associated PP2A (Fig 5.5.B) compared to controls. Sister centromeres were categorised into three groups; sister centromeres where Sgo2-PP2A colocalised centrally between centromeres (Fig 5.5.A1), others where the Sgo2-PP2A signal was displaced from the centre of the centromeres (Fig 5.5.B3) and finally some, where characterisation was not possible due to doubt and/or bad IF staining. Classification of numerous sister centromere pairs based on the "Central" or "Off-Centred" localisation of Sgo2-PP2A showed that there were significant ($P<0.001$) differences between control and BI 2536-treated oocytes (Fig. 5.5.C), with the "Off-Centred" configuration becoming prevalent in the presence of BI 2536. For example, in control oocytes 85% of late prometaphase

centromeres had a centrally localised Sgo2-PP2A signal, whereas the respective proportion in BI 2536-treated oocytes was just 33%.

These results indicate that the centromeric localisation of Sgo2 and PP2A, which is required for the maintenance of centromeric sister chromatid cohesion until the onset of anaphase II, is disrupted in oocytes in the presence of BI 2536. Based on these findings, I propose that centromeric cohesin might be partially "exposed" to the effect of seperase, and consequently cleaved, during anaphase I, thus leading to precocious sister-chromatid separation.

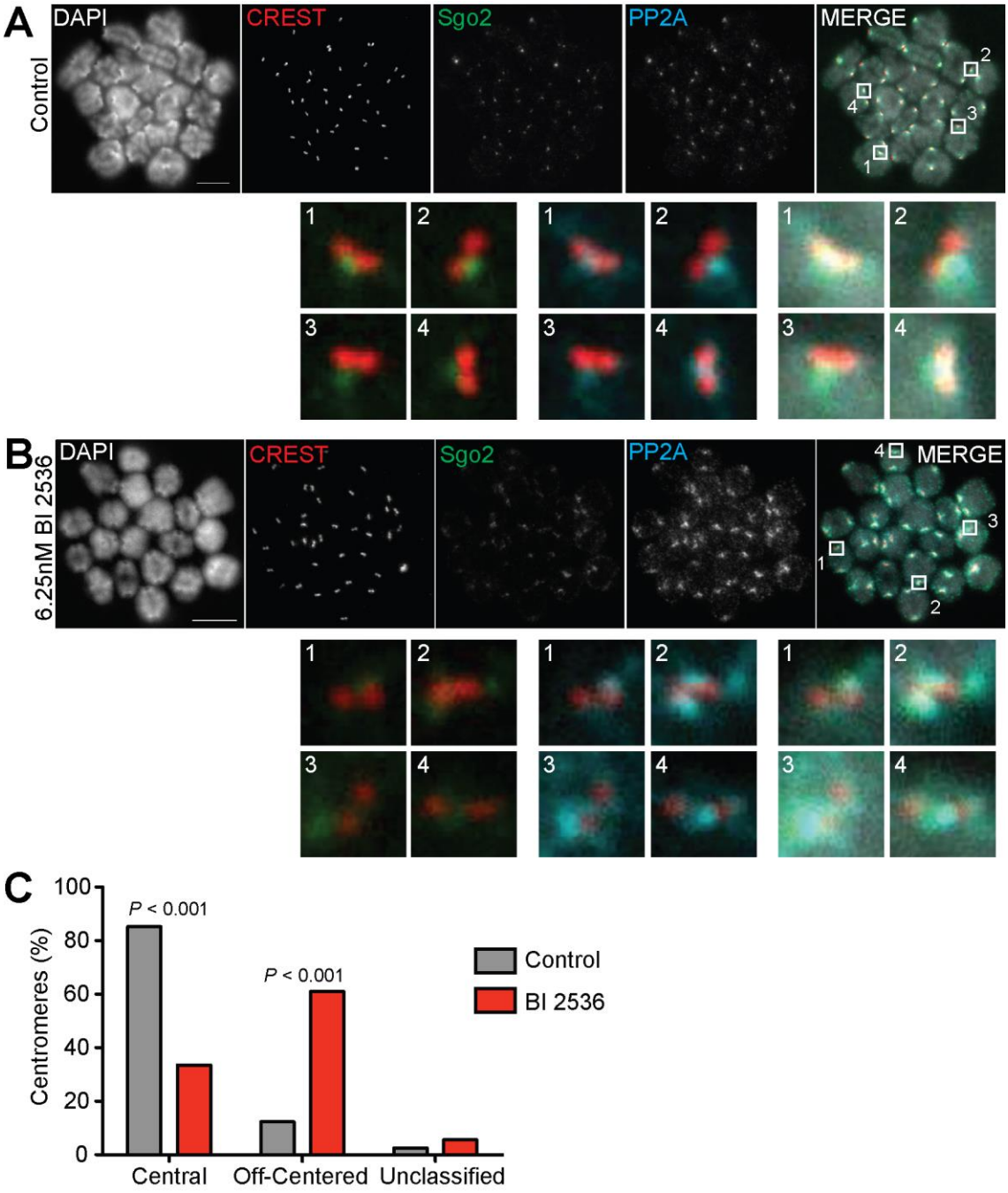

Figure 5.5 The effect of BI 2536 on centromeric localisation of Sgo2-PP2A in late prometaphase of MI

Representative images showing DNA, Sgo2, PP2A and CREST staining of chromosome spreads prepared during late prometaphase (GVBD + 7 hr) of oocytes cultured in **(A)** control medium (23 oocytes from 3 mice) and **(B)** in medium supplemented with 6.25nM BI 2536 (16 oocytes from 3 mice). Enlarged images show four numbered representative examples of sister centromeres. Notice the diffused and "off-centred" localisation of both Sgo2 and PP2A on the sister centromeres of BI 2536-treated oocytes compared to control oocytes. BI 2536-treated oocytes also appear to have higher levels of chromosome-associated PP2A. **(C)** Graph shows the proportions of centromeres in control (n = 400 centromeres; 10 oocytes from three mice) and BI 2536-treated (n = 440 centromeres; 11 oocytes from three mice) oocytes showing "Central" (e.g.A1), "Off-centred" (e.g. B3), and "Unclassified" localisation of Sgo2-PP2A. The proportion of sister centromeres with "Central" localisation of Sgo2-PP2A was significantly ($P < 0.001$) reduced in BI 2536-treated oocytes, whereas the proportion of "Off-Centred" Sgo2-PP2A foci was significantly ($P < 0.001$) higher compared to control oocytes. Scale bars represent 10μm.

5.7 BI 2536 does not affect the levels of chromosome-associated cohesin during prometaphase of MI.

The finding that centromeric cohesin is increased in the presence of BI 2536 (Fig 5.4), raised the possibility that some cohesin might be removed by a Plk1-dependent mechanism such as a meiotic equivalent of the Plk1-dependent prophase pathway. However, in vertebrate cells, the prophase pathway targets arm cohesin rather than centromeric cohesin (Sumara *et al.*, 2002; Hauf *et al.*, 2005) and as shown in section 5.4, the scope for quantitative analysis was limited to centromere-associated cohesin. I therefore asked what is the effect of BI 2536 on arm cohesin in mouse oocytes.

In preliminary experiments to identify a suitable "house-keeping" target to improve quantification of arm-associated cohesin, TO-PRO-3, a sequence-independent DNA stain, which binds specifically and stoichiometrically to the sugar phosphate back bone (Bink *et al.*, 2001; Ploeger *et al.*, 2008) was used (data not shown). Overall, TO-PRO-3 gave promising results in prometaphase oocytes, however, the staining pattern in BI 2536-treated oocytes was less reproducible and unfortunately this approach was abandoned.

Measurement of arm cohesin is also complicated by the fact that chromosomes become hyper-condensed in the presence of BI 2536. Therefore, although a first look at the IF signal of arm-associated cohesin in BI 2536-treated oocytes gives the impression that it is brighter compared to controls, implying a role of Plk1 in the removal of arm cohesin, it could also be an optical artifact due to chromatin hyper-condensation. To overcome this difficulty, I decided to investigate the effect of BI 2536 on chromosome arm-associated cohesin levels in aged oocytes. The rationale behind that decision was that the age-associated depletion of cohesin would allow me to distinguish a possible increase in its levels in the presence of BI 2536.

To test this idea, fully-grown prophase-arrested oocytes from 12-months old *Rec8-myc* mice were harvested and were allowed to mature in control medium or medium supplemented with 12.5nM BI 2536. Chromosome spreads were produced using oocytes at late prometaphase of MI (GVBD+6h) and were immunolabeled for CREST, and Rec8-myc (Fig 5.6A/B/C). Subsequent image analysis revealed that consistent with our previous observations (Lister *et al.*, 2010) Rec8 is significantly depleted in oocytes of aged mice (Fig 5.6B/D). However, only a slight and not particularly convincing increase was apparent in the levels of chromosome associated Rec8 in BI 2536-treated oocytes compared to control oocytes (Fig 5.6C/D).

These results suggest that in mouse oocytes arm-cohesin is generally resistant to removal by a Plk1-dependent pathway during progression through MI.

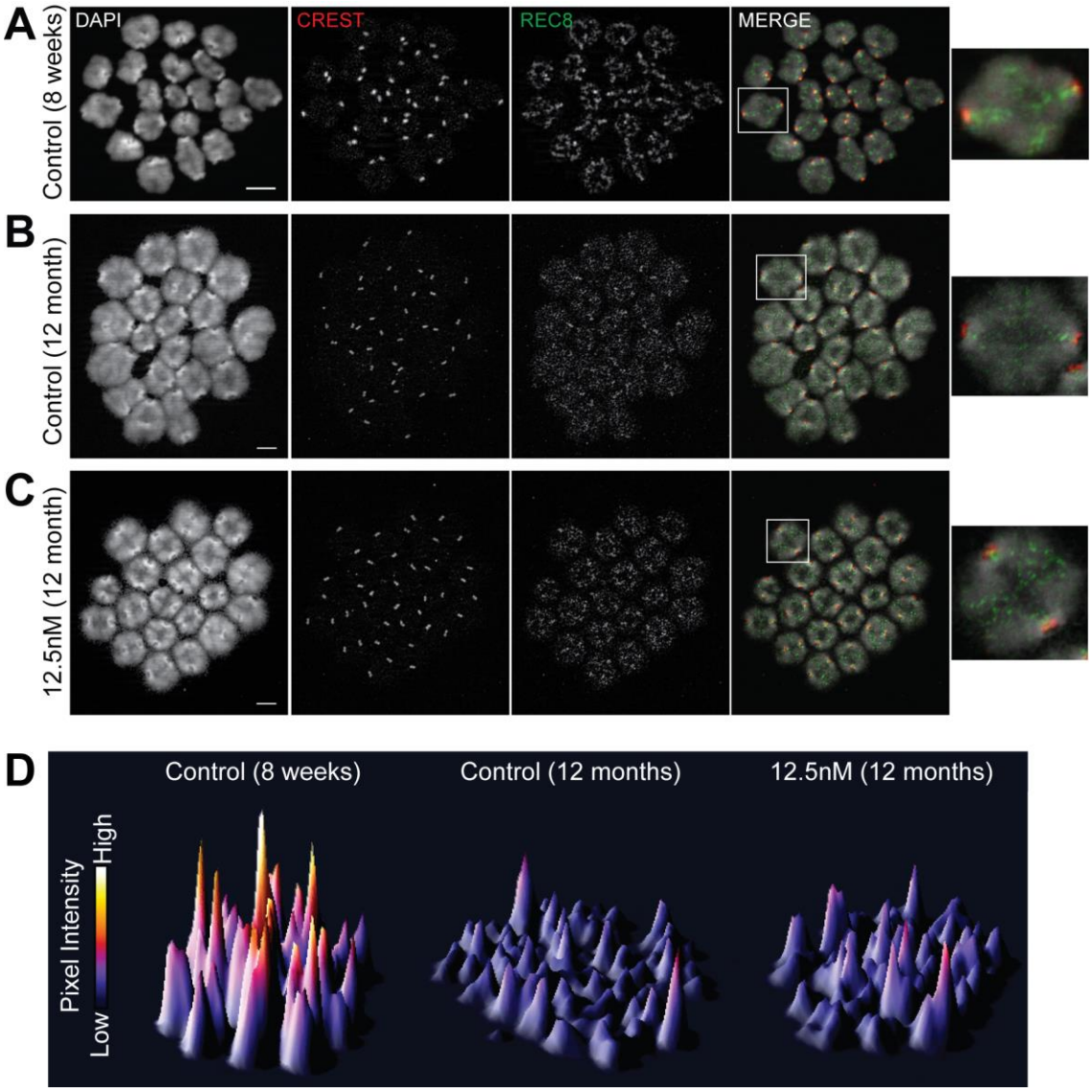

Figure 5.6 The effect of BI 2536 on chromosome-associated cohesin levels in late prometaphase I

Representative images showing DNA, Rec8, and CREST staining of chromosome spreads prepared during late prometaphase of MI (GVBD + 6 hr) of oocytes from **(A)** 8-weeks-old Rec8-myc mice, cultured in control media, **(B)** 12-months-old Rec8-myc mice, cultured in control media and **(C)** 12-months-old Rec8-myc mice, cultured in media supplemented with 12.5nM BI 2536. Chromosomes surrounded by white boxes are shown in the enlarged images. Notice the reduced Rec8 levels on chromosomes of oocytes from 8-weeks-old compared to 12-months-old mice. BI 2536-treated oocytes appear to have higher levels of chromosome-associated cohesin. Scale bars represent 10μm. **(D)** 3D surface plots of (A/B/C) showing higher Rec8 fluorescence intensity on chromosomes of 8-weeks-old compared with 12-month-old oocytes and a slight increase in Rec8 fluorescence intensity on chromosomes of 12-month-old control compared with 12-month-old BI 2536-treated oocytes.

5.8 Discussion

In this chapter I aimed to investigate the role of Plk1 in regulating chromosome segregation and cohesin removal during MI in mouse oocytes. I have provided evidence that Plk1 kinase activity is required for timely degradation of securin and successful cytokinesis in MI. My findings also indicate that Plk1 is required for the crucial meiotic function of protecting centromeric cohesin during MI, most likely through an effect on Sgo2-PP2A localisation. However, I found that, in contrast to its role in somatic cells (Sumara *et al.*, 2002; Hauf *et al.*, 2005), Plk1 does not appear to play a major role in removing cohesin before the onset of anaphase. This indicates that meiotic cohesin is largely resistant to removal by the propahse pathway.

5.8.1 The role of Plk1 in the protection of centromeric cohesion

To date most research has focused on the role of Plk1 and other Plks in the phosphorylation events that either directly promote cohesin dissociation (Sumara *et al.*, 2002; Hauf *et al.*, 2005) or prime cohesin for cleavage by separase (Lee and Amon, 2003; Kudo *et al.*, 2009; Katis *et al.*, 2010). Here, for the first time I present evidence that Plk1 kinase function is crucial for the protection of centromeric cohesin and thus its stepwise removal during mouse meiosis.

5.8.1.1 Effect of low concentrations of BI2536 on exit form MI

To study Plk1 function in regulating events during exit from MI, I took advanatage of the fact that a subset of ocytes produced polar bodies in the presence of low concentrations (≤12.5nM) of BI2536. My findings indicate a delay in securin degradation in the presence of BI 2536 (Fig 5.1). This is consistent with the findings I presented in Chapter 4, that Plk1 is required for APC/C activation.

Notably, polar body extrusion was also massively perturbed in the presence of BI 2536, with oocytes extruding fragmented and occasionally very large (Fig

5.1.C) polar bodies. Failed abscission attempts were also observed. This is consistent with observations in mitosis, where exposure of HeLa cells to BI 2536 during anaphase has been shown to block the ingression of the cleavage furrow resulting in cytokinesis failure (Brennan *et al.*, 2007a; Petronczki *et al.*, 2007).

5.8.1.2 BI 2536 promotes premature separation of sisters in a dose-dependent manner

In control MetII-arrested oocytes, dyads (pairs of sister chromatids) were predominantly observed (Fig 5.2A), albeit approximately 12% of the oocytes (Fig 5.2B) exhibited 2-4 separated sisters (Fig 5.2C), presumably due to mechanical stress during chromosome spreading. In striking contrast, however, oocytes that developed to MetII in the presence of BI 2536 showed a marked prevalence of separated single chromatids (Fig 5.2A). BI 2536-treated oocytes exhibited a mixture of single chromatids and intact dyads at MetII stage (Fig 5.2A), with the number of single sisters increasing with higher concentrations of BI 2536 (Fig 5.2C). Thus, BI 2536 induces premature separation of sisters indicating that Plk1 is required for the crucial function of protecting centromeric cohesin during MI.

5.8.1.3 Post-PBE inhibition of Plk1 does not promote premature sister separation

Given that separated sisters were detected in oocytes that had already exited MI, it was important to determine whether sister separation occurred during exit form MI or during MII arrest. To distinguish between these two possibilities, I incubated oocytes in BI 2536 shortly after PBE and prepared chromosome spreads to assess the extent of sister separation. I found no significant differences in the number of single sisters between BI 2536-treated and control oocytes (Fig 5.3B/C). Therefore, it is likely that the single chromatids arise during anaphase I, when cohesin is normally removed from chromosome arms, but is retained at centromeres.

5.8.1.4 Centromeric cohesin is not depleted during prometaphase I in BI 2536-treated oocytes.

Having established that inhibition of Plk1 induces premature separation of sisters, I asked whether centromeric cohesin was already depleted before the onset of anaphase. To test this idea I measured intercentromeric distances and levels of centromeric cohesin in control and BI 2536-treated *Rec8-myc* oocytes at late prometaphase of MI. Consistent with my previous observations in oocytes from CD1 mice (Fig 4.7), BI 2536 caused an increase in the intercentromeric distances at late prometaphase of MI (5.4D). However, the results indicate that centromeric cohesin was not depleted during late prometaphase in BI 2536-treated oocytes. These data, together with absence of an effect on MetII oocytes, imply that Plk1 is required to protect centromeric cohesin during anaphase of MI, rather than before or after it.

5.8.1.4 BI 2536 compromises centromeric Sgo2-PP2A localisation in prometaphase of MI

In yeast and vertebrate meiosis, Rec8 must be phosphorylated in order to be cleaved by separase during anaphase I (Lee and Amon, 2003; Kudo *et al.*, 2009; Katis *et al.*, 2010; Rumpf *et al.*, 2010). To prevent precocious separation of sister chromatids in MI, centromeric cohesin must be protected/de-phosphorylated. In both budding and fission yeast this is achieved through the phosphatase activity of PP2A, which is recruited to the centromere by Sgo1 and counteracts phosphorylation of Rec8 (Kitajima *et al.*, 2006; Riedel *et al.*, 2006). In mouse meiocytes, Sgo2 is responsible for recruitment of PP2A and protection of centromeric cohesin during MI (Lee *et al.*, 2008). Previous studies have shown that Aurora B and Bub1 are required for centromeric recruitment of Sgo2 in vertebrate somatic cells (Huang *et al.*, 2007) and that Bub1 might be involved in the recruitment of shugoshin proteins to centromeres in mouse oocytes (McGuinness *et al.*, 2009) . Could Plk1 activity at the centromere somehow also be involved in this process?

To test the idea that loss of centromeric cohesin during anaphase of MI was due to impaired protection, I asked whether Sgo2 and PP2A, are recruited to centromeres in the presence of BI 2536. Immunolabelling for Sgo2 and PP2A revealed a striking difference in the centromeric localisation of the Sgo2-PP2A complex between control and BI 2536-treated oocytes, with the latter being characterised by sister centromeres where Sgo2-PP2A was displaced from the centre of the centromeres (Fig 5.5). Presuming that Sgo2-PP2A should localise physically close to centromeric cohesin, in order to fulfill its protective role, then the off-centred positioning of Sgo2-PP2A is unlikely to be effective in protecting the cohesin complexes between sister centromeres from cleavage by separase.

It remains to be established whether mislocalisation of Sgo2 and PP2A is linked to the increased distance between sister centromeres observed in BI 2536-treated oocytes. The reason for the increased distance between sisters is also obscure, but it may be linked to the hyper-condensed state of the chromatin in the presence of BI 2536. In other words, hyper-condensation of pericentromeric chromatin may push sister centromeres apart. An alternative possibility is that Plk1 is required for monopolar attachment and that the increased distance between sisters is caused by bi-oriented sisters being pulled towards opposite poles. However, my analysis of kinetochore-microtubule attachments presented in the previous chapter provided no convincing evidence that biorientation of sisters is prevalent during MI in BI 2536-treated oocytes. Taken together the data suggest that that mislocalisation of Sgo2, due to either a direct or indirect effect of Plk1 inhibition, is sufficient to explain loss of centromeric cohesin during anaphase of MI.

Further experimentation to dissect the mechanisms of Plk1 function would involve the use of nocodazole or taxol in order to examine whether absence of

Mt attachments or tension, respectively, alters the observed effect of BI 2536 on Sgo2-PP2A localisation. The effects of hyper-condensation would be harder to assess, as I am not currently aware of a method that could counteract this effect of BI 2536 on chromosome condensation, without interfering with other known Plk1 functions.

5.8.2 No evidence of prophase pathway-like activity in MI

In vertebrate mitosis, the bulk of chromosome arm-associated cohesin is removed during prometaphase by phosphorylation of the SA2 (and presumably SA1) cohesin subunit by Plk1; this process is separase-independent and is referred to as the prophase pathway (Waizenegger *et al.*, 2000; Sumara *et al.*, 2002; Hauf *et al.*, 2005). The presence or absence of this pathway has not yet been experimentally confirmed in vertebrate meiocytes, although Plk1 has been shown to be highly active during prometaphase I in mouse oocytes (Pahlavan *et al.*, 2000). It seems logical though to presume that the prophase pathway is very tightly regulated, if not completely inhibited, as precocious removal of arm cohesin prior to anaphase I would result in premature resolution of chiasmata leading to devastating effects for meiosis (Roeder, 1997). However, this assumption does not exclude the possibility that Plk1 kinase activity might somehow contribute to arm-associated cohesin depletion in oocytes during the prolonged prophase arrest stage and/or the prometaphase I stage, which lasts longer in meiosis (~6h, mouse; ~20h, human) than in mitosis (~45min, human). Such an effect of Plk1 during meiotic maturation would have adverse effects especially on aged oocytes as these oocytes both spend more time in prophase arrest and resume MI with depleted levels of chromosome associated cohesin (Chapter 1).

To test the hypothesis that Plk1 activity might contribute to cohesin depletion during prometaphase I, I initially decided to inhibit it and examine for differences in chromosome arm-associated cohesin levels at late prometaphase

of MI in oocytes from young (8wks old) *Rec8-myc* mice. Unfortunately, this approach proved inefficient, because the combination of high levels of cohesin in young oocytes and chromosome hyper-condensation rendered my immuno-fluorescence intensity quantification methods non-applicable. To overcome this I decided to follow the same approach, but to use oocytes from aged mice instead, assuming that a change in cohesin levels would be more distinguishable when using oocytes with already depleted levels of chromosome-associated cohesin. The results (Fig 5.6) revealed no apparent difference in the levels of chromosome-associated Rec8 between control and BI 2536-treated oocytes. In contrast to what has been shown in mitotic cells (Lenart *et al.*, 2007), these data suggest that Plk1-mediated removal of cohesin is negligible, I any, in mouse oocytes. It could be argued that Plk1 activity might be removing Scc1-containing cohesin, instead of Rec8-containing ones, from chromosomes during prophase and/or prometaphase I. However, a recent study suggested that Scc1-containing cohesin does not contribute to sister chromatid cohesion in MI (Tachibana-Konwalski *et al.*, 2010).

Assuming that Plk1 activity actually poses a threat to arm-associated cohesin during prometaphase of MI, what might be the protection mechanisms against it? In mitosis separase-independent removal of cohesin through the prophase pathway is achieved through Plk1-dependent phosphorylation of its SA2 subunit (Hauf *et al.*, 2005). However, in invertebrate meiocytes SA1 and SA2 subunits are replaced by the meiosis-specific SA3 (Prieto *et al.*, 2001). I have used Clustal Omega (http://www.ebi.ac.uk/Tools/msa/clustalo/) to align the nucleotide sequences of SA1, SA2 and SA3 and I found that although all the known Plk1 phosphorylation sites on SA2 (Hauf *et al.*, 2005) are conserved in SA1, only 5 out of 21 (~24%) are conserved in SA3 (data not shown). Unfortunately, my limited bioinformatics knowledge has not allowed me to investigate for putative Plk1 binding sites on SA3. Could this reduction in Plk1 phosphorylation sites indicate a role for SA3 in protecting arm-associated

cohesin from Plk1 activity? This hypothesis would actually be consistent with previous findings showing that in mammalian oocytes SA3 localises to the interchromatid domain during prometaphase I, but is not detected on chromosomes after anaphase I (Prieto *et al.*, 2001). Further research in our lab (Randy Ballesteros) has shown that Plk1 is mostly kept outside the nucleus during oocyte growth suggesting another mechanism in place for restricting putative Plk1 effects on chromosomal cohesin during prophase arrest. Taken together the above data indicate that Plk1 is not likely to be a major contributor to its loss during mammalian female reproductive ageing.

In summary, my findings indicate that the major role of Plk1 in relation to the regulation of cohesin, rests in the protection of centromeric cohesin from separase during anaphase I, rather than in the removal of arm cohesin via a meiotic equivalent of the prophase pathway.

Chapter 6 . Conclusion & Future Directions

The work described in this thesis makes a significant contribution towards a better understanding of the mechanisms regulating chromosome segregation in mammalian oocytes. This was achieved by pursuing three lines of investigation: 1) The effect of ageing on cohesin and its protector, Sgo2; 2) Characterisation of Plk1 function in oocytes; 3) The role of Plk1 in cohesin protection and removal in oocyte meiosis.

6.1 Cohesin and female reproductive ageing

During recent years evidence is accumulating to support the hypothesis that cohesin deterioration is an age-dependent process and correlates with an increasing incidence of aneuploidies (Hodges *et al.*, 2005; Liu and Keefe, 2008; Chiang *et al.*, 2010; Lister *et al.*, 2010; Chiang *et al.*, 2011).

In support of the above, in this thesis I show that age-related depletion of chromosomal cohesin occurs during the prolonged period of prophase arrest experienced by oocytes from older females. I also document an increase in intercentromere distance in older oocytes. Interestingly, I also find that the cohesin protector Sgo2 is also reduced with increasing age, that it is not recruited to chromosomes until the transition from prophase to prometaphase of MI and that its recruitment is impaired in cohesin-deficient oocytes. On the basis of these findings, we propose a scenario where the depletion of cohesin during the extended prophase arrest causes impaired recruitment or retention of Sgo2 to chromosomes during late prophase, which in turn renders the remaining cohesin vulnerable to removal during prometaphase I resulting in disruption of the unique chromosome architecture required for normal segregation of homologues during anaphase of MI.

Support for this model comes from recent findings in mouse oocytes that bivalent stability depends on cohesin complexes loaded in S-phase (Revenkova *et al.*, 2010; Tachibana-Konwalski *et al.*, 2010). This also implies that intervention strategies based on replenishment of cohesin are not likely to rescue age-related defects. Thus, the immediate focus of future research would be to uncover the primary mechanisms of cohesin loss and to determine whether the model can be applied to reproductive ageing in women.

Depletion of chromosome- associated cohesin in oocytes of older females may be a consequence of protein damage, or removal by a separase-independent or separase-dependent pathway. In support of the latter, preliminary experiments in our lab indicate that separase is expressed in prophase-arrested mouse oocytes. This is consistent with findings in budding yeast (Katis *et al.*, 2010) and raises the possibility that even a very low level of separase activity might result in significant depletion of cohesin during the extended period of prophase arrest in aged females.

Another important question is whether cohesin loss occurs during the relatively quiescent primordial stage and whether it occurs uniformly across all stages of oocyte development. A marked difference between young and aged oocytes at the primordial stage would be consistent with a gradual loss of cohesin during prolonged prophase arrest. By contrast, if the difference becomes apparent only in growing oocytes, it could be speculated that the age-related depletion of cohesin is linked either to movement of the cohesin ring during the massive burst of transcriptional activity (Kagey *et al.*, 2010), and/or due to protein damage associated with increased metabolic activity. Answering these questions is crucial to understanding the underlying mechanisms of cohesin loss and to gaining insight into the feasibility of preventative strategies.

6.2 Plk1 function in mouse oocytes and its association with cohesin

The previously reported (Wianny *et al.*, 1998) association of Plk1 with meiotic chromosomes, has received very little attention in studies of the enzyme in mammalian meiosis. Consistent with what has been observed in mitotic cells (Petronczki *et al.*, 2008), the punctate localisation of Plk1 that I have described in this thesis leaves no doubt that it associates with the kinetochore region of meiotic chromosomes. Importantly, by using a low concentration of BI 2536, I have unmasked a function for Plk1 in protecting centromeric cohesin during anaphase of MI. My findings indicate that loss of centromeric cohesin in the presence of BI 2536 is due to mislocalisation of the cohesin protector Sgo2. These findings indicate that Plk1 is required not only for accurate kinetochore function, but also for accurate chromosome segregation during meiosis. It is interesting how Plk1 almost disappears from the kinetochore region of Met-II chromosomes, which no longer necessitate protection of centromeric cohesion by Sgo2.

An additional important finding is that APC/C activation in MI appears to be Plk1-dependent. This contrasts with findings in mitosis where Plk1 inhibition leads to prometaphase arrest by activating the SAC and not through an effect on the core APC/C (Lenart *et al.*, 2007). The key question that needs to be answered in the future is whether Plk1 is required to suppress an inhibitor of the APC/C in meiosis or whether phosphorylation by Plk1 is required for efficient activation of the APC/C during exit from MI.

Moreover, the finding that inhibition of Plk1 activity, permissive for anaphase to occur, had no effect on MI chromosome segregation indicates that Rec8 and/or separase phosphorylation by Plk1 is not required for Rec8 cleavage by separase. This finding challenges a previous report that phosphorylation by Plk1 is essential for mouse Rec8 cleavage by separase *in vitro* (Kudo *et al.*, 2009). It is conceivable that either Rec8 phosphorylation by Plk1 is not important for

MI chromosome segregation or there are additional protein kinases phosphorylating Rec8 *in vivo*. However, we cannot at this stage exclude the possibility that residual Plk1 activity was present at the concentrations of BI 2536 used in the experiments described in this thesis.

Finally, I have investigated for evidence of Plk1-mediated removal of cohesin from meiotic chromosomes in a mechanism analogous to the prophase pathway. I present data indicating that removal of cohesin by a Plk1-mediated mechanism is unlikely to be a major mechanism of cohesin removal during prometaphase of MI and is therefore unlikely to contribute to an age-related loss of cohesin during progression through prometaphase. This triggers the question of how is arm-cohesin immunized against Plk1 activity, which is highly active during the prolonged prometaphase of MI in oocytes.

Plk1 has already been assigned a plethora of roles in mitosis; therefore it is not surprising to discover similar or additional functions in meiosis. However, we cannot exclude the possibility that the observed chromatin hyper-condensation in the presence of BI 2536 might cause deformations of the centromere and kinetochore, thus further interrupting the balance between levels of kinase-phosphatase activities at kinetochores, which is known to depend highly on Plk1 activity (Archambault and Carmena, 2012).

Taken together, our findings indicate that Plk1 has previously unknown functions during mammalian meiosis involving activation of the APC/C and stepwise removal of cohesin, both of which are essential for normal segregation of chromosomes. Moreover, we show that Plk1 activity is not likely to be a major contributor to cohesin loss during mammalian female ageing. The identification of Plk1's exact role and position in the molecular pathways that govern these processes during meiosis remain to be elucidated. Although the small-molecule inhibitors BI 2536 has proven to be a fantastic research tool for

dissecting the spatio-temporal function of Plk1, further research into the molecular mechanisms will necessitate different approaches.

6.3 Clinical Relevance

Female ageing is the most important aetiological factor for genetic abnormalities and infertility in humans (Nagaoka *et al.*, 2012). Despite this, recent birth statistics show that the number of babies born to mothers older than 35 years of age increased by 46% between 1996 and 2006 (Morris and Alberman, 2009). The impact of this on human reproductive health is highlighted by a 70% increase in the incidence of Down's syndrome pregnancy during the past 20 years (Morris and Alberman, 2009). The trend for women to delay childbearing also has enormous implications for general health, wellbeing and socio-economic stability. For example, a report from the actuarial profession in the UK (*More babies? Who needs them?*, 2004) predicts that the declining birth rate will reduce the support ratio (defined as the number of working people per person aged >65 years) from 3.9 in 2004 to 2.2 by 2050. Thus, the trend for women to postpone reproduction is a double-edged sword, which cuts the support ratio while creating the additional problems of age-related infertility and health care demands of prenatal testing, pregnancy terminations and, in the event of birth defects, care of the disabled. The work presented in this thesis constitutes a significant step towards understanding the primary causes of female age-related chromosome defects. This will provide us with insights into the feasibility of developing strategies to prevent or reduce cohesin loss.

Abbreviations

Ama1	Activator of meiotic anaphase complex
APC/C	Anaphase promoting complex/ Cyclosome
Ark1	Aurora kinase 1
ATP	Adenosine tri-phosphate
Bub1-3	Budding uninhibited by benzimidazoles 1-3 homolog
BubR1	Budding uninhibited by benzimidazoles 1 homologue beta
BSA	Bovine serum albumin
cAMP	Cyclic adenosine mono-phosphate
Cdc20	Cell division cycle 20
Cdh1	Cell division cycle 20 homologue 1
Cdk1	Cell dependent kinase 1
cDNA	Complementary DNA
CENP A-F	Centromeric protein A-F
CO_2	Carbon dioxide
CPC	Chromosomal passenger complex
CREST	Calcinosis, Raynaud phenomenon, esophageal dismotility, sclerodactyly, telangiectasia
CSF	Cytostatic factor
Cyclin B1-GFP	Green fluorescent tagged cyclin B1
DAPI	4',6-diamidino-2-phenylindole
DIC	Differential interference contrast
DNA	Deoxyribonucleic acid
DTT	Dithiothreitol
FSH	Follicle stimulating hormone
GAPDH	Glyceraldehyde 3-phosphate dehydrogenase
GFP	Green fluorescent protein
GV	Germinal vesicle
GVBD	Germinal vesicle breakdown
H2B-RFP	Histone 2B-red fluorescent protein
IBMX	Isobutylmethylxanthine
LH	Luteinising hormone
Mad2	Mitotic-arrest deficient 2
MAPK	Mitogen-activated protein kinase
MCC	Mitotic checkpoint complex
ME-S332	Meiotic from Salaria 332
MetI	Metaphase I
MetII	Metaphase II
MI	Meiosis I
µg	Microgram
µl	Microliter
µm	Micrometre
µM	Micromolar
MII	Meiosis II
mM	Millimolar
M	Molar
mRNA	Messenger RNA
MTOC	Microtubule organizing centre

Myc	Myelocytomatosis viral oncogene
na	Numerical Aperture
NaOH	Sodium hydroxide
NEBD	Nuclear envelope breakdown
NLS	Nuclear localisation sequence
nM	Nanomolar
PB	Polar body
PBE	Polar body extrusion
PBS	Phosphate buffered saline
PCR	Polymerase chain reaction
PFA	Paraformaldehyde
PGC	Primordial germ cell
Plk1/Plx1	Polo-like kinase 1
PMSG	Pregnant mare serum gonodotrophin
PP2A	Protein phosphastase 2A
Rad21	Double strand break repair protein Rad21 homologue
Rec8	Meiotic recombination protein Rec8 homologue
RFP	Red fluorescence protein
RNAi	Ribonucleic acid interference
RNAse	Ribonuclease
RT	Room temperature
SA1-3	Stromal antigen protein 1-3
SAC	Spindle assembly checkpoint
SAM	Senescence accelerated mouse
Scc1-4	Sister chromatid cohesion protein 1-4
Sgo1-2	Shugoshin 1-2
siRNA	Small interference RNA
Smc1-3	Structural maintenance of chromosomes 1-3
Sycp3	Synaptonemal complex protein 3
UTR	Untranslated region
v/v	By volume
w/v	By weight
YFP	Yellow fluorescent protein

Acquaviva, C. and Pines, J. (2006) 'The anaphase-promoting complex/cyclosome: APC/C', *J Cell Sci*, 119(Pt 12), pp. 2401-4.

Ahonen, L.J., Kallio, M.J., Daum, J.R., Bolton, M., Manke, I.A., Yaffe, M.B., Stukenberg, P.T. and Gorbsky, G.J. (2005) 'Polo-like kinase 1 creates the tension-sensing 3F3/2 phosphoepitope and modulates the association of spindle-checkpoint proteins at kinetochores', *Curr Biol*, 15(12), pp. 1078-89.

Archambault, V. and Carmena, M. (2012) 'Polo-like kinase-activating kinases: Aurora A, Aurora B and what else?', *Cell Cycle*, 11(8), pp. 1490-5.

Archambault, V. and Glover, D.M. (2009) 'Polo-like kinases: conservation and divergence in their functions and regulation', *Nat Rev Mol Cell Biol*, 10(4), pp. 265-75.

Arnaud, L., Pines, J. and Nigg, E.A. (1998) 'GFP tagging reveals human Polo-like kinase 1 at the kinetochore/centromere region of mitotic chromosomes', *Chromosoma*, 107(6-7), pp. 424-9.

Aulia, S. and Tang, B.L. (2006) 'Cdh1-APC/C, cyclin B-Cdc2, and Alzheimer's disease pathology', *Biochem Biophys Res Commun*, 339(1), pp. 1-6.

Baker, D.J., Dawlaty, M.M., Galardy, P. and van Deursen, J.M. (2007) 'Mitotic regulation of the anaphase-promoting complex', *Cell Mol Life Sci*, 64(5), pp. 589-600.

Bannister, L.A., Reinholdt, L.G., Munroe, R.J. and Schimenti, J.C. (2004) 'Positional cloning and characterization of mouse mei8, a disrupted allelle of the meiotic cohesin Rec8', *Genesis*, 40(3), pp. 184-94.

Barford, D. (2011) 'Structural insights into anaphase-promoting complex function and mechanism', *Philos Trans R Soc Lond B Biol Sci*, 366(1584), pp. 3605-24.

Beaumont, H.M. and Mandl, A.M. (1961) ' A quantitative and cytological study of oogonia and oocytes in the foetal and neonatal rat', *Proc R Soc London B*, 155, pp. 557–579.

Bentley, A.M., Normand, G., Hoyt, J. and King, R.W. (2007) 'Distinct sequence elements of cyclin B1 promote localization to chromatin, centrosomes, and kinetochores during mitosis', *Mol Biol Cell*, 18(12), pp. 4847-58.

Bink, K., Walch, A., Feuchtinger, A., Eisenmann, H., Hutzler, P., Hofler, H. and Werner, M. (2001) 'TO-PRO-3 is an optimal fluorescent dye for nuclear counterstaining in dual-colour FISH on paraffin sections', *Histochem Cell Biol*, 115(4), pp. 293-9.

Blat, Y. and Kleckner, N. (1999) 'Cohesins bind to preferential sites along yeast chromosome III, with differential regulation along arms versus the centric region', *Cell*, 98(2), pp. 249-59.

Bornslaeger, E.A., Mattei, P. and Schultz, R.M. (1986) 'Involvement of cAMP-dependent protein kinase and protein phosphorylation in regulation of mouse oocyte maturation', *Dev Biol*, 114(2), pp. 453-62.

Bornslaeger, E.A., Mattei, P.M. and Schultz, R.M. (1988) 'Protein phosphorylation in meiotically competent and incompetent mouse oocytes', *Mol Reprod Dev*, 1(1), pp. 19-25.

Brar, G.A. and Amon, A. (2008) 'Emerging roles for centromeres in meiosis I chromosome segregation', *Nat Rev Genet*, 9(12), pp. 899-910.

Brar, G.A., Kiburz, B.M., Zhang, Y., Kim, J.E., White, F. and Amon, A. (2006) 'Rec8 phosphorylation and recombination promote the step-wise loss of cohesins in meiosis', *Nature*, 441(7092), pp. 532-6.

Brennan, I.M., Peters, U., Kapoor, T.M. and Straight, A.F. (2007a) 'Polo-like kinase controls vertebrate spindle elongation and cytokinesis', *PLoS One*, 2(5).

Brennan, I.M., Peters, U., Kapoor, T.M. and Straight, A.F. (2007b) 'Polo-like kinase controls vertebrate spindle elongation and cytokinesis', *PLoS One*, 2(5), p. e409.

Brunet, S., Maria, A.S., Guillaud, P., Dujardin, D., Kubiak, J.Z. and Maro, B. (1999) 'Kinetochore fibers are not involved in the formation of the first meiotic spindle in mouse oocytes, but control the exit from the first meiotic M phase', *J Cell Biol*, 146(1), pp. 1-12.

Brunet, S., Pahlavan, G., Taylor, S. and Maro, B. (2003) 'Functionality of the spindle checkpoint during the first meiotic division of mammalian oocytes', *Reproduction*, 126(4), pp. 443-50.

Brunet, S., Polanski, Z., Verlhac, M.H., Kubiak, J.Z. and Maro, B. (1998) 'Bipolar meiotic spindle formation without chromatin', *Curr Biol*, 8(22), pp. 1231-4.

Buonomo, S.B., Clyne, R.K., Fuchs, J., Loidl, J., Uhlmann, F. and Nasmyth, K. (2000) 'Disjunction of homologous chromosomes in meiosis I depends on proteolytic cleavage of the meiotic cohesin Rec8 by separin', *Cell*, 103(3).

Burkard, M.E., Randall, C.L., Larochelle, S., Zhang, C., Shokat, K.M., Fisher, R.P. and Jallepalli, P.V. (2007) 'Chemical genetics reveals the requirement for Polo-like kinase 1 activity in positioning RhoA and triggering cytokinesis in human cells', *Proc Natl Acad Sci U S A*, 104(11), pp. 4383-8.

Byskov, A.G. (1974) 'Cell kinetic studies of follicular atresia in the mouse ovary', *J Reprod Fertil*, 37(2), pp. 277–285.

Casenghi, M., Barr, F.A. and Nigg, E.A. (2005) 'Phosphorylation of Nlp by Plk1 negatively regulates its dynein-dynactin-dependent targeting to the centrosome', *J Cell Sci*, 118(Pt 21), pp. 5101-8.

Casenghi, M., Meraldi, P., Weinhart, U., Duncan, P.I., Korner, R. and Nigg, E.A. (2003) 'Polo-like kinase 1 regulates Nlp, a centrosome protein involved in microtubule nucleation', *Dev Cell*, 5(1), pp. 113-25.

Chelysheva, L., Diallo, S., Vezon, D., Gendrot, G., Vrielynck, N., Belcram, K., Rocques, N., Marquez-Lema, A., Bhatt, A.M., Horlow, C., Mercier, R., Mezard, C. and Grelon, M. (2005) 'AtREC8 and AtSCC3 are essential to the monopolar orientation of the kinetochores during meiosis', *J Cell Sci*, 118(Pt 20), pp. 4621-32.

Chiang, T., Duncan, F.E., Schindler, K., Schultz, R.M. and Lampson, M.A. (2010) 'Evidence that weakened centromere cohesion is a leading cause of age-related aneuploidy in oocytes', *Curr Biol*, 20(17), pp. 1522-8.

Chiang, T., Schultz, R.M. and Lampson, M.A. (2011) 'Age-dependent susceptibility of chromosome cohesion to premature separase activation in mouse oocytes', *Biol Reprod*, 85(6), pp. 1279-83.

Ciosk, R., Shirayama, M., Shevchenko, A., Tanaka, T., Toth, A. and Nasmyth, K. (2000) 'Cohesin's binding to chromosomes depends on a separate complex consisting of Scc2 and Scc4 proteins', *Mol Cell*, 5(2), pp. 243-54.

Clyne, R.K., Katis, V.L., Jessop, L., Benjamin, K.R., Herskowitz, I., Lichten, M. and Nasmyth, K. (2003) 'Polo-like kinase Cdc5 promotes chiasmata formation and cosegregation of sister centromeres at meiosis I', *Nat Cell Biol*, 5(5), pp. 480-5.

Coucouvanis, E.C., Sherwood, S.W., Carswell-Crumpton, C., Spack, E.G. and Jones, P.P. (1993) 'Evidence that the mechanism of prenatal germ cell death in the mouse is apoptosis', *Exp Cell Res*, 209(2), pp. 238-47.

Cross, F.R. (2003) 'Two redundant oscillatory mechanisms in the yeast cell cycle', *Dev Cell*, 4(5), pp. 741-52.

de Rooij, D.G. and Grootegoed, J.A. (1998) 'Spermatogonial stem cells', *Curr Opin Cell Biol*, 10(6), pp. 694-701.

Dehapiot, B., Carriere, V., Carroll, J. and Halet, G. (2013) 'Polarized Cdc42 activation promotes polar body protrusion and asymmetric division in mouse oocytes', *Dev Biol*, 377(1), pp. 202-12.

den Elzen, N. and Pines, J. (2001) 'Cyclin A is destroyed in prometaphase and can delay chromosome alignment and anaphase', *J Cell Biol*, 153(1), pp. 121-36.

Descombes, P. and Nigg, E.A. (1998) 'The polo-like kinase Plx1 is required for M phase exit and destruction of mitotic regulators in Xenopus egg extracts', *EMBO J*, 17(5), pp. 1328-35.

Di Fiore, B. and Pines, J. (2007) 'Emi1 is needed to couple DNA replication with mitosis but does not regulate activation of the mitotic APC/C', *J Cell Biol*, 177(3), pp. 425-37.

Ditchfield, C., Johnson, V.L., Tighe, A., Ellston, R., Haworth, C., Johnson, T., Mortlock, A., Keen, N. and Taylor, S.S. (2003) 'Aurora B couples chromosome alignment with anaphase by targeting BubR1, Mad2, and Cenp-E to kinetochores', *J Cell Biol*, 161(2), pp. 267-80.

Earnshaw, W.C. and Cooke, C.A. (1989) 'Proteins of the inner and outer centromere of mitotic chromosomes', *Genome*, 31(2), pp. 541-52.

Eijpe, M., Offenberg, H., Jessberger, R., Revenkova, E. and Heyting, C. (2003) 'Meiotic cohesin REC8 marks the axial elements of rat synaptonemal complexes before cohesins SMC1beta and SMC3', *J Cell Biol*, 160(5), pp. 657-70.

Elia, A.E.H., Cantley, L.C. and Yaffe, M.B. (2003a) 'Proteomic screen finds pSer/pThr-binding domain localizing Plk1 to mitotic substrates', *Science*, 299(5610).

Elia, A.E.H., Rellos, P., Haire, L.F., Chao, J.W., Ivins, F.J., Hoepker, K., Mohammad, D., Cantley, L.C., Smerdon, S.J. and Yaffe, M.B. (2003b) 'The molecular basis for phosphodependent substrate targeting and regulation of Plks by the Polo-box domain', *Cell*, 115(1).

Elowe, S., Hummer, S., Uldschmid, A., Li, X. and Nigg, E.A. (2007) 'Tension-sensitive Plk1 phosphorylation on BubR1 regulates the stability of kinetochore microtubule interactions', *Genes Dev*, 21(17), pp. 2205-19.

Eppig, J.J. (2001) 'Oocyte control of ovarian follicular development and function in mammals', *Reproduction*, 122(6), pp. 829–838.

Eytan, E., Braunstein, I., Ganoth, D., Teichner, A., Hittle, J.C., Yen, T.J. and Hershko, A. (2008) 'Two different mitotic checkpoint inhibitors of the anaphase-promoting complex/cyclosome antagonize the action of the activator Cdc20', *Proc Natl Acad Sci U S A*, 105(27), pp. 9181-5.

Faddy, M.J. (2000) 'Follicle dynamics during ovarian ageing', *Mol Cell Endocrinol*, 163(1-2), pp. 43-8.

Faddy, M.J., Gosden, R.G., Gougeon, A., Richardson, S.J. and Nelson, J.F. (1992) 'Accelerated disappearance of ovarian follicles in mid-life: implications for forecasting menopause', *Hum Reprod*, 7(10), pp. 1342-6.

Fan, H.Y., Tong, C., Teng, C.B., Lian, L., Li, S.W., Yang, Z.M., Chen, D.Y., Schatten, H. and Sun, Q.Y. (2003) 'Characterization of Polo-like kinase-1 in rat oocytes and early embryos implies its functional roles in the regulation of meiotic maturation, fertilization, and cleavage', *Mol Reprod Dev*, 65(3), pp. 318-29.

Gandhi, R., Gillespie, P.J. and Hirano, T. (2006) 'Human Wapl is a cohesin-binding protein that promotes sister-chromatid resolution in mitotic prophase', *Curr Biol*, 16(24), pp. 2406-17.

Ge, S., Skaar, J.R. and Pagano, M. (2009) 'APC/C- and Mad2-mediated degradation of Cdc20 during spindle checkpoint activation', *Cell Cycle*, 8(1), pp. 167-71.

Gilbert, S.F. (2006) *Developmental Biology*. 8 edn. Sanderland,USA: Sinaeur Associates Inc.

Gimenez-Abian, J.F., Sumara, I., Hirota, T., Hauf, S., Gerlich, D., de la Torre, C., Ellenberg, J. and Peters, J.M. (2004) 'Regulation of sister chromatid cohesion between chromosome arms', *Curr Biol*, 14(13), pp. 1187-93.

Golan, A., Yudkovsky, Y. and Hershko, A. (2002) 'The cyclin-ubiquitin ligase activity of cyclosome/APC is jointly activated by protein kinases Cdk1-cyclin B and Plk', *J Biol Chem*, 277(18), pp. 15552-7.

Golsteyn, R.M., Mundt, K.E., Fry, A.M. and Nigg, E.A. (1995) 'Cell cycle regulation of the activity and subcellular localization of Plk1, a human protein kinase implicated in mitotic spindle function', *J Cell Biol*, 129(6), pp. 1617-28.

Gorr, I.H., Boos, D. and Stemmann, O. (2005) 'Mutual inhibition of separase and Cdk1 by two-step complex formation', *Mol Cell*, 19(1), pp. 135-41.

Gruber, S., Haering, C.H. and Nasmyth, K. (2003) 'Chromosomal cohesin forms a ring', *Cell*, 112(6), pp. 765-77.

Guacci, V., Koshland, D. and Strunnikov, A. (1997) 'A direct link between sister chromatid cohesion and chromosome condensation revealed through the analysis of MCD1 in S. cerevisiae', *Cell*, 91(1), pp. 47-57.

Guardavaccaro, D., Kudo, Y., Boulaire, J., Barchi, M., Busino, L., Donzelli, M., Margottin-Goguet, F., Jackson, P.K., Yamasaki, L. and Pagano, M. (2003) 'Control of meiotic and mitotic progression by the F box protein beta-Trcp1 in vivo', *Dev Cell*, 4(6), pp. 799-812.

Gui, L. and Homer, H. (2012) 'Spindle assembly checkpoint signalling is uncoupled from chromosomal position in mouse oocytes', *Development*, 139(11), pp. 1941-6.

Gutierrez-Caballero, C., Cebollero, L.R. and Pendas, A.M. (2012) 'Shugoshins: from protectors of cohesion to versatile adaptors at the centromere', *Trends Genet*, 28(7), pp. 351-60.

Gutierrez-Caballero, C., Herran, Y., Sanchez-Martin, M., Suja, J.A., Barbero, J.L., Llano, E. and Pendas, A.M. (2011) 'Identification and molecular characterization of the mammalian alpha-kleisin RAD21L', *Cell Cycle*, 10(9), pp. 1477-87.

Hamant, O., Golubovskaya, I., Meeley, R., Fiume, E., Timofejeva, L., Schleiffer, A., Nasmyth, K. and Cande, W.Z. (2005) 'A REC8-dependent plant Shugoshin is required for maintenance of centromeric cohesion during meiosis and has no mitotic functions', *Curr Biol*, 15(10), pp. 948-54.

Hansen, D.V., Loktev, A.V., Ban, K.H. and Jackson, P.K. (2004) 'Plk1 regulates activation of the anaphase promoting complex by phosphorylating and triggering SCFbetaTrCP-dependent destruction of the APC Inhibitor Emi1', *Mol Biol Cell*, 15(12), pp. 5623-34.

Hassold, T. and Hunt, P. (2001) 'To err (meiotically) is human: the genesis of human aneuploidy', *Nat Rev Genet*, 2(4), pp. 280-91.

Hassold, T. and Hunt, P. (2009) 'Maternal age and chromosomally abnormal pregnancies: what we know and what we wish we knew', *Curr Opin Pediatr*, 21(6), pp. 703-8.

Hassold, T.J. and Jacobs, P.A. (1984) 'Trisomy in man', *Annu Rev Genet*, 18, pp. 69-97.

Hauf, S., Roitinger, E., Koch, B., Dittrich, C.M., Mechtler, K. and Peters, J.-M. (2005) 'Dissociation of cohesin from chromosome arms and loss of arm cohesion during early mitosis depends on phosphorylation of SA2', *PLoS Biol*, 3(3), p. e69.

Hauf, S. and Watanabe, Y. (2004) 'Kinetochore orientation in mitosis and meiosis', *Cell*, 119(3), pp. 317-27.

Herbert, M., Levasseur, M., Homer, H., Yallop, K., Murdoch, A. and McDougall, A. (2003) 'Homologue disjunction in mouse oocytes requires proteolysis of securin and cyclin B1', *Nat Cell Biol*, 5(11), pp. 1023-5.

Herran, Y., Gutierrez-Caballero, C., Sanchez-Martin, M., Hernandez, T., Viera, A., Barbero, J.L., de Alava, E., de Rooij, D.G., Suja, J.A., Llano, E. and Pendas, A.M. (2011) 'The cohesin subunit RAD21L functions in meiotic synapsis and exhibits sexual dimorphism in fertility', *EMBO J*, 30(15), pp. 3091-105.

Hershko, A. (2005) 'The ubiquitin system for protein degradation and some of its roles in the control of the cell division cycle', *Cell Death Differ*, 12(9), pp. 1191-7.

Hodges, C.A., Revenkova, E., Jessberger, R., Hassold, T.J. and Hunt, P.A. (2005) 'SMC1beta-deficient female mice provide evidence that cohesins are a missing link in age-related nondisjunction', *Nat Genet*, 37(12), pp. 1351-5.

Hoffman, D.B., Pearson, C.G., Yen, T.J., Howell, B.J. and Salmon, E.D. (2001) 'Microtubule-dependent changes in assembly of microtubule motor proteins and mitotic spindle checkpoint proteins at PtK1 kinetochores', *Mol Biol Cell*, 12(7), pp. 1995-2009.

Hoffmann, S., Maro, B., Kubiak, J.Z. and Polanski, Z. (2011) 'A single bivalent efficiently inhibits cyclin B1 degradation and polar body extrusion in mouse oocytes indicating robust SAC during female meiosis I', *PLoS One*, 6(11), p. e27143.

Homer, H., Gui, L. and Carroll, J. (2009a) 'A spindle assembly checkpoint protein functions in prophase I arrest and prometaphase progression', *Science*, 326(5955), pp. 991-4.

Homer, H., Gui, L. and Carroll, J. (2009b) 'A spindle assembly checkpoint protein functions in prophase I arrest and prometaphase progression', *Science*, 326(5955).

Homer, H.A., McDougall, A., Levasseur, M., Murdoch, A.P. and Herbert, M. (2005a) 'Mad2 is required for inhibiting securin and cyclin B degradation following spindle depolymerisation in meiosis I mouse oocytes', *Reproduction*, 130(6), pp. 829-43.

Homer, H.A., McDougall, A., Levasseur, M., Yallop, K., Murdoch, A.P. and Herbert, M. (2005b) 'Mad2 prevents aneuploidy and premature proteolysis of cyclin B and securin during meiosis I in mouse oocytes', *Genes Dev*, 19(2), pp. 202-7.

Hoque, M.T. and Ishikawa, F. (2002) 'Cohesin defects lead to premature sister chromatid separation, kinetochore dysfunction, and spindle-assembly checkpoint activation', *J Biol Chem*, 277(44), pp. 42306-14.

Huang, H., Feng, J., Famulski, J., Rattner, J.B., Liu, S.T., Kao, G.D., Muschel, R., Chan, G.K. and Yen, T.J. (2007) 'Tripin/hSgo2 recruits MCAK to the inner centromere to correct defective kinetochore attachments', *J Cell Biol*, 177(3), pp. 413-24.

Hunt, P. and Hassold, T. (2010) 'Female meiosis: coming unglued with age', *Curr Biol*, 20(17), pp. R699-702.

Ishiguro, K., Kim, J., Fujiyama-Nakamura, S., Kato, S. and Watanabe, Y. (2011) 'A new meiosis-specific cohesin complex implicated in the cohesin code for homologous pairing', *EMBO Rep*, 12(3), pp. 267-75.

Jackman, M., Lindon, C., Nigg, E.A. and Pines, J. (2003) 'Active cyclin B1-Cdk1 first appears on centrosomes in prophase', *Nat Cell Biol*, 5(2), pp. 143-8.

Jacobs, P.A. (1992) 'The chromosome complement of human gametes', *Oxf Rev Reprod Biol*, 14, pp. 47-72.

Jeffreys, C.A., Burrage, P.S. and Bickel, S.E. (2003) 'A model system for increased meiotic nondisjunction in older oocytes', *Curr Biol*, 13(6), pp. 498-503.

Jeong, K., Jeong, J.Y., Lee, H.O., Choi, E. and Lee, H. (2010) 'Inhibition of Plk1 induces mitotic infidelity and embryonic growth defects in developing zebrafish embryos', *Dev Biol*, 345(1), pp. 34-48.

Jessberger, R. (2011) 'Cohesin complexes get more complex: the novel kleisin RAD21L', *Cell Cycle*, 10(13), pp. 2053-4.

Jones, K.T. (2008) 'Meiosis in oocytes: predisposition to aneuploidy and its increased incidence with age', *Hum Reprod Update*, 14(2), pp. 143-58.

Kagey, M.H., Newman, J.J., Bilodeau, S., Zhan, Y., Orlando, D.A., van Berkum, N.L., Ebmeier, C.C., Goossens, J., Rahl, P.B., Levine, S.S., Taatjes, D.J., Dekker, J. and Young, R.A. (2010) 'Mediator and cohesin connect gene expression and chromatin architecture', *Nature*, 467(7314), pp. 430-5.

Katis, V.L., Galova, M., Rabitsch, K.P., Gregan, J. and Nasmyth, K. (2004) 'Maintenance of cohesin at centromeres after meiosis I in budding yeast requires a kinetochore-associated protein related to MEI-S332', *Curr Biol*, 14(7), pp. 560-72.

Katis, V.L., Lipp, J.J., Imre, R., Bogdanova, A., Okaz, E., Habermann, B., Mechtler, K., Nasmyth, K. and Zachariae, W. (2010) 'Rec8 phosphorylation by casein kinase 1 and Cdc7-Dbf4 kinase regulates cohesin cleavage by separase during meiosis', *Dev Cell*, 18(3), pp. 397-409.

Kerrebrock, A.W., Moore, D.P., Wu, J.S. and Orr-Weaver, T.L. (1995) 'Mei-S332, a Drosophila protein required for sister-chromatid cohesion, can localize to meiotic centromere regions', *Cell*, 83(2), pp. 247-56.

Kitajima, T.S., Kawashima, S.A. and Watanabe, Y. (2004) 'The conserved kinetochore protein shugoshin protects centromeric cohesion during meiosis', *Nature*, 427(6974), pp. 510-7.

Kitajima, T.S., Ohsugi, M. and Ellenberg, J. (2011) 'Complete kinetochore tracking reveals error-prone homologous chromosome biorientation in mammalian oocytes', *Cell*, 146(4), pp. 568-81.

Kitajima, T.S., Sakuno, T., Ishiguro, K.-i., Iemura, S.-i., Natsume, T., Kawashima, S.A. and Watanabe, Y. (2006) 'Shugoshin collaborates with protein phosphatase 2A to protect cohesin', *Nature*, 441(7089), pp. 46-52.

Kleckner, N. (2006) 'Chiasma formation: chromatin/axis interplay and the role(s) of the synaptonemal complex', *Chromosoma*, 115(3), pp. 175-94.

Klein, F., Mahr, P., Galova, M., Buonomo, S.B., Michaelis, C., Nairz, K. and Nasmyth, K. (1999) 'A central role for cohesins in sister chromatid cohesion, formation of axial elements, and recombination during yeast meiosis', *Cell*, 98(1), pp. 91-103.

Kotani, S., Tugendreich, S., Fujii, M., Jorgensen, P.M., Watanabe, N., Hoog, C., Hieter, P. and Todokoro, K. (1998) 'PKA and MPF-activated polo-like kinase regulate anaphase-promoting complex activity and mitosis progression', *Mol Cell*, 1(3), pp. 371-80.

Kouznetsova, A., Lister, L., Nordenskjold, M., Herbert, M. and Hoog, C. (2007) 'Bi-orientation of achiasmatic chromosomes in meiosis I oocytes contributes to aneuploidy in mice', *Nat Genet*, 39(8), pp. 966-8.

Kraft, C., Herzog, F., Gieffers, C., Mechtler, K., Hagting, A., Pines, J. and Peters, J.M. (2003) 'Mitotic regulation of the human anaphase-promoting complex by phosphorylation', *EMBO J*, 22(24), pp. 6598-609.

Kudo, N.R., Anger, M., Peters, A.H., Stemmann, O., Theussl, H.C., Helmhart, W., Kudo, H., Heyting, C. and Nasmyth, K. (2009) 'Role of cleavage by separase of the Rec8 kleisin subunit of cohesin during mammalian meiosis I', *J Cell Sci*, 122(Pt 15), pp. 2686-98.

Kudo, N.R., Wassmann, K., Anger, M., Schuh, M., Wirth, K.G., Xu, H., Helmhart, W., Kudo, H., McKay, M., Maro, B., Ellenberg, J., de Boer, P. and Nasmyth, K. (2006) 'Resolution of chiasmata in oocytes requires separase-mediated proteolysis', *Cell*, 126(1), pp. 135-46.

Kueng, S., Hegemann, B., Peters, B.H., Lipp, J.J., Schleiffer, A., Mechtler, K. and Peters, J.M. (2006) 'Wapl controls the dynamic association of cohesin with chromatin', *Cell*, 127(5), pp. 955-67.

Kuliev, A., Cieslak, J. and Verlinsky, Y. (2005) 'Frequency and distribution of chromosome abnormalities in human oocytes', *Cytogenet Genome Res*, 111(3-4), pp. 193-8.

Kulukian, A., Han, J.S. and Cleveland, D.W. (2009) 'Unattached kinetochores catalyze production of an anaphase inhibitor that requires a Mad2 template to prime Cdc20 for BubR1 binding', *Dev Cell*, 16(1), pp. 105-17.

Lamb, N.E., Feingold, E., Savage, A., Avramopoulos, D., Freeman, S., Gu, Y., Hallberg, A., Hersey, J., Karadima, G., Pettay, D., Saker, D., Shen, J., Taft, L., Mikkelsen, M., Petersen, M.B., Hassold, T. and Sherman, S.L. (1997) 'Characterization of susceptible chiasma configurations that increase the risk for maternal nondisjunction of chromosome 21', *Hum Mol Genet*, 6(9), pp. 1391-9.

Lamb, N.E., Feingold, E. and Sherman, S.L. (1996) 'Statistical models for trisomic phenotypes', *Am J Hum Genet*, 58(1), pp. 201-12.

Lamb, N.E., Yu, K., Shaffer, J., Feingold, E. and Sherman, S.L. (2005) 'Association between maternal age and meiotic recombination for trisomy 21', *Am J Hum Genet*, 76(1), pp. 91-9.

Lampson, M.A. and Kapoor, T.M. (2005) 'The human mitotic checkpoint protein BubR1 regulates chromosome-spindle attachments', *Nat Cell Biol*, 7(1), pp. 93-8.

Lane, H.A. and Nigg, E.A. (1996) 'Antibody microinjection reveals an essential role for human polo-like kinase 1 (Plk1) in the functional maturation of mitotic centrosomes', *J Cell Biol*, 135(6 Pt 2), pp. 1701-13.

Lane, S.I., Yun, Y. and Jones, K.T. (2012) 'Timing of anaphase-promoting complex activation in mouse oocytes is predicted by microtubule-kinetochore attachment but not by bivalent alignment or tension', *Development*, 139(11), pp. 1947-55.

Lee, B.H. and Amon, A. (2003) 'Role of Polo-like kinase CDC5 in programming meiosis I chromosome segregation', *Science*, 300(5618), pp. 482-6.

Lee, J. and Hirano, T. (2011) 'RAD21L, a novel cohesin subunit implicated in linking homologous chromosomes in mammalian meiosis', *J Cell Biol*, 192(2), pp. 263-76.

Lee, J., Kitajima, T.S., Tanno, Y., Yoshida, K., Morita, T., Miyano, T., Miyake, M. and Watanabe, Y. (2008) 'Unified mode of centromeric protection by shugoshin in mammalian oocytes and somatic cells', *Nat Cell Biol*, 10(1), pp. 42-52.

LeMaire-Adkins, R., Radke, K. and Hunt, P.A. (1997) 'Lack of checkpoint control at the metaphase/anaphase transition: a mechanism of meiotic nondisjunction in mammalian females', *J Cell Biol*, 139(7), pp. 1611-9.

Lemaire, P., Garrett, N. and Gurdon, J.B. (1995) 'Expression cloning of Siamois, a Xenopus homeobox gene expressed in dorsal-vegetal cells of blastulae and able to induce a complete secondary axis', *Cell*, 81(1), pp. 85-94.

Lenart, P., Petronczki, M., Steegmaier, M., Di Fiore, B., Lipp, J.J., Hoffmann, M., Rettig, W.J., Kraut, N. and Peters, J.M. (2007) 'The small-molecule inhibitor BI 2536 reveals novel insights into mitotic roles of polo-like kinase 1', *Curr Biol*, 17(4), pp. 304-15.

Lengronne, A., McIntyre, J., Katou, Y., Kanoh, Y., Hopfner, K.P., Shirahige, K. and Uhlmann, F. (2006) 'Establishment of sister chromatid cohesion at the S. cerevisiae replication fork', *Mol Cell*, 23(6), pp. 787-99.

Lens, S.M., Voest, E.E. and Medema, R.H. (2010) 'Shared and separate functions of polo-like kinases and aurora kinases in cancer', *Nat Rev Cancer*, 10(12), pp. 825-41.

Li, G.Q. and Zhang, H.F. (2004) 'Mad2 and p27 expression profiles in colorectal cancer and its clinical significance', *World J Gastroenterol*, 10(21), pp. 3218-20.

Li, X. and Dawe, R.K. (2009) 'Fused sister kinetochores initiate the reductional division in meiosis I', *Nat Cell Biol*, 11(9), pp. 1103-8.

Lister, L.M., Kouznetsova, A., Hyslop, L.A., Kalleas, D., Pace, S.L., Barel, J.C., Nathan, A., Floros, V., Adelfalk, C., Watanabe, Y., Jessberger, R., Kirkwood, T.B., Hoog, C. and Herbert, M. (2010) 'Age-related meiotic segregation errors in mammalian oocytes are preceded by depletion of cohesin and Sgo2', *Curr Biol*, 20(17), pp. 1511-21.

Liu, L. and Keefe, D.L. (2008) 'Defective cohesin is associated with age-dependent misaligned chromosomes in oocytes', *Reprod Biomed Online*, 16(1), pp. 103-12.

Llamazares, S., Moreira, A., Tavares, A., Girdham, C., Spruce, B.A., Gonzalez, C., Karess, R.E., Glover, D.M. and Sunkel, C.E. (1991) 'polo encodes a protein kinase homolog required for mitosis in Drosophila', *Genes Dev*, 5(12A), pp. 2153-65.

Llano, E., Gomez, R., Gutierrez-Caballero, C., Herran, Y., Sanchez-Martin, M., Vazquez-Quinones, L., Hernandez, T., de Alava, E., Cuadrado, A., Barbero, J.L., Suja, J.A. and Pendas, A.M. (2008) 'Shugoshin-2 is essential for the completion of meiosis but not for mitotic cell division in mice', *Genes Dev*, 22(17), pp. 2400-13.

Losada, A., Hirano, M. and Hirano, T. (1998) 'Identification of Xenopus SMC protein complexes required for sister chromatid cohesion', *Genes Dev*, 12(13), pp. 1986-97.

Losada, A., Hirano, M. and Hirano, T. (2002) 'Cohesin release is required for sister chromatid resolution, but not for condensin-mediated compaction, at the onset of mitosis', *Genes Dev*, 16(23), pp. 3004-16.

Losada, A., Yokochi, T., Kobayashi, R. and Hirano, T. (2000) 'Identification and characterization of SA/Scc3p subunits in the Xenopus and human cohesin complexes', *J Cell Biol*, 150(3), pp. 405-16.

Madgwick, S., Hansen, D.V., Levasseur, M., Jackson, P.K. and Jones, K.T. 'Mouse Emi2 is required to enter meiosis II by reestablishing cyclin B1 during interkinesis', *J Cell Biol*, 174(6).

Magidson, V., O'Connell, C.B., Loncarek, J., Paul, R., Mogilner, A. and Khodjakov, A. (2011) 'The spatial arrangement of chromosomes during prometaphase facilitates spindle assembly', *Cell*, 146(4), pp. 555-67.

Marangos, P., Verschuren, E.W., Chen, R., Jackson, P.K. and Carroll, J. (2007) 'Prophase I arrest and progression to metaphase I in mouse oocytes are controlled by Emi1-dependent regulation of APC(Cdh1)', *J Cell Biol*, 176(1), pp. 65-75.

Margottin-Goguet, F., Hsu, J.Y., Loktev, A., Hsieh, H.M., Reimann, J.D. and Jackson, P.K. (2003) 'Prophase destruction of Emi1 by the SCF(betaTrCP/Slimb) ubiquitin ligase activates the anaphase promoting complex to allow progression beyond prometaphase', *Dev Cell*, 4(6), pp. 813-26.

Maro, B., Howlett, S.K. and Webb, M. (1985) 'Non-spindle microtubule organizing centers in metaphase II-arrested mouse oocytes', *J Cell Biol*, 101(5 Pt 1), pp. 1665-72.

Marston, A.L. and Amon, A. (2004) 'Meiosis: cell-cycle controls shuffle and deal', *Nat Rev Mol Cell Biol*, 5(12), pp. 983-997.

McGuinness, B.E., Anger, M., Kouznetsova, A., Gil-Bernabe, A.M., Helmhart, W., Kudo, N.R., Wuensche, A., Taylor, S., Hoog, C., Novak, B. and Nasmyth, K. (2009) 'Regulation of APC/C activity in oocytes by a Bub1-dependent spindle assembly checkpoint', *Curr Biol*, 19(5), pp. 369-80.

McGuinness, B.E., Hirota, T., Kudo, N.R., Peters, J.-M. and Nasmyth, K. (2005) 'Shugoshin prevents dissociation of cohesin from centromeres during mitosis in vertebrate cells', *PLoS Biol*, 3(3), p. e86.

Messinger, S.M. and Albertini, D.F. (1991) 'Centrosome and microtubule dynamics during meiotic progression in the mouse oocyte', *J Cell Sci*, 100 (Pt 2), pp. 289-98.

Michaelis, C., Ciosk, R. and Nasmyth, K. (1997) 'Cohesins: chromosomal proteins that prevent premature separation of sister chromatids', *Cell*, 91(1), pp. 35-45.

Moore, D.P. and Orr-Weaver, T.L. (1998) 'Chromosome segregation during meiosis: building an unambivalent bivalent', *Curr Top Dev Biol*, 37, pp. 263-99.

Moore, G.P. (1975) 'The RNA polymerase activity of the preimplantation mouse embryo', *J Embryol Exp Morphol*, 34(2), pp. 291–298.

Moore, G.P. and Lintern-Moore, S. (1978) 'Transcription of the mouse oocyte genome', *Biol Reprod*, 18(5), pp. 865–870.

More babies? Who needs them? (2004). Available at: http://www.actuaries.org.uk/research-and-resources/documents/more-babies-who-needs-them-discussion-paper-actuarial-profession (Accessed: 21/12/2012).

Morris, J.K. and Alberman, E. (2009) 'Trends in Down's syndrome live births and antenatal diagnoses in England and Wales from 1989 to 2008: analysis of data from the National Down Syndrome Cytogenetic Register', *BMJ*, 339, p. b3794.

Morton, N.E., Jacobs, P.A., Hassold, T. and Wu, D. (1988) 'Maternal age in trisomy', *Ann Hum Genet*, 52(Pt 3), pp. 227-35.

Moshe, Y., Bar-On, O., Ganoth, D. and Hershko, A. (2011) 'Regulation of the action of early mitotic inhibitor 1 on the anaphase-promoting complex/cyclosome by cyclin-dependent kinases', *J Biol Chem*, 286(19), pp. 16647-57.

Moshe, Y., Boulaire, J., Pagano, M. and Hershko, A. (2004) 'Role of Polo-like kinase in the degradation of early mitotic inhibitor 1, a regulator of the anaphase promoting complex/cyclosome', *Proc Natl Acad Sci U S A*, 101(21), pp. 7937-42.

Musacchio, A. and Salmon, E.D. (2007) 'The spindle-assembly checkpoint in space and time', *Nat Rev Mol Cell Biol*, 8(5), pp. 379-93.

Nagaoka, S.I., Hassold, T.J. and Hunt, P.A. (2012) 'Human aneuploidy: mechanisms and new insights into an age-old problem', *Nat Rev Genet*, 13(7), pp. 493-504.

Nagaoka, S.I., Hodges, C.A., Albertini, D.F. and Hunt, P.A. (2011) 'Oocyte-specific differences in cell-cycle control create an innate susceptibility to meiotic errors', *Curr Biol*, 21(8), pp. 651-7.

Nakajima, H., Toyoshima-Morimoto, F., Taniguchi, E. and Nishida, E. (2003) 'Identification of a consensus motif for Plk (Polo-like kinase) phosphorylation reveals Myt1 as a Plk1 substrate', *J Biol Chem*, 278(28), pp. 25277-80.

Nakayama, K.I. and Nakayama, K. (2006) 'Ubiquitin ligases: cell-cycle control and cancer', *Nat Rev Cancer*, 6(5), pp. 369-381.

Nasmyth, K. (2005) 'How do so few control so many?', *Cell*, 120(6), pp. 739-46.

Nasmyth, K. (2011) 'Cohesin: a catenase with separate entry and exit gates?', *Nat Cell Biol*, 13(10), pp. 1170-7.

Nasmyth, K. and Haering, C.H. (2005) 'The structure and function of SMC and kleisin complexes', *Annu Rev Biochem*, 74, pp. 595-648.

Nasmyth, K. and Haering, C.H. (2009) 'Cohesin: its roles and mechanisms', *Annu Rev Genet*, 43, pp. 525-58.

Niault, T., Hached, K., Sotillo, R., Sorger, P.K., Maro, B., Benezra, R. and Wassmann, K. (2007) 'Changing Mad2 levels affects chromosome segregation and spindle assembly checkpoint control in female mouse meiosis I', *PLoS One*, 2(11), p. e1165.

Nilsson, J., Yekezare, M., Minshull, J. and Pines, J. (2008) 'The APC/C maintains the spindle assembly checkpoint by targeting Cdc20 for destruction', *Nat Cell Biol*, 10(12), pp. 1411-20.

Orth, M., Mayer, B., Rehm, K., Rothweiler, U., Heidmann, D., Holak, T.A. and Stemmann, O. (2011) 'Shugoshin is a Mad1/Cdc20-like interactor of Mad2', *EMBO J*, 30(14), pp. 2868-80.

Pacchierotti, F., Adler, I.D., Eichenlaub-Ritter, U. and Mailhes, J.B. (2007) 'Gender effects on the incidence of aneuploidy in mammalian germ cells', *Environ Res*, 104(1), pp. 46-69.

Pahlavan, G., Polanski, Z., Kalab, P., Golsteyn, R., Nigg, E.A. and Maro, B. (2000) 'Characterization of polo-like kinase 1 during meiotic maturation of the mouse oocyte', *Dev Biol*, 220(2), pp. 392–400.

Pasierbek, P., Jantsch, M., Melcher, M., Schleiffer, A., Schweizer, D. and Loidl, J. (2001) 'A Caenorhabditis elegans cohesion protein with functions in meiotic chromosome pairing and disjunction', *Genes Dev*, 15(11), pp. 1411-20.

Passmore, L.A., McCormack, E.A., Au, S.W., Paul, A., Willison, K.R., Harper, J.W. and Barford, D. (2003) 'Doc1 mediates the activity of the anaphase-promoting complex by contributing to substrate recognition', *EMBO J*, 22(4), pp. 786-96.

Penrose, L.S. (2009) 'The relative effects of paternal and maternal age in mongolism. 1933', *J Genet*, 88(1), pp. 9-14.

Pesin, J.A. and Orr-Weaver, T.L. (2008) 'Regulation of APC/C activators in mitosis and meiosis', *Annu Rev Cell Dev Biol*, 24, pp. 475-99.

Peters, H. (1970) 'Migration of gonocytes into the mammalian gonad and their differentiation', *Philos Trans R Soc Lond B Biol Sci*, 259(828), pp. 91-101.

Peters, J.-M., Tedeschi, A. and Schmitz, J. (2008) 'The cohesin complex and its roles in chromosome biology', *Genes Dev*, 22(22), pp. 3089-114.

Peters, J.M. (2006) 'The anaphase promoting complex/cyclosome: a machine designed to destroy', *Nat Rev Mol Cell Biol*, 7(9), pp. 644-56.

Peters, U., Cherian, J., Kim, J.H., Kwok, B.H. and Kapoor, T.M. (2006) 'Probing cell-division phenotype space and Polo-like kinase function using small molecules', *Nat Chem Biol*, 2(11), pp. 618-26.

Petronczki, M., Glotzer, M., Kraut, N. and Peters, J.M. (2007) 'Polo-like kinase 1 triggers the initiation of cytokinesis in human cells by promoting recruitment of the RhoGEF Ect2 to the central spindle', *Dev Cell*, 12(5), pp. 713-25.

Petronczki, M., Lenart, P. and Peters, J.M. (2008) 'Polo on the Rise-from Mitotic Entry to Cytokinesis with Plk1', *Dev Cell*, 14(5), pp. 646-59.

Petronczki, M., Siomos, M.F. and Nasmyth, K. (2003) 'Un menage a quatre: the molecular biology of chromosome segregation in meiosis', *Cell*, 112(4), pp. 423-440.

Pezzi, N., Prieto, I., Kremer, L., Perez Jurado, L.A., Valero, C., Del Mazo, J., Martinez-A, C. and Barbero, J.L. (2000) 'STAG3, a novel gene encoding a protein involved in meiotic chromosome pairing and location of STAG3-related genes flanking the Williams-Beuren syndrome deletion', *Faseb J*, 14(3), pp. 581-92.

Pfleger, C.M. and Kirschner, M.W. (2000) 'The KEN box: an APC recognition signal distinct from the D box targeted by Cdh1', *Genes Dev*, 14(6), pp. 655-65.

Pidoux, A.L. and Allshire, R.C. (2004) 'Kinetochore and heterochromatin domains of the fission yeast centromere', *Chromosome Res*, 12(6), pp. 521-34.

Pines, J. (2006) 'Mitosis: a matter of getting rid of the right protein at the right time', *Trends Cell Biol*, 16(1), pp. 55-63.

Ploeger, L.S., Dullens, H.F., Huisman, A. and van Diest, P.J. (2008) 'Fluorescent stains for quantification of DNA by confocal laser scanning microscopy in 3-D', *Biotech Histochem*, 83(2), pp. 63-9.

Prieto, I., Suja, J.A., Pezzi, N., Kremer, L., Martinez-A, C., Rufas, J.S. and Barbero, J.L. (2001) 'Mammalian STAG3 is a cohesin specific to sister chromatid arms in meiosis I', *Nat Cell Biol*, 3(8), pp. 761-6.

Prieto, I., Tease, C., Pezzi, N., Buesa, J.M., Ortega, S., Kremer, L., Martinez, A., Martinez-A, C., Hulten, M.A. and Barbero, J.L. (2004) 'Cohesin component

dynamics during meiotic prophase I in mammalian oocytes', *Chromosome Res*, 12(3), pp. 197-213.

Prinz, S., Hwang, E.S., Visintin, R. and Amon, A. (1998) 'The regulation of Cdc20 proteolysis reveals a role for APC components Cdc23 and Cdc27 during S phase and early mitosis', *Curr Biol*, 8(13), pp. 750-60.

Rai, R. and Regan, L. (2006) 'Recurrent miscarriage', *Lancet*, 368(9535), pp. 601-11.

Rapley, J., Baxter, J.E., Blot, J., Wattam, S.L., Casenghi, M., Meraldi, P., Nigg, E.A. and Fry, A.M. (2005) 'Coordinate regulation of the mother centriole component nlp by nek2 and plk1 protein kinases', *Mol Cell Biol*, 25(4), pp. 1309-24.

Reijo, R., Lee, T.Y., Salo, P., Alagappan, R., Brown, L.G., Rosenberg, M., Rozen, S., Jaffe, T., Straus, D. and Hovatta, O. (1995) 'Diverse spermatogenic defects in humans caused by Y chromosome deletions encompassing a novel RNA-binding protein gene', *Nat Genet*, 10(4), pp. 383-93.

Reimann, J.D., Freed, E., Hsu, J.Y., Kramer, E.R., Peters, J.M. and Jackson, P.K. (2001a) 'Emi1 is a mitotic regulator that interacts with Cdc20 and inhibits the anaphase promoting complex', *Cell*, 105(5).

Reimann, J.D., Gardner, B.E., Margottin-Goguet, F. and Jackson, P.K. (2001b) 'Emi1 regulates the anaphase-promoting complex by a different mechanism than Mad2 proteins', *Genes Dev*, 15(24).

Reis, A., Chang, H.-Y., Levasseur, M. and Jones, K.T. (2006a) 'APCcdh1 activity in mouse oocytes prevents entry into the first meiotic division', *Nat Cell Biol*, 8(5), pp. 539–540.

Reis, A., Levasseur, M., Chang, H.Y., Elliott, D.J. and Jones, K.T. (2006b) 'The CRY box: a second APCcdh1-dependent degron in mammalian cdc20', *EMBO Rep*, 7(10), pp. 1040-5.

Reis, A., Madgwick, S., Chang, H.-Y., Nabti, I., Levasseur, M. and Jones, K.T. (2007) 'Prometaphase APCcdh1 activity prevents non-disjunction in mammalian oocytes', *Nat Cell Biol*, 9(10), pp. 1192–1198.

Revenkova, E., Eijpe, M., Heyting, C., Gross, B. and Jessberger, R. (2001) 'Novel meiosis-specific isoform of mammalian SMC1', *Mol Cell Biol*, 21(20), pp. 6984-98.

Revenkova, E., Eijpe, M., Heyting, C., Hodges, C.A., Hunt, P.A., Liebe, B., Scherthan, H. and Jessberger, R. (2004) 'Cohesin SMC1 beta is required for meiotic chromosome dynamics, sister chromatid cohesion and DNA recombination', *Nat Cell Biol*, 6(6), pp. 555-62.

Revenkova, E., Herrmann, K., Adelfalk, C. and Jessberger, R. (2010) 'Oocyte cohesin expression restricted to predictyate stages provides full fertility and prevents aneuploidy', *Curr Biol*, 20(17), pp. 1529-33.

Revenkova, E. and Jessberger, R. (2005) 'Keeping sister chromatids together: cohesins in meiosis', *Reproduction*, 130(6), pp. 783-90.

Riedel, C.G., Katis, V.L., Katou, Y., Mori, S., Itoh, T., Helmhart, W., Galova, M., Petronczki, M., Gregan, J., Cetin, B., Mudrak, I., Ogris, E., Mechtler, K., Pelletier, L., Buchholz, F., Shirahige, K. and Nasmyth, K. (2006) 'Protein phosphatase 2A protects centromeric sister chromatid cohesion during meiosis I', *Nature*, 441(7089), pp. 53-61.

Rieder, C.L., Cole, R.W., Khodjakov, A. and Sluder, G. (1995) 'The checkpoint delaying anaphase in response to chromosome monoorientation is mediated by an inhibitory signal produced by unattached kinetochores', *J Cell Biol*, 130(4), pp. 941-8.

Rieder, C.L., Schultz, A., Cole, R. and Sluder, G. (1994) 'Anaphase onset in vertebrate somatic cells is controlled by a checkpoint that monitors sister kinetochore attachment to the spindle', *J Cell Biol*, 127(5), pp. 1301-10.

Roeder, G.S. (1997) 'Meiotic chromosomes: it takes two to tango', *Genes Dev*, 11(20), pp. 2600-21.

Rosenbusch, B.E. and Schneider, M. (2006) 'Cytogenetic analysis of human oocytes remaining unfertilized after intracytoplasmic sperm injection', *Fertil Steril*, 85(2), pp. 302-7.

Roshak, A.K., Capper, E.A., Imburgia, C., Fornwald, J., Scott, G. and Marshall, L.A. (2000) 'The human polo-like kinase, PLK, regulates cdc2/cyclin B through phosphorylation and activation of the cdc25C phosphatase', *Cell Signal*, 12(6), pp. 405-11.

Rowlatt, C., Chesterman, F.C. and Sheriff, M.U. (1976) 'Lifespan, age changes and tumour incidence in an ageing C57BL mouse colony', *Lab Anim*, 10(10), pp. 419-42.

Roy, J. and Cyert, M.S. (2009) 'Cracking the phosphatase code: docking interactions determine substrate specificity', *Sci Signal*, 2(100), p. re9.

Rudner, A.D., Hardwick, K.G. and Murray, A.W. (2000) 'Cdc28 activates exit from mitosis in budding yeast', *J Cell Biol*, 149(7), pp. 1361-76.

Rudner, A.D. and Murray, A.W. (2000) 'Phosphorylation by Cdc28 activates the Cdc20-dependent activity of the anaphase-promoting complex', *J Cell Biol*, 149(7), pp. 1377-90.

Rumpf, C., Cipak, L., Dudas, A., Benko, Z., Pozgajova, M., Riedel, C.G., Ammerer, G., Mechtler, K. and Gregan, J. (2010) 'Casein kinase 1 is required for efficient removal of Rec8 during meiosis I', *Cell Cycle*, 9(13), pp. 2657-62.

Sakuno, T., Tanaka, K., Hauf, S. and Watanabe, Y. (2011) 'Repositioning of aurora B promoted by chiasmata ensures sister chromatid mono-orientation in meiosis I', *Dev Cell*, 21(3), pp. 534-45.

Sakuno, T. and Watanabe, Y. (2009) 'Studies of meiosis disclose distinct roles of cohesion in the core centromere and pericentromeric regions', *Chromosome Res*, 17(2), pp. 239-49.

Santamaria, A., Neef, R., Eberspacher, U., Eis, K., Husemann, M., Mumberg, D., Prechtl, S., Schulze, V., Siemeister, G., Wortmann, L., Barr, F.A. and Nigg, E.A. (2007) 'Use of the novel Plk1 inhibitor ZK-thiazolidinone to elucidate functions of Plk1 in early and late stages of mitosis', *Mol Biol Cell*, 18(10), pp. 4024-36.

Schreiber, A., Stengel, F., Zhang, Z., Enchev, R.I., Kong, E.H., Morris, E.P., Robinson, C.V., da Fonseca, P.C. and Barford, D. (2011) 'Structural basis for the subunit assembly of the anaphase-promoting complex', *Nature*, 470(7333), pp. 227-32.

Schuh, M. and Ellenberg, J. (2007) 'Self-organization of MTOCs replaces centrosome function during acentrosomal spindle assembly in live mouse oocytes', *Cell*, 130(3).

Schuh, M. and Ellenberg, J. (2008) 'A new model for asymmetric spindle positioning in mouse oocytes', *Curr Biol*, 18(24), pp. 1986-92.

Schultz, R.M., Montgomery, R.R. and Belanoff, J.R. (1983) 'Regulation of mouse oocyte meiotic maturation: implication of a decrease in oocyte cAMP and protein dephosphorylation in commitment to resume meiosis', *Dev Biol*, 97(2), pp. 264-73.

Schwab, M., Neutzner, M., Mocker, D. and Seufert, W. (2001) 'Yeast Hct1 recognizes the mitotic cyclin Clb2 and other substrates of the ubiquitin ligase APC', *EMBO J*, 20(18), pp. 5165-75.

Scott, K. (ed.) (2009) *Meiosis: Cytological Methods* (2 vols). Humana Press.

Shteinberg, M., Protopopov, Y., Listovsky, T., Brandeis, M. and Hershko, A. (1999) 'Phosphorylation of the cyclosome is required for its stimulation by Fizzy/cdc20', *Biochem Biophys Res Commun*, 260(1), pp. 193-8.

Sonoda, E., Matsusaka, T., Morrison, C., Vagnarelli, P., Hoshi, O., Ushiki, T., Nojima, K., Fukagawa, T., Waizenegger, I.C., Peters, J.M., Earnshaw, W.C. and

Takeda, S. (2001) 'Scc1/Rad21/Mcd1 is required for sister chromatid cohesion and kinetochore function in vertebrate cells', *Dev Cell*, 1(6), pp. 759-70.

Sorensen, R.A. and Wassarman, P.M. (1976) 'Relationship between growth and meiotic maturation of the mouse oocyte', *Dev Biol*, 50(2), pp. 531–536.

Steegmaier, M., Hoffmann, M., Baum, A., Lenart, P., Petronczki, M., Krssak, M., Gurtler, U., Garin-Chesa, P., Lieb, S., Quant, J., Grauert, M., Adolf, G.R., Kraut, N., Peters, J.M. and Rettig, W.J. (2007) 'BI 2536, a potent and selective inhibitor of polo-like kinase 1, inhibits tumor growth in vivo', *Curr Biol*, 17(4), pp. 316-22.

Stemmann, O., Zou, H., Gerber, S.A., Gygi, S.P. and Kirschner, M.W. (2001a) 'Dual inhibition of sister chromatid separation at metaphase', *Cell*, 107(6).

Stemmann, O., Zou, H., Gerber, S.A., Gygi, S.P. and Kirschner, M.W. (2001b) 'Dual inhibition of sister chromatid separation at metaphase', *Cell*, 107(6), pp. 715-26.

Sternberg, S.R. (1983) 'Biomedical Image Processing', *Computer*, 16(1), pp. 22-34.

Suijkerbuijk, S.J., Vleugel, M., Teixeira, A. and Kops, G.J. (2012) 'Integration of Kinase and Phosphatase Activities by BUBR1 Ensures Formation of Stable Kinetochore-Microtubule Attachments', *Dev Cell*, 23(4), pp. 745-55.

Sumara, I., Gimenez-Abian, J.F., Gerlich, D., Hirota, T., Kraft, C., de la Torre, C., Ellenberg, J. and Peters, J.M. (2004) 'Roles of polo-like kinase 1 in the assembly of functional mitotic spindles', *Curr Biol*, 14(19), pp. 1712-22.

Sumara, I., Vorlaufer, E., Stukenberg, P.T., Kelm, O., Redemann, N., Nigg, E.A. and Peters, J.-M. (2002) 'The dissociation of cohesin from chromosomes in prophase is regulated by Polo-like kinase', *Mol Cell*, 9(3), pp. 515-25.

Sunkel, C.E. and Glover, D.M. (1988) 'polo, a mitotic mutant of Drosophila displaying abnormal spindle poles', *J Cell Sci*, 89 (Pt 1), pp. 25-38.

Suzumori, N., Ogata, T., Mizutani, E., Hattori, Y., Matsubara, K., Kagami, M. and Sugiura-Ogasawara, M. (2010) 'Prenatal findings of paternal uniparental disomy 14: Delineation of further patient', *Am J Med Genet A*, 152A(12).

Tachibana-Konwalski, K., Godwin, J., van der Weyden, L., Champion, L., Kudo, N.R., Adams, D.J. and Nasmyth, K. (2010) 'Rec8-containing cohesin maintains bivalents without turnover during the growing phase of mouse oocytes', *Genes Dev*, 24(22), pp. 2505-16.

Tanaka, T., Cosma, M.P., Wirth, K. and Nasmyth, K. (1999) 'Identification of cohesin association sites at centromeres and along chromosome arms', *Cell*, 98(6), pp. 847-58.

Taniguchi, E., Toyoshima-Morimoto, F. and Nishida, E. (2002) 'Nuclear translocation of plk1 mediated by its bipartite nuclear localization signal', *J Biol Chem*, 277(50), pp. 48884-8.

Taylor, S. and Peters, J.M. (2008) 'Polo and Aurora kinases: lessons derived from chemical biology', *Curr Opin Cell Biol*, 20(1), pp. 77-84.

Telfer, E.E. and McLaughlin, M. (2007) 'Natural history of the mammalian oocyte', *Reprod Biomed Online*, 15(3), pp. 288-95.

Thornton, B.R., Ng, T.M., Matyskiela, M.E., Carroll, C.W., Morgan, D.O. and Toczyski, D.P. (2006) 'An architectural map of the anaphase-promoting complex', *Genes Dev*, 20(4), pp. 449-60.

Tomonaga, T., Nagao, K., Kawasaki, Y., Furuya, K., Murakami, A., Morishita, J., Yuasa, T., Sutani, T., Kearsey, S.E., Uhlmann, F., Nasmyth, K. and Yanagida, M. (2000) 'Characterization of fission yeast cohesin: essential anaphase proteolysis of Rad21 phosphorylated in the S phase', *Genes Dev*, 14(21), pp. 2757-70.

Tong, C., Fan, H.-Y., Lian, L., Li, S.-W., Chen, D.-Y., Schatten, H. and Sun, Q.-Y. (2002) 'Polo-like kinase-1 is a pivotal regulator of microtubule assembly during mouse oocyte meiotic maturation, fertilization, and early embryonic mitosis', *Biol Reprod*, 67(2), pp. 546–554.

Toth, A., Ciosk, R., Uhlmann, F., Galova, M., Schleiffer, A. and Nasmyth, K. (1999) 'Yeast cohesin complex requires a conserved protein, Eco1p(Ctf7), to establish cohesion between sister chromatids during DNA replication', *Genes Dev*, 13(3), pp. 320-33.

Toth, A., Rabitsch, K.P., Galova, M., Schleiffer, A., Buonomo, S.B. and Nasmyth, K. (2000) 'Functional genomics identifies monopolin: a kinetochore protein required for segregation of homologs during meiosis i', *Cell*, 103(7), pp. 1155-68.

Toyoshima-Morimoto, F., Taniguchi, E. and Nishida, E. (2002) 'Plk1 promotes nuclear translocation of human Cdc25C during prophase', *EMBO Rep*, 3(4), pp. 341-8.

Toyoshima-Morimoto, F., Taniguchi, E., Shinya, N., Iwamatsu, A. and Nishida, E. (2001) 'Polo-like kinase 1 phosphorylates cyclin B1 and targets it to the nucleus during prophase', *Nature*, 410(6825), pp. 215-20.

Uhlmann, F. (2003) 'Separase regulation during mitosis', *Biochem Soc Symp*, (70), pp. 243-51.

Uhlmann, F. (2004) 'The mechanism of sister chromatid cohesion', *Exp Cell Res*, 296(1), pp. 80-5.

Uhlmann, F., Lottspeich, F. and Nasmyth, K. (1999) 'Sister-chromatid separation at anaphase onset is promoted by cleavage of the cohesin subunit Scc1', *Nature*, 400(6739), pp. 37-42.

Uhlmann, F., Wernic, D., Poupart, M.A., Koonin, E.V. and Nasmyth, K. (2000) 'Cleavage of cohesin by the CD clan protease separin triggers anaphase in yeast', *Cell*, 103(3), pp. 375-86.

van de Weerdt, B.C. and Medema, R.H. (2006) 'Polo-like kinases: a team in control of the division', *Cell Cycle*, 5(8), pp. 853-64.

Vanderheyden, V., Wakai, T., Bultynck, G., De Smedt, H., Parys, J.B. and Fissore, R.A. (2009) 'Regulation of inositol 1,4,5-trisphosphate receptor type 1 function during oocyte maturation by MPM-2 phosphorylation', *Cell Calcium*, 46(1), pp. 56-64.

Verlhac, M.H., Lefebvre, C., Guillaud, P., Rassinier, P. and Maro, B. (2000) 'Asymmetric division in mouse oocytes: with or without Mos', *Curr Biol*, 10(20), pp. 1303-6.

Vodermaier, H.C., Gieffers, C., Maurer-Stroh, S., Eisenhaber, F. and Peters, J.M. (2003) 'TPR subunits of the anaphase-promoting complex mediate binding to the activator protein CDH1', *Curr Biol*, 13(17), pp. 1459-68.

Waizenegger, I.C., Hauf, S., Meinke, A. and Peters, J.M. (2000) 'Two distinct pathways remove mammalian cohesin from chromosome arms in prophase and from centromeres in anaphase', *Cell*, 103(3), pp. 399-410.

Warren, W.D. and Gorringe, K.L. (2006) 'A molecular model for sporadic human aneuploidy', *Trends Genet*, 22(4).

Wassmann, K., Niault, T. and Maro, B. (2003) 'Metaphase I arrest upon activation of the Mad2-dependent spindle checkpoint in mouse oocytes', *Curr Biol*, 13(18), pp. 1596-608.

Watanabe, N., Arai, H., Nishihara, Y., Taniguchi, M., Hunter, T. and Osada, H. (2004) 'M-phase kinases induce phospho-dependent ubiquitination of somatic Wee1 by SCFbeta-TrCP', *Proc Natl Acad Sci U S A*, 101(13), pp. 4419-24.

Watanabe, Y. (2005) 'Sister chromatid cohesion along arms and at centromeres', *Trends Genet*, 21(7), pp. 405-12.

Watanabe, Y. and Nurse, P. (1999) 'Cohesin Rec8 is required for reductional chromosome segregation at meiosis', *Nature*, 400(6743), pp. 461-4.

Waters, J.C. (2009) 'Accuracy and precision in quantitative fluorescence microscopy', *J Cell Biol*, 185(7), pp. 1135-48.

Wells, D. and Delhanty, J.D. (2000) 'Comprehensive chromosomal analysis of human preimplantation embryos using whole genome amplification and single cell comparative genomic hybridization', *Mol Hum Reprod*, 6(11), pp. 1055-62.

Wianny, F., Tavares, A., Evans, M.J., Glover, D.M. and Zernicka-Goetz, M. (1998) 'Mouse polo-like kinase 1 associates with the acentriolar spindle poles, meiotic chromosomes and spindle midzone during oocyte maturation', *Chromosoma*, 107(6-7), pp. 430–439.

Xu, H., Beasley, M.D., Warren, W.D., van der Horst, G.T.J. and McKay, M.J. (2005) 'Absence of mouse REC8 cohesin promotes synapsis of sister chromatids in meiosis', *Dev Cell*, 8(6), pp. 949-61.

Yamamoto, A., Guacci, V. and Koshland, D. (1996) 'Pds1p, an inhibitor of anaphase in budding yeast, plays a critical role in the APC and checkpoint pathway(s)', *J Cell Biol*, 133(1), pp. 99-110.

Yokobayashi, S. and Watanabe, Y. (2005) 'The kinetochore protein Moa1 enables cohesion-mediated monopolar attachment at meiosis I', *Cell*, 123(5), pp. 803-17.

Yu, H. (2007) 'Cdc20: a WD40 activator for a cell cycle degradation machine', *Mol Cell*, 27(1), pp. 3-16.

Zhang, D., Ma, W., Li, Y.H., Hou, Y., Li, S.W., Meng, X.Q., Sun, X.F., Sun, Q.Y. and Wang, W.H. (2004) 'Intra-oocyte localization of MAD2 and its relationship with kinetochores, microtubules, and chromosomes in rat oocytes during meiosis', *Biol Reprod*, 71(3), pp. 740-8.

Zhang, Y. and Lees, E. (2001) 'Identification of an overlapping binding domain on Cdc20 for Mad2 and anaphase-promoting complex: model for spindle checkpoint regulation', *Mol Cell Biol*, 21(15), pp. 5190-9.